# VARIABLE-PRESSURE ^{2}H NMR STUDIES OF BICELLAR MIXTURES IN THE PRESENCE AND ABSENCE OF DMPG

ASHKAN RAHMANI
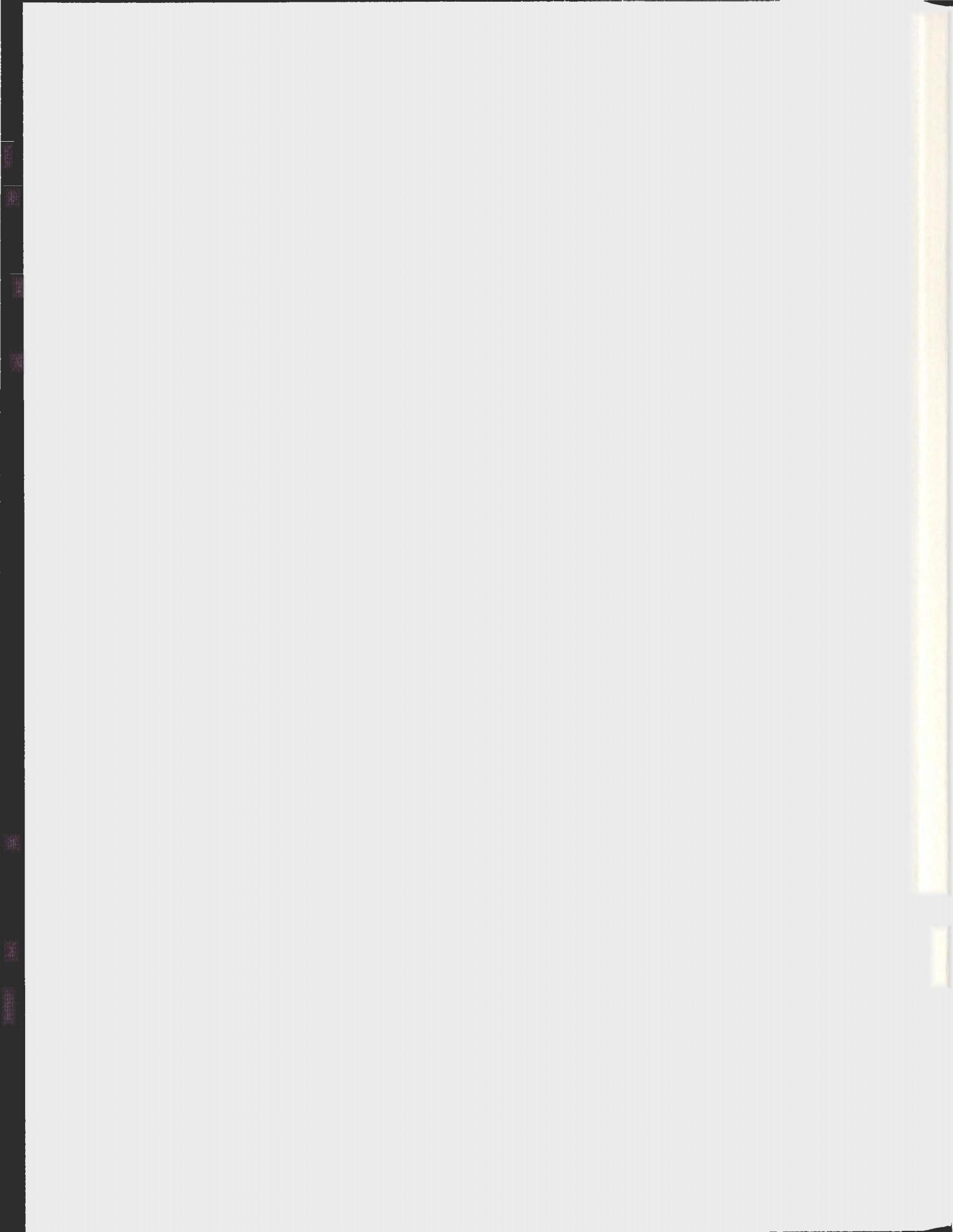
Variable-pressure ^{2}H NMR studies of bicellar mixtures in the presence and absence of DMPG

by

©Ashkan Rahmani

A Thesis submitted to the School of Graduate Studies in partial fulfillment of the requirements for the degree of

Master's of Science

Physics and physical oceanography

Memorial University of Newfoundland

June 27th 2013

St. John's

Newfoundland

Abstract

Lipid dispersions with planar regions enriched in long chain lipids and highly curved regions enriched in short chain lipids can exhibit complex phase behaviour. Such "bicellar" mixtures provide insight into how the morphology of self-assembled soft structures are determined by component heterogeneity. Bicellar dispersion properties can be affected both by surface charge and the application of pressure. Variable pressure deuterium nuclear magnetic resonance (^{2}H NMR) studies were carried out on bicellar lipid mixtures comprising the short chain lipid 1,2-dihexanoyl-sn-glycero-3-phosphocholine (DHPC), the long chain lipid 1,2-dimyristoyl-sn-glycero-3-phosphocholine (DMPC) and the anionic lipid 1,2-dimyristoyl-sn-glycero-3-phospho-(1'-rac-glycerol) (sodium salt) (DMPG). Samples of DMPC-d_{54}/DMPG/DHPC (3:1:1), DMPC/DMPG-d_{54}/DHPC (3:1:1) and, for comparison, DMPC-d_{54}/DHPC (4:1) were prepared and hydrated in HEPES buffer at lipid weight fractions of 10%. DMPC-d_{54}/DMPG/DHPC (3:1:1) sample was also prepared with the same sample preparation protocol but the sonication and freeze-thaw omitted. Spectra and quadrupole echo decays were obtained, between 4 °C and 65 °C, for both warming and cooling at ambient pressure, 41.4 Mpa, and 82.7 Mpa. At ambient pressure, all mixtures form isotropically reorienting small particles at low temperature. On warming past the DMPC gel-to-liquid crystal transition temperature, the particles coalesce into larger structures that can be magnetically oriented. At higher temperatures, the disper-

sions form more randomly oriented lamellar phases. On cooling at ambient pressure, the lamellar phase persists to lower temperature where it transforms directly to the isotropic phase. Application of pressure raises the transition temperatures for DMPC-d_{54}/DHPC (4:1) but does not significantly change the phases observed. For DMPC-d_{54}/DMPG/DHPC (3:1:1), pressure can stabilize the isotropically reorienting phase to higher temperature on warming. On cooling under pressure, DMPC-d_{54}/DMPG/DHPC (3:1:1) can reorganize into a highly ordered gel phase with spectra similar to those of the high pressure interdigitated gel phases of some phospholipids. The same phase behavior was observed for non-sonicated DMPC-d_{54}/DMPG/DHPC (3:1:1) and for DMPC/DMPG-d_{54}/DHPC (3:1:1). Once nucleated, the highly ordered gel phase appears to be stable even at ambient pressure. These observations demonstrate the sensitivity of dispersion morphology to details of mixed-lipid sample's thermal and pressure history.

Acknowledgements

I wish to offer my foremost and sincerest gratitude to my supervisor, Dr. Michael Morrow, who has supported me throughout my thesis with his patience and knowledge. I attribute the level of my Master's degree to his encouragement and effort and without him this thesis, too, would not have been completed or written. One could not wish for a better supervisor.

I also wish to show my sincere appreciation to my teachers, Dr. Stephanie Curnoe, Dr. Erika Merschrod and Dr. Anand Yethiraj. I am also deeply thankful to Dr. Todd Andrews, the graduate coordinator, for his immediate and priceless helps in tough times. I also thank Dr. Valerie Booth and her research team for their interesting and informative group meetings.

I warmly thank my colleges Alanna Flynn, Lauren MacEachern, Alexander Sylvester and Collin Knight for their useful collaboration many times during the program and it was a good time working with them in lab. I specially thank Donna Jackman for providing the required buffer solution. I also wish to thank Wayne Holly from the cryogenics facility for providing required support to keep the lab running.

In my office, I was surrounded by knowledgeable and friendly people who helped me

Table of Contents

List of Tables

List of Figures

Chapter 1

Introduction

Lipid bilayers are the main structural element of cell membranes. There are 10^6 lipid molecules in a 1 μm^2 area of lipid bilayer in the plasma membrane of an animal's cells [1]. Lipids are amphiphilic molecules. In amphiphilic structures, one end associates with water and is called hydrophilic whereas the other end avoids water and is called hydrophobic. One of the most abundant types of lipid in a cell is phospholipid which has a glycerol backbone, acyl chains, a phosphate group, and a simple organic group such as choline in the headgroup. The hydrophilic part of a phospholipid is the headgroup which can be zwitteronic or charged depending on the chemical structure of the headgroup. The hydrophobic end consists of the hydrocarbon chains which can have different lengths depending on the type of phospholipid. Such molecules form bilayers in cells and when dispersed in water. Phospholipids are important parts of biological systems and a deeper understanding of them provides insights into biological processes involving cell membranes or lipid assemblies.

Lipids play significant roles in a variety of cell functions including cell division or fusion, transport, energy storage, hormone biosynthesis, provision of a structured en-

vironment for enzymes and so on [1, 6, 7, 8]. The ability of some bilayer dispersions, namely bicellar mixtures, to align in magnetic fields also makes them excellent platforms for NMR studies of membrane-associated proteins [1, 2, 4, 8].

The studies of bilayered micelle properties and phase behavior described in this thesis provide information not only about specific model systems but also give some insight into the conditions under which lipid assemblies can reorganize. Accordingly, the results reported here may be more broadly relevant to biological processes involving bilayer or membrane structure. They are also relevant to the understanding of this particular class of self-assembled soft material.

1.1 Bilayers structures

1.1.1 Dispersions in water

Although dry phospholipids are crystalline, they form bilayer vesicles or micelles spontaneously upon hydration due to their amphiphilic nature [9]. The dominant force in self-assembly is hydrophobic. The mode of assembly upon hydration can vary with degree of hydration and composition of the dispersion. Hydrated dispersions of lipids with longer lipid chains (more than 10 carbons on each chain), such as 1,2-dimyristoyl-*sn*-3-phosphocholine (DMPC), form bilayers or lamellae. Lipids with shorter lipid chains (6 carbons per chain or shorter), such as 1,2-dihexanoyl-*sn*-glycero-3-phosphocholine (DHPC), form micelles for a wide range of temperature [10, 11, 12]. Molecules in bilayers are arranged in a way that hydrocarbon chains are roughly parallel to each other. The hydrophilic part of the bilayer is formed by a monolayer of polar head group(s). Two monolayers, each arranged as described, face toward each

other to form a bilayer. Other morphologies, such as micelles and hexagonal phase can be formed by varying temperature, pressure, hydration and composition.

1.1.2   Synthetic lipid assemblies

Cell membranes are made of bilayered lipids. Studying synthetic lipid assemblies adds to our understanding about their response to physical parameters as well as their structural characteristics and roles in biological processes. These lipid assemblies can be used as models for biological membranes [1].

Due to the ability of lipids to form different assemblies, some structures they form can be used for specific purposes. For example, vesicles can be formed spontaneously after dispersion in a water based solution. This structure is a lipid bilayer rolled into a spherical shell with water enclosed in the vesicle. These vesicles can be used for the purpose of encapsulation by substituting the enclosed water based solution by any desirable solution. For example vesicles made of synthetic lipids can be used as drug delivery agents [48, 49].

Lipid mixtures containing two or three different phospholipid components can be used to study the interactions among the components. One important class of lipid mixtures is one in which one or more long chain lipid component(s) is mixed with one short chain component. Such mixtures are commonly called "bicellar mixtures" [9, 18, 24]. The mismatch between components' chain lengths results in very interesting morphologies and phase behaviors. In such mixtures, at low temperatures, lipids with longer chains (more than 10 carbons) can locate on planar parts of the lipid assembly while lipids with shorter chains locate preferentially in highly curved areas or

edges. [18, 21, 22, 23, 24]. The low temperature, bilayered micelle structures are relatively small, planar particles between 10 nm to 100 nm in diameter.

1.1.3 Phases

The morphologies of lipid phases reflect the balance between interactions in the head-group and chain regions. Lipid assemblies are thermotropic meaning that the phase depends on temperature. For longer chain lipids($\sim$10 or more carbons per acyl chains) bilayers are found to be in the lamellar gel phase at lower temperature and in the lamellar liquid crystalline phase at higher temperature [20].

In the lamellar gel phase, hydrocarbon chains are mostly ordered in all-trans configurations. This phase exists mainly at low temperatures or high pressure. As lipid bilayers enter this phase on cooling, the area per lipid decreases as a result of the increase in chain order. Full extension of chains in this phase results in an increased bilayer thickness [61]. Some specific gel phase structures are described below. Figure 1.1 shows a general schematic representation of ordered lipids in the gel phase.
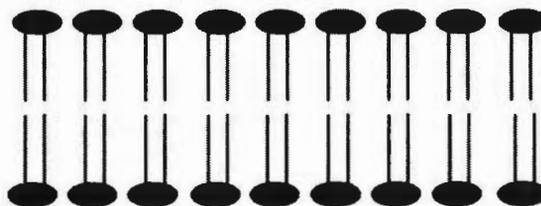
Figure 1.1: Gel Phase

The ripple gel phase happens at low temperature. It results from a mismatch between

acyl chain and head group area. Figure 1.2 shows a schematic representation of the ripple gel phase.
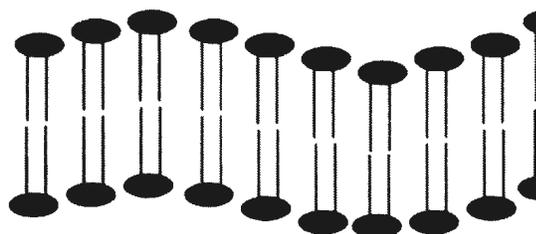
Figure 1.2: Schematic representation of the rippled gel phase.

The tilted lamellar gel phase is also known as $L_{\beta'}$. It occurs for lipids with relatively larger head groups such as PCs [61]. The tilt angle is measured to be $\sim 32°$ for a wide range of temperature [61, 62]. In this sub-phase, lipids are tilted with respect to the membrane normal [7, 59]. A schematic representation of the tilted gel phase is shown as Figure 1.3.
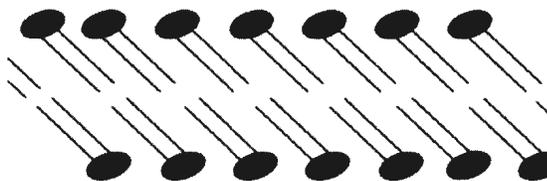
Figure 1.3: Schematic representation of the tilted gel phase.

The lamellar liquid crystalline phase is characterized by fast, axially symmetric reorientation of acyl chain segments and is typical of bilayer dispersions at high temperature and ambient pressure. In this arrangement, chains are disordered by trans-gauche

isomerisation around carbon-carbon bonds. In this phase, lipid molecules diffuse laterally through the bilayer. Such fluidity is characteristic of membranes under biologically relevant conditions [7, 59]. The liquid crystalline phase is denoted as L_α. The schematic representation of liquid crystal phase is shown as Figure 1.4.
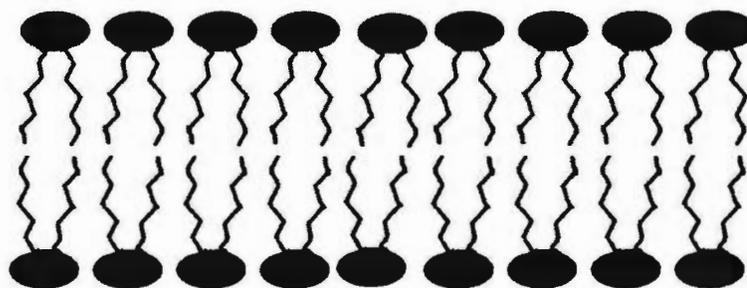
Figure 1.4: Schematic representation of the liquid crystalline phase.

1.2 Bicellar mixtures

In this thesis, the term "bicellar mixture" refers to a mixture of phospholipids composed of 1,2-dimyristoyl-*sn*-glycero-3-phosphocholine (DMPC) as the long chain lipid and 1,2-dihexanoyl-*sn*-glycero-3-phosphocholine (DHPC) as the short chain lipid. Bicellar mixtures doped with lipids having anionic head groups will be referred to "anionic bicellar" or "doped bicellar". The anionic lipid used in this work is 1,2-dimyristoyl-*sn*-glycero-3-phospho-(1'-rac-glycerol) (sodium salt) or DMPG. Figure 1.5 shows the chemical structures of DMPC, DHPC and DMPG. DMPC and DMPG each have 14 carbons in their acyl chain. These are used as long chain lipids in this work. For bicellar mixtures in this work DHPC, with 6 carbons in the acyl chain, has been
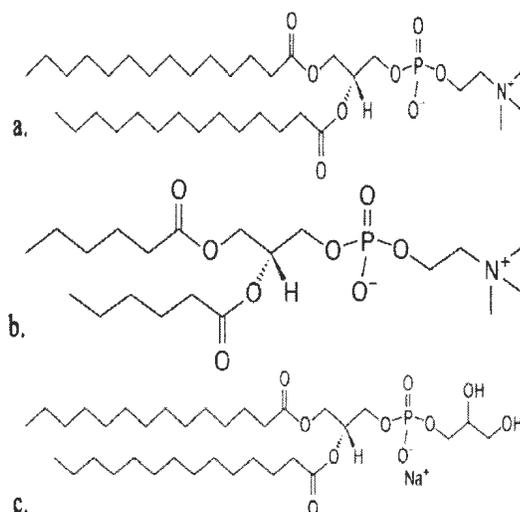
Figure 1.5: Schematic structures for (a) DMPC, (b) DHPC, and (c) DMPG.

used as the short chain lipid.

The interesting morphologies and phase behaviors in bicellar materials result from competition between the entropic cost of separating long chain and short chain lipids and the enthalpic cost of accommodating substantial chain length mismatch [77]. One important determinant of bicellar mixture morphology and phase behavior is the specific set of components contained in the lipid mixture. Bicelle particle size and morphology depend on the molar ratio of long and short chain lipids, $Q = \frac{[DMPC]}{[DHPC]}$.

Several different experimental methods such as NMR spectroscopy, IR spectroscopy, neutron scattering, light scattering, x-ray diffraction, Raman spectroscopy, and fluorescence based techniques, have been employed to study either lipid bilayers or bicellar mixtures [28, 29, 30, 31, 32, 33, 34, 56, 57, 59]. ^{2}H NMR gives us very useful information about molecular orientation in bicellar assemblies due to bicellar mixtures'

be magnetically oriented.

Previous NMR studies of DMPC-d_{54}/DHPC bicellar dispersions, where DMPC-d_{54} denotes chain-perdeuterated DMPC, have shown the formation of bilayered disks with fast isotropic reorientation at lower temperatures, axially-symmetric reorientation about an axis oriented perpendicular to the applied magnetic field over a small range of intermediate temperatures and axially symmetric reorientation about spherically-distributed bilayer normal orientations at high temperature [18, 21, 23].

Small angle neutron scattering, SANS, has confirmed these observations [38]. Studies employing SANS showed that the morphological phases of a mixture of long-chain phospholipid/short-chain phospholipid (i.e. DMPC/DHPC) encountered on warming from low to high temperature are an isotropic phase, consisting of bicellar disks experiencing rapid thermal reorientation, a magnetically alignable chiral nematic phase consisting of entangled worm-like micelles, and a multilamellar bilayer vesicle (MLV) phase [35, 37]. The progression of isotropic, nematic and lamellar structures for mixtures of long-chain lipids and short-chain lipids is now widely accepted [18, 23, 24, 35, 37, 38, 43, 44, 45]. However, some studies have suggested that bicellar materials pass through phases with different morphologies under some specific circumstances [15, 16, 17].

Bicellar mixtures containing three lipid components can also be studied. One of the most interesting candidates for a third bicellar lipid component is a lipid with a charged headgroup but with the same chain length as the longer chain zwitteronic lipid component. For instance, bicellar mixtures with 25% of DMPG or DMPS which have negative and positive headgroups respectively, are used to study myristoylated

peptides [39, 40]. Anionic lipids (e.g. DMPG) are of interest as a component of bicellar mixtures for use as surfactant lipid models in NMR studies of hydrophobic lung surfactants proteins [41]. Such mixtures can also be used to study the interaction among headgroups in the kinds of structures formed by bicellar mixtures. In terms of anionic bicellar mixtures, another parameter must be defined in addition to Q to denote the molar ratio of the third lipid component. This parameter is the molar ratio of charged to zwitteronic long-chain component (i.e. $\frac{[DMPG]}{[DMPC]}$) and it is called R.

1.2.1 Phases and arrangements

As noted above, small angle neutron scattering studies have provided important insights into the properties of bicellar phases observed at different temperatures [35, 46, 80]. In particular, various bicellar dispersion phases have been identified with specific lyotropic liquid crystal symmetries.

For Q > 2, bicellar mixtures experience three distinct ranges of behavior as follows. For temperatures below the gel-to-liquid crystal temperature of DMPC, long-chain and short-chain components are strongly separated to form small bilayered disk micelles with fast isotropic reorientation. In other words, at a particular instant in time, bilayered disks are uniformly oriented in every direction [26, 27]. Figure 1.6 shows a schematic representation of a bicellar mixture in the isotropic phase. The blue regions (lighter color in black and white copies) represent short chain lipids while red areas (darker in black and white copies) represent long chain lipids.

In the bicelle disk phase mentioned above, the chains of long-chain lipids (e.g. DMPC) are ordered or extended. The parameter Q determines the ratio between planar area
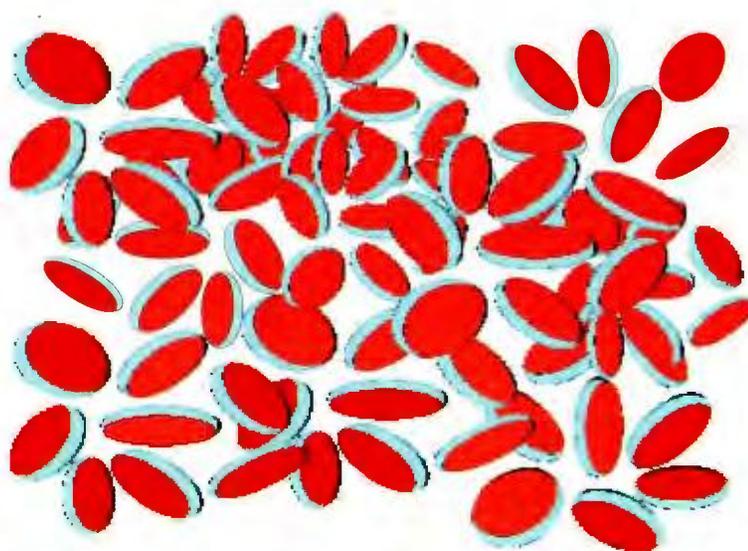
Figure 1.6: Isotropically oriented bicellar disks. This figure is modified and reprinted with the permission of its creator, Dr. Michael Morrow.

and disk perimeter. Area per lipid in planar regions is constrained by the perimeter. These disks have no long range positional or orientational order which, in additional to their size, results in low viscosity and transparency [78].

When temperature increases through the main gel to liquid transition temperature (T_m), area per lipid for the long chain component exceeds the disk perimeter constraint imposed by Q [77]. As a result, larger assemblies form with long-chain and short-chain components still largely separated [36]. In this phase, lipid segments are worm-like micelles or bilayer sheets. These structures are magnetically alignable. The schematic representation of a bilayer sheet is shown in Figure 1.7. The resulting aggregates form a nematic phase [80]. This phase exhibits long range orientational order. One characteristic of this aggregation is higher viscosity than the isotropic phase which is the result of entanglement of the elongated bilayers micelles which still maintain some fluidity [37]. In addition to temperature, composition also affects the
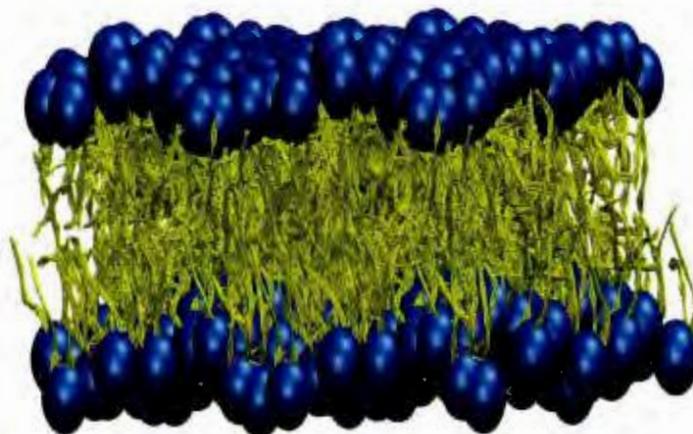
Figure 1.7: Bilayer sheets that may be aligned parallel or perpendicular to B_o. This figure is reprinted with the permission of its creator, Mohammad Hassan Khatami.

properties of lipid assemblies. Studies have shown that magnetic orientation occurs when $2 < Q < 6$ [18, 23, 25].

At temperatures higher than the magnetic orientation phase temperature range, DHPC molecules start to interact with the other components more strongly [63]. This can cause instability of the edges. In other words, the short-chain lipids (e.g. DHPC) may migrate into the planar bilayer regions. This instability can cause the bilayered sheets to fold into spherical bilayered shells of perforated lamellae [19, 35, 37, 81]. The rims of pores in this arrangement are formed by short chain lipids. This arrangement can contain a single bilayered sphere or multiple spheres. The first arrangement is called unilamellar vesicle and the latter one is called multilamellar vesicles. An MLV is larger in size compared to ULV. In either case, the thickness of bilayer is smaller than the size of either MLV or ULV. Viscosity drops slightly in this phase [37]. Figure 1.8 shows a schematic representation of a multilamellar vesicle.
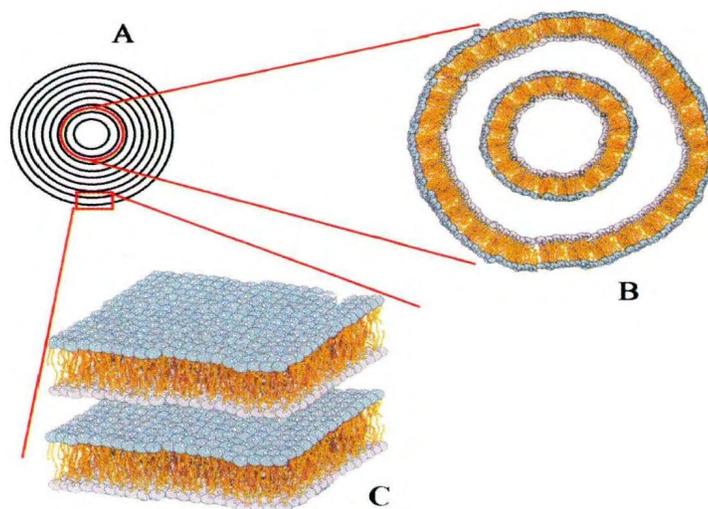
Figure 1.8: A schematic representation of a multilamellar vesicle. This figure is reprinted here with the permission from its creator Dr. Michael Morrow.

1.3 Hydrostatic pressure

Amphiphilic structures are known to be very sensitive to pressure. Studying the response of lipid and surfactant systems to pressure can yield new information on their structure, energetics and phase behavior and on the transition kinetics between mesophases. Pressure increases the order of membranes, thus simulating the effects of cooling [45]. Hydrostatic pressure is known to be a parameter that can affect the structure, energetics, phase behavior and dynamics of biomolecules [45]. Studying bilayers at high pressure can contribute to better understanding of the role of bilayer composition in deep-sea marine organisms living at high-pressure (up to 0.1 Gpa) habitats [47]. Hydrostatic pressure influences physiology of cells in every level. However, the biological membrane is the most pressure sensitive cellular component [45].

The effects of pressure on bicellar structures have been previously studied extensively. A tentative pressure-temperature phase diagram for the DMPC/DHPC system has been found employing X-ray scattering [45]. This shows that applying pressure raises the isotropic-nematic and nematic-lamellar transition temperatures. In addition to this, it has been observed by SANS studies [45, 31] and deuterium NMR studies [17] that applying pressure can lead to a highly ordered phase for bilayer membranes with more than 16 carbons in their acyl chains. This phase is referred to as the interdigitated gel phase in this thesis and it is shown schematically in Figure 1.9. In other words, hydrostatic pressure contributes to the formation of arrangements which are not accessible at ambient pressure(e.g. interdigitated gel phase).
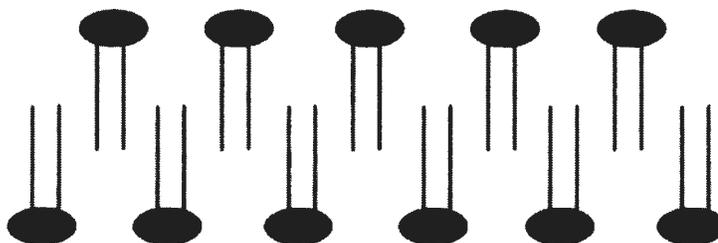
Figure 1.9: Schematic representation of an interdigitated gel phase. In this Figure, it is assumed that the mixture contains one species of lipid.

^{2}H NMR studies at high pressure have been employed to examine both phase behaviour [17, 56] and head group orientation [55] of bilayers. An interdigitated gel phase has been reported for bilayers under a variety of experimental conditions [13, 14, 15, 16, 17]. Based on the literature review done in this work, interdigitated gel

phase has only been observed after being exposed to high pressure [17, 51, 52, 56, 59] or the presence of small molecules that perturb the order of headgroups [13, 16]. If bilayers in the liquid crystalline phase are cooled under pressure, chain orientational order increases until the transition to a more-ordered phase [50, 17]. Chain orientational order is described in detail in the second chapter.

The sensitivity of phospholipid chain ordering to pressure in mixtures containing a single phospholipid species depends on the proximity of the temperature to T_m for that phospholipid [54]. For mixtures composed of two non-identical phospholipids, however, both species show sensitivity to ordering caused by pressure. This sensitivity falls between the values of either species individually [50].

At fixed temperature, increasing pressure increases mean lipid chain orientational order [17, 50, 54, 56, 57]. Thus, hydrostatic pressure increases the temperature for the main transition from gel to liquid crystalline, isotropic-nematic and nematic-lamellar if present [63, 17, 54, 56, 57, 58, 59]. ^{2}H NMR studies have reported the pressure sensitivity of the main transition temperature for DMPC mixtures as 0.19 °C/MPa [54].

In addition to the influence of hydrostatic pressure on lipid chains and their orientational order, studies have shown different responses to pressure for bilayers composed of lipids with different headgroups. Comparison between DPPC and DPPG bilayers have shown that DPPG tend to undergo a transition to an interdigitated gel phase at a lower pressure than DPPC bilayers. The lowest pressure at which DPPG bilayers undergo a transition to an interdigitated gel phase is approximately 60 MPa. For DPPC bilayers, this pressure is approximately 150 MPa [17]. The lower interdigitation pressure for DPPG might be due to electrostatic interactions between the negatively

charged DPPG headgroups. The same study reported that, above the lowest pressure at which interdigitation is observed for each lipid, both DPPC-d_{62} and DPPG-d$_{62}$ display an interdigitated gel phase at high temperature, a non-interdigitated gel phase at intermediate temperature and a chain-immobilized ordered phase at low temperature [17].

DSC and variable pressure NMR have also been used to study bicellar mixtures (DMPC/DHPC) [35, 64, 63]. It has been reported that the isotropic-nematic transition rises by $\sim 0.19\,^\circ$C/MPa for DMPC/DHPC (4.4:1) and by $\sim 0.15\,^\circ$C/MPa for DMPC/DHPC (3:1). The pressure sensitivity of nematic-lamellar transition has also been reported to be $\sim 0.18\,^\circ$C/MPa for DMPC/DHPC (4.4:1) and $\sim 0.14\,^\circ$C/MPa for DMPC/DHPC (3:1) [63]. This study reported that DMPC/DHPC (4:1) mixtures do not undergo a transition into an interdigitated gel phase at pressures up to 135 MPa while being warmed.

1.4   This work

Bicellar mixtures, containing one long chain lipid and one short chain lipid, have shown very interesting morphology and phase behavior and have been studied extensively [21, 22. 24, 25, 39]. The effects of hydrostatic pressure on bicellar properties have only recently been examined [63]. Studies of DMPC/DHPC with molar ratios between 2 to 4 and either perdeuterated DMPC or DHPC have shown no sign of interdigitation [63] at different pressures up to 135 MPa.

This work is partially motivated by previous observations of how bilayers with different

headgroups respond to hydrostatic pressure. Previous observation of gel interdigitation at lower pressure for anionic lipids than for zwitteronic lipids provides some clues about the sensitivity of bilayer structure to the balance between headgroup and chain interactions. It has been observed that lipid mixtures with a PG headgroup tend to transform to an interdigitated gel phase at a pressures higher than 60 MPa while lipids with a PC headgroup undergo the transition into an interdigitated phase at 150 MPa and higher. [17]. The effect of anionic lipids on the response of bicellar mixtures to pressure has not been studied.

Adding anionic lipid components to a bicellar mixture is of interest due to the morphology of bicellar structures. Studies have shown that adding 25% of DMPG to DMPC/DHPC (Q=3, R=0.33) modifies the behavior of the bicellar mixture and bilayer dynamics in the high temperature phase. The DMPC/DMPG/DHPC (3:1:1) mixture, however, displays the same progression of phases as DMPC/DHPC (Q=4) [77]. On the other hand, SANS studies using oscillating shear to induce magnetic alignment have been interpreted as showing that DMPC/DMPG/DHPC with R=0.02 and R=1 transforms directly from isotropically reorienting disks to a smectic lamellar phase whereas DMPC/DHPC mixtures pass through the intermediate nematic ribbon-like phase [42]. The apparent discrepancy between the behaviours inferred from the NMR and SANS observations has not been resolved.

The work reported in this thesis is motivated by the question of how the presence of charged lipid affects the response of bilayered micelle structures to hydrostatic pressure. Specific objectives are :

1. To examine how the presence of DMPG in DMPC/DMPG/DHPC (3:1:1) disper-

sions affects the dependence of observed transition temperatures on hydrostatic pressure:

2. To determine whether the presence of DMPG in the bilayered micelle dispersion results in the observation of pressure stabilized phases that are not observed at ambient pressure :

and

3. To determine whether the presence of DMPG in the bilayered micelle dispersion affects the morphology of phases observed at high pressure.

For these purposes, several bicellar mixtures were prepared with the following compositions: DMPC-d_{54}/DHPC with molar ratio Q$\simeq$ 4; DMPC-d_{54}/DMPG/DHPC, with Q$\simeq$ 4 and R$\simeq$ 0.33; and DMPC/DMPG-d_{54}/DHPC (3:1:1) (the same molar ratio but different perdeuterated carbon chains). The ratio of long chain to short chain lipids was kept constant at the value used for previous DMPC/DHPC studies [63]. Samples containing either perdeuterated DMPC or DMPG were prepared to study the response, participation and morphology of either DMPG or DMPC under various experimental circumstances in different assemblies. Variable pressure ^{2}H NMR has been employed to study either perdeuterated DMPC or DMPG in each doped bicellar mixtures. An anionic bicellar mixture was also prepared using an alternative sample preparation protocol in order to determine how sensitive observed behavior was to sample preparation methods.

This thesis is organized in the following way. The objective of the present work, a brief review of earlier works and a broader image of lipid assemblies and phases are presented in chapter 1. Chapter 2 gives a brief background about ^{2}H NMR theory

relevant to this work including some necessary technical information about magnets being used. Experimental techniques and methods used are described in chapter 3. Results and discussions are presented in chapter 4. The last chapter includes a summary of this work and conclusions.

Chapter 2

NMR background

Nuclear Magnetic Resonance (NMR) is a common method of studying phospholipid dispersions containing a single species, or a binary or bicellar mixture. One reason that NMR is popular among different methods of studying bicellar mixtures is that bilayers in bicellar mixtures can be magnetically orientable over a particular range of temperature. This characteristic makes magnetic-based methods ideal for these types of studies.

Nuclei with angular momentum and magnetic moments precess with a specific frequency in the presence of a magnetic field. If a current flows to a coil perpendicular to the magnetic field with the same frequency as the nuclear precession, it can tip the magnetic moments away from the applied field. If the duration of this radio frequency (RF) pulse is chosen in such a way as to leave the moments precessing in a plane perpendicular to magnetic field, the precessing magnetization can be detected via an oscillating voltage induced in the coil. Information about the motions and environment of molecules containing the nuclei can be obtained from interactions that perturb the precession frequency [66]. This is a very simplified way to describe how

NMR works.

NMR can be used for any isotopes that contain an odd number of protons and/or neutrons. These isotopes have a natural magnetic moment and angular momentum. In other words, a nonzero spin is required for the purpose of NMR. Among the most commonly used nuclei are ^1H, ^{13}C and ^{15}N. ^1H is common due to its high natural abundance and can provide information about organic molecules and the hydrocarbon chains. This high natural abundance can cause issues. For example, the proton NMR spectrum of a large organic molecule can be very complex and consist of many resonances. ^{13}C is not highly abundant but is a very useful isotope for studies of organic structures [66]. NMR methods have been developed for isotopes of many other elements ,e.g. ^2H, ^6L, ^{10}B, ^{11}B, ^{14}N, ^{17}O, ^{19}F, ^{23}Na, ^{29}Si, ^{31}P, ^{35}Cl, ^{113}Cd, ^{129}Xe , and ^{195}Pt. The advantages and disadvantages in using each isotope will not be discussed further in this thesis in any detail. The focus, in this thesis, is on ^2H NMR.

^2H NMR has been widely employed to study partially ordered systems containing deuterated organic molecules especially lipid membranes. The deuterium nucleus has spin=1 (one proton and one neutron) and its natural abundance is 0.016%. In order to take full advantage of ^2H NMR, synthetically deuterated molecules are required. Based on the type of required information, the chain or headgroup can be deuterated.

2.1 Theory of solid-state ^{2}H NMR

2.1.1 Theory of deuterium NMR in the absence of molecular motion

The Hamiltonian of a ^{2}H nucleus in presence a magnetic field, H_o, has four terms and it is given by

$$\mathcal{H} = \mathcal{H}_Z + \mathcal{H}_Q + \mathcal{H}_{CS} + \mathcal{H}_D \tag{2.1}$$

where $\mathcal{H}_Z$ stands for the Zeeman effect, $\mathcal{H}_Q$ for the quadrupole energy, $\mathcal{H}_{CS}$ for the anisotropic chemical shift due to shielding by electron density around the ^{2}H nucleus and $\mathcal{H}_D$ is the dipolar coupling resulting from the interaction between two magnetic dipoles. The approximate magnitudes of the perturbations caused by each interaction to the deuteron precession frequency can differ significantly. It is known that chemical shift for deuterium is less than 1 kHz for typical magnetic fields and that the dipolar interaction perturbation is approximately 4 kHz in the case of two deuterons. These magnitudes can be neglected in comparison to quadrupolar coupling splitting which is $\sim$ 250 kHz for deuterium in a static C-D bond. Thus, the total Hamiltonian of this system can be written as

$$\mathcal{H} = \mathcal{H}_Z + \mathcal{H}_Q. \tag{2.2}$$

The Zeeman effect is the splitting of energy levels corresponding to different azimuthal quantum numbers and it is caused by external magnetic field. For deuterium, there are three azimuthal quantum numbers, m=-1,0,1. Deuterium with I=1 has a non-spherical charge distribution and consequently an electric quadrupole moment. This non-spherical nuclear charge distribution causes an electrostatic interaction between the nuclear quadrupolar moment and the electric field gradient (EFG), due to the carbon-deuterium bond, at the position of nucleus. As shown in Figure 2.1, the de-

generacy between the transitions is removed resulting in two allowed transitions.
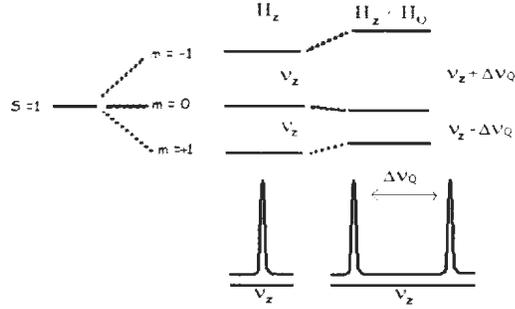
Figure 2.1: Perturbation of the Zeeman energy levels by the quadrupole interaction. The resulting ^{2}H NMR spectra are shown with and without quadrupole interactions, respectively, at right and left

The Hamiltonian associated with the Zeeman interaction between the magnetic moment and the static magnetic field can be expressed as [65]

$$\mathcal{H}_Z = -\gamma h(\vec{I}.\vec{H}_o) = -h\nu_o I_z \tag{2.3}$$

where $\vec{I}$ is the spin angular moment, γ is the gyromagnetic ratio and $\nu_o = \gamma H_o$ is the Larmor frequency [66]. The corresponding eigenvalue for this Hamiltonian can be written as

$$E_m = -\gamma h\nu_o m. \tag{2.4}$$

On the other hand, the quadrupole Hamiltonian can be written as [65, 70]

$$\mathcal{H}_Q = \frac{e^2 qQ}{8h}[3I_z^2 - I(I+1)][(3\cos^2\theta - 1) + \eta\sin^2\theta\cos 2\phi] \tag{2.5}$$

where θ and ϕ indicate the orientation of the EFG tensor with respect to the external

magnetic field (H_o), and η is the asymmetry parameter which reflects departures of the electric field gradient from axial symmetry. In the case of C-D bonds, The EFG tensor is known to be approximately symmetric ($\eta \leq 0.05$) which causes the last term to vanish. Thus, Eq. 2.3 becomes

$$\mathcal{H}_Q = \frac{e^2qQ}{8}[3I_z^2 - I(I+1)][(3\cos^2\theta - 1) \tag{2.6}$$

Therefore, the total Hamiltonian for deuterium nucleus is expressed as

$$\mathcal{H} = -\gamma h H_o I_z + \frac{e^2qQ}{8}[3I_z^2 - I(I+1)][(3\cos^2\theta - 1) \tag{2.7}$$

And the total energy for a deuteron with spin=1 is correspondingly

$$E_m = -\gamma h H_o m + \frac{e^2qQ}{8}[(3m^2 - 2)(3\cos^2\theta - 1)] \tag{2.8}$$

where different energy levels due to different values of m are

$$E_{+1} = -\gamma h H_o + \frac{e^2qQ}{8}(3\cos^2\theta - 1), \tag{2.9}$$

$$E_o = \frac{e^2qQ}{4}(3\cos^2\theta - 1) \tag{2.10}$$

and

$$E_{-1} = \gamma h H_o + \frac{e^2qQ}{8}(3\cos^2\theta - 1). \tag{2.11}$$

Selection rules [1] result in the resonance energies

$$h\nu_Q^- = E_{-1} - E_0 = \gamma h H_o + \frac{3e^2qQ}{8}(3\cos^2\theta - 1) \tag{2.12}$$

[1] $\triangle m = \pm 1$

and

$$h\nu_Q^+ = E_o - E_{+1} = \gamma h H_o - \frac{3e^2qQ}{8}(3\cos^2\theta - 1). \qquad (2.13)$$

The quadrupole splitting, $\triangle\nu_Q \equiv \nu_Q^- - \nu_Q^+$ can be written in terms of constants and θ as

or

$$\triangle\nu_Q = \frac{3e^2qQ}{4h}(3\cos^2\theta - 1) \qquad (2.14)$$

where $\dfrac{e^2qQ}{h}$, also known as the static deuteron quadrupole coupling constant, is measured to be ~ 167 kHz for a single deuterium nucleus in a C-D bond [65, 68].

2.1.2 ^{2}H NMR spectrum associated with molecular motion

In this section, the effects of molecular motions such as reorientation about the bilayer normal and chain conformational fluctuations, will be taken into account. The ^{2}H NMR spectrum of a deuteron on a lipid chain is affected by fast motions of the C-D bond about the bilayer normal. This can include rotations, fluctuation and trans-gauche isomerization. The instantaneous orientation of the bond can be characterized by the angle, θ, between C-D bond and bilayer normal. The observed spectrum also depends on the angle between bilayer normal and the applied magnetic field, β, which changes only slowly. These two angles are shown in Figure 2.2. After two different transformations and choosing Euler angles appropriately [66, 69, 70], the mean value of Hamiltonian over time can be expressed as

$$\langle \mathcal{H}_Q \rangle = \frac{e^2qQ}{16}[3\cos^2\beta - 1]\langle(3\cos^2\theta_n - 1) + \eta\sin^2\theta\cos^2\phi\rangle[3I_z^2 - 2] \qquad (2.15)$$

where the angular brackets indicate a time average over chain motions in the time scale of the experiment and θ_n is the angle between the bilayer normal and the nth C-D bond in the bilayer chain. For axially symmetric chain reorientation, η is very close to zero and the term with η can be neglected.

If the chain reorientation is axially symmetric with respect to the bilayer normal, the quadrupole splitting is then given by the following equation or

$$\langle \nu_Q \rangle = \triangle \nu_Q = \frac{3e^2 qQ}{4h}(3\cos^2 \beta - 1)S_{CD} \tag{2.16}$$

where S_{CD} is the orientational order parameter and is defined as

$$S_{CD} = \frac{1}{2}\langle 3\cos^2 \theta - 1\rangle. \tag{2.17}$$
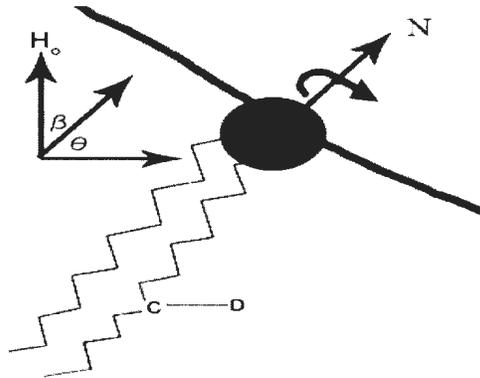
Figure 2.2: Schematic representation of the orientation of the magnetic field direction H_o, bilayer normal, N and the C-D bond orientation relative to the magnetic field direction, H_o.

The average in Eq. 2.18 is over chain motions that modulate the quadrupole Hamiltonian on the time scale ($\sim 10^{-5}$s) of the ^{2}H NMR experiment.

The average in the orientational order parameter reflects the motions of the CD bond, with respect to the bilayer normal, in the hydrocarbon chains of the lipid molecules. If all of the C-D bonds on a lipid acyl chain are deuterated, the resulting spectrum is superposition of different doublets with splittings corresponding to different values of S_{CD}. As shown in Figure 2.3 each doublet splitting indicates a specific C-D bond. The number of resolvable doublets depends on the resolution of a given spectrum and on the transverse relaxation time for that doublet.
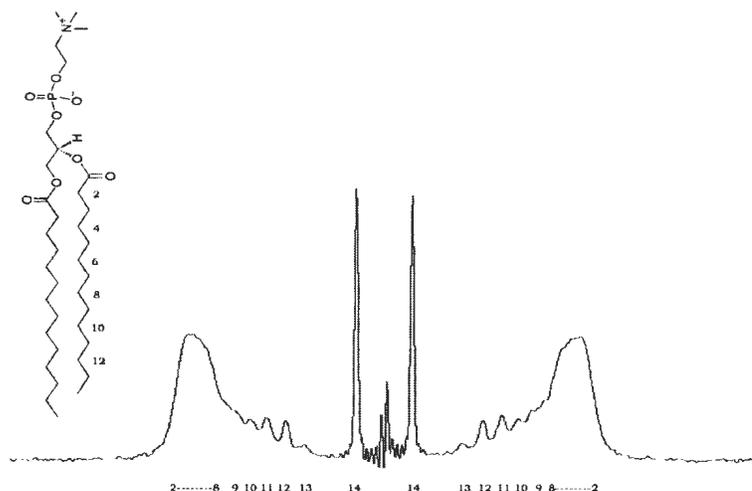
Figure 2.3: Deuterium NMR spectrum of predeuterated DMPC-d_{54} in DMPC-d_{54}/DMPG/DHPC(3:1:1) at 34 °C in the oriented phase.

The smallest quadrupole splitting comes from methyl (CD$_3$) groups at the end of each chain. The motions of methyl groups are the least constrained. Therefore, they result in the smallest quadrupole splitting. The greatest quadrupole splitting corresponds to the methylene (CD$_2$) groups near the headgroup. Motions are the most constrained for these methylene groups. Quadrupole splitting decreases from the C-D bonds near

the headgroup to the methyl groups located furthest from the headgroup.

2.2 Spectra for bicellar dispersion phases

2.2.1 Isotropic reorientation

At temperatures lower than the main transition temperature (T_m) of the longer chain lipid component in the bicellar mixture, bilayered disk micelles reorient isotropically when viewed over the ^{2}H NMR timescale. This averages the quadrupole interactions for all chain deuterons to zero. For this reason, the spectrum for a typical bicellar mixture dispersion in this range of temperature has a high intensity at ν_o and approximately zero intensity everywhere else. An example of the spectrum corresponding to isotropically reorienting bicelle disks is shown in Figure 2.4.
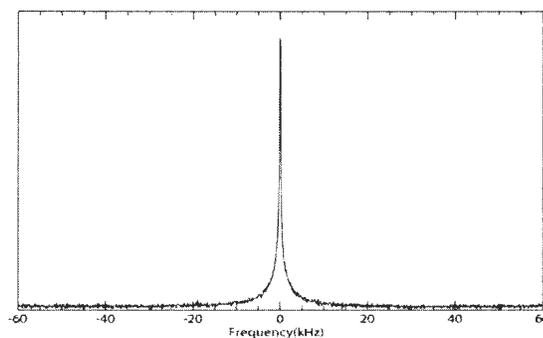
Figure 2.4: Lipids with isotropically reorientation for DMPC-d_{54}/DMPG/DHPC(3:1:1) at 18 °C.
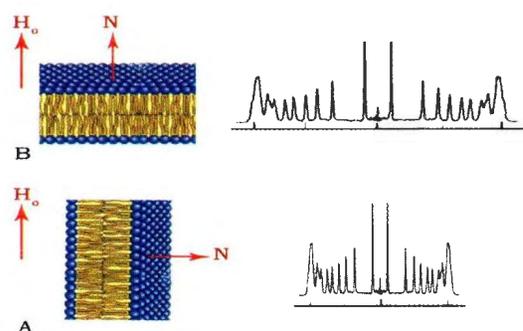
Figure 2.5: ^{2}H NMR spectra for bilayers with normal directions oriented (a) perpendicular to the magnetic field and (b) parallel to the magnetic field.

2.2.2 Oriented bilayers

Bilayered micelles at intermediate temperature can orient in a magnetic field. Thus, there is one single value for β which results in a superposition of sharp doublets, rather than Pake doublets (or powder patterns), corresponding to the deuterons contributing to the deuterium NMR spectrum. The corresponding spectrum, obtained when bilayer normal is perpendicular to the magnetic field, is shown in Figure 2.5.a whereas the one for bilayer normal alignment parallel to the applied magnetic field is shown in Figure 2.5.b. Such a difference in the angle between bilayer normal and magnetic field changes β by 90° whereas the range over which θ_n varies for each CD bond remains the same. The splitting of the doublet for the perpendicular orientation is scaled by a factor of $-\frac{1}{2}$ while this factor is 1 for the parallel alignment. An example of a deuterium NMR spectrum for DMPC-d_{54}/DMPG/DHPC(3:1:1) in oriented phase is shown in Figure 2.6.

2.2.3 High temperature bicellar dispersion phase

In the high temperature bicellar phase, the observed spectra resemble those for multilamellar vesicles with bilayer normals directed in every direction with equal probability.
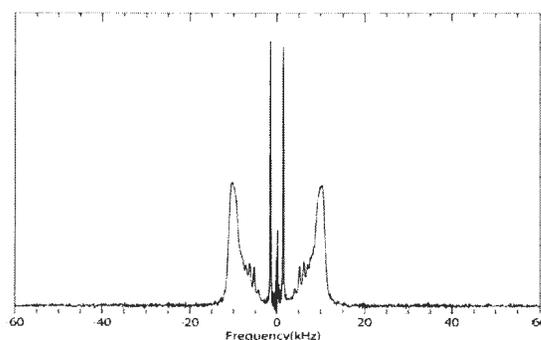
Figure 2.6: ^{2}H NMR spectrum of DMPC-d_{54}/DMPG/DHPC(3:1:1) in the oriented phase at $34\,^\circ$C with $\beta = 90\,^\circ$.

β can take all values in the range of 0 and $180\,^\circ$. The weighting of contributions from different orientations is proportional to the fraction of a spherical surface corresponding to that orientation. Thus, the intensity of each contribution to a spectrum is a function of the value of β corresponding to that contribution. A schematic representation of such a spectrum is shown in Figure 2.7.
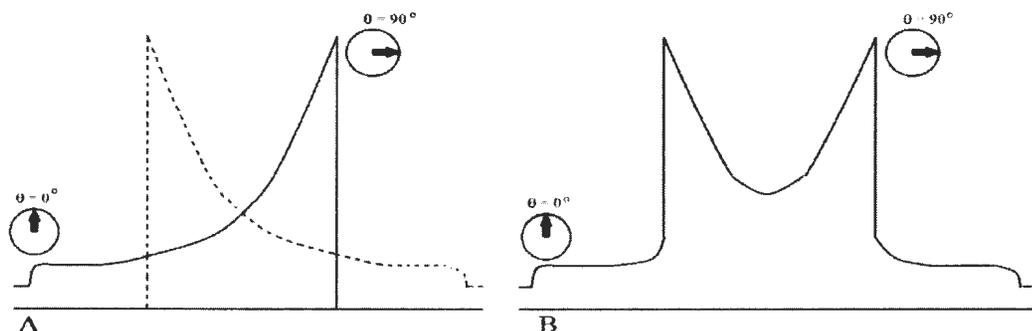
Figure 2.7: **A)** Separation of the deuterium powder spectrum (solid and dashed lines) corresponding to the two deuteron transitions.**B)** Schematic spectrum of lipids in lamellar vesicle phase.

This spectrum is a superposition of quadrupole doublets with different values corresponding to different values of β with different weights. This shape is called a

Pake-doublet. It is symmetric about the Larmor frequency. The highest doublet intensity indicates the regions of the spherical vesicle whose bilayer normals are perpendicular to the magnetic field. The lowest intensity represents the region of the spherical vesicle with the bilayer normals parallel to the applied magnetic field. The doublet splitting for regions with $\beta = 90\,^{\circ}$ is half of that for the regions with $\beta = 0\,^{\circ}$ as shown in Eq.2.15.

The weights for these two regions are also not equal. The abundance of lipids with $\beta = 90\,^{\circ}$ is maximum in spherical vesicles. The number of lipids with $\beta = 0\,^{\circ}$ (contributing to intensity in spectral region is shown by the arrows in figure 2.8) is minimum. In this thesis, the quadrupole splitting is defined as the doublet splitting corresponding to regions with $\beta = 90\,^{\circ}$. Figure 2.8. shows an actual spectrum for DMPC-d_{54}/DMPG/DHPC (3:1:1) at 40 $^{\circ}$C which corresponds to the lamellar vesicle phase. This spectrum is a superposition of doublets which are corresponding to different values of β.
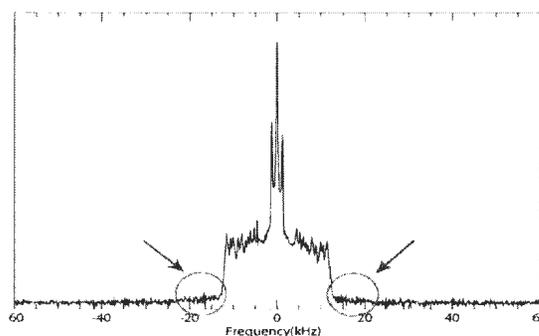
Figure 2.8: A ^{2}H NMR spectrum collected from DMPC-d_{54}/DMPG/DHPC (3:1:1) at 40 $^{\circ}$C which corresponds to the MLV phase for this sample. The red arrows show the spectral segments which represent lipids with $\beta = 0\,^{\circ}$.

2.2.4 Interdigitated gel phase

At high pressure, some samples displayed spectral characteristics of lipid chains in a highly ordered phase [17]. This was interpreted as an interdigitated gel phase based on comparison with previously observed spectra of DPPC-d_{62} and DPPG-d_{62} in the interdigitated gel phase [17]. In this phase the C-D bonds are more constrained. A spectrum for lipids in this phase is shown in Figure 2.9. The doublet splitting is double the oriented phase spectrum for the same sample.
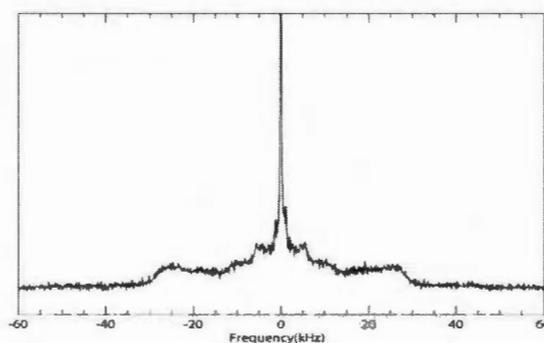
Figure 2.9: A ^{2}H NMR spectrum collected from DMPC-d_{54}/DMPG/DHPC (3:1:1) at 48 °C and applied pressure of 85 MPa. The sample is in the interdigitated phase.

Note that the doublet splitting corresponding to methyl (CD$_3$) groups is also two times bigger than the methyl doublet splitting for the same sample in a non-interdigitated phase. Overlap of chains, which are more ordered in the interdigitated phase, from opposite sides of the bilayer packs the lipids. This reduces the available area per lipid acyl chain that in a way increases the order parameter. Therefore, the quadrupole splitting will be approximately doubled according to Eq. 2.16 or Eq. 2.17.

2.3   Quadrupole echo decay

An RF pulse is employed, in a pulse NMR experiment, to excite nuclear spins in the sample. For deuterium NMR, the RF pulse must contain energy over a broad spectral range. For this reason, this RF pulse must be a short, high power pulse. For the purpose of protecting the spectrometer, which is designed to detect weak signals, the spectrometer switches from its "protected" state to "collecting" state using diodes. This, along with oscillations in the react of components in the preamplifier (ringing), takes longer than the free induction decay time. Therefore, to obtain a broad spectrum, an echo experiment using two pulses is required so that signal acquisition can be delayed until after the spectrometer receiver has recovered from the pulse effects [71]. The first pulse is a $\frac{\pi}{2}$ pulse. After a delay time of τ, a second $\frac{\pi}{2}$ pulse, shifted by $90°$ in phase, is applied. After the second pulse, the spins which precess faster than average are behind the net magnetization but converging with the net magnetization. The spins that precess slower than average are ahead of the net magnetization. These two spin populations refocus to form an echo at a time 2τ after the initial pulse. This process allows the spectrometer to recover to the collecting state and collect a signal that, except for relaxation effects, is the same as the signal after the first pulse. For spin 1 nuclei, a sequence of $\frac{\pi}{2}$ pulses is used to obtain echo whereas π pulse sequence is used for spin 1/2 nuclei. Further information about this process and using $\frac{\pi}{2}$ pulse sequence for spin 1 nuclei can be found here [67]. A schematic representation of quadrupole echo decay pulse sequence is shown in Figure 2.10.

The amplitude of the echo can be expressed as [71]

$$S(2\tau) = A = A_o \exp(\frac{-2\tau}{T_2^{qe}}) \tag{2.18}$$
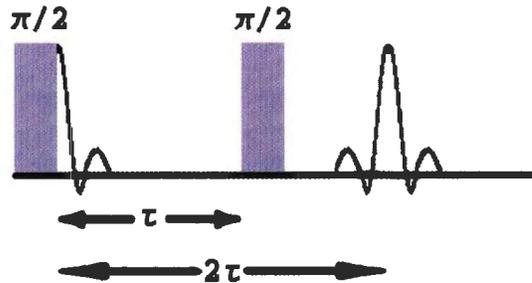
Figure 2.10: Schematic representation of quadrupole echo decay pulse sequence introduced by James Davis and co-workers [71]

where T_2^{qe} is the echo decay time. Eq. 2.19 can be rewritten as

$$\ln(\frac{A}{A_o}) = \frac{-2\tau}{T_2^{qe}} \tag{2.19}$$

Therefore, $\frac{1}{T_2^{qe}}$ is the slope of the plot of $\log(\frac{A}{A_o})$ versus 2τ. T_2^{qe} yields useful information about the motions that cause the quadrupole signal to decay in different phases. The echo decay rate, R, depends on the second moment ($\triangle M_2$). This second moment correspond to a portion of the quadrupole Hamiltonian which is resulted by a given motion with a specific correlation time (τ_c). Slow motions can be characterized as having correlation times that satisfies the condition [72, 73]

$$\tau_c \gg \frac{1}{\sqrt{\triangle M_2}} \tag{2.20}$$

and contributions to the echo decay rate,

$$R \times \frac{1}{\tau_c}. \tag{2.21}$$

For fast motions,

$$\tau_c \ll \frac{1}{\sqrt{\triangle M_2}} \tag{2.22}$$

and

$$R \propto \tau_c. \tag{2.23}$$

The echo decay times pass through a minimum during a phase transition from a phase with echo decay dominated by fast motions to a phase with echo decay dominated by slow motions. Through this minimum, the echo decay time is dominated by the motions with correlation times that are closest to the timescale of the experiment.

In the liquid crystalline phase of multilamellar vesicle dispersions, echo decay is influenced by both slow long-range motions and fast short-range motions. This gives a plateau region with long decay times [74]. Motions are slower for a lipid assembly in the gel phase which occurs at low temperatures. These slow motions have longer correlation times and the echo decay time increases as the correlation times increase with decreasing temperature of bicellar mixtures. Thus, T_2^{qc} reaches a minimum at the transition where the dominant motions are at an intermediate timescale. In other words, T_2^{qc} reaches a minimum because fast motions related to the liquid crystal phase approach the timescale of the experiment while passing through this transition.

Chapter 3

Materials and method

3.1 Sample preparation

Chain perdeuterated DMPC and DMPG along with non-deuterated DMPC, DMPG, and DHPC were purchased from Avanti Polar Lipids (Pelham, AL). These lipids were used without any further purification. The molecular weight and molecular formula of used lipids are shown in Table 1. A solution of 10 mM HEPES with pH=7.0 was used as the buffer solution. This solution was prepared by Donna Jackman (Department of Biochemistry, Memorial University of Newfoundland).

lipid	Molecular formula	Molecular weight
DMPC	$C_{36}H_{72}NO_8P$	677.933
DMPC-d_{54}	$C_{36}H_{18}NO_8PD_{54}$	732.265
DMPG	$C_{34}H_{66}O_{10}PNa$	688.845
DMPG-d_{54}	$C_{34}H_{12}O_{10}PNaD_{54}$	743.178
DHPC	$C_{20}H_{40}NO_8P$	453.507

Table 3.1: Lipids molecular formulas and their molecular weights. These information have been obtained from Avanti Lipids website.

3.1.1 Preparation of bicellar mixtures

Dry, powder, chain perdeuterated 1,2-dimyristoyl-*sn*-glycero-3-phosphocholine-d_{54} (DMPC-d_{54}) and non-deuterated dry 1,2-dihexanoyl-*sn*-glycero-3-phosphocholine (DHPC) were combined for the purpose of making the bicellar mixture. DMPC-d_{54}, with 14 carbons in its chain, was utilized as the long chain lipid. DHPC with 6 carbons in its chain was used as the short chain lipid component. They were combined with the molar ratio of (4:1) at lipid weight fractions of ~0.1 g of lipid per ml of water. Details of the samples preparation follow.

To prepare DMPC-d_{54}/DHPC (4:1), 20 mg of chain perdeuterated DMPC and 3.1 mg of DHPC were weighed into different culture tubes. Each lipid was dissolved in adequate chloroform/methanol (2:1) (v:v) solution (few milliliters) to completely dissolve all of the lipids. The dissolved lipid solutions were combined in a round bottom flask. The solvent was removed by rotary evaporation at 40 °C. The sample was then held under vacuum in a desiccation chamber for about five hours. This sample was then hydrated by using 250 μL of 100 mM HEPES buffer (pH=7). The hydrated mixture was then sonicated in a sonicating bath at room temperature for 15 minutes. The sample, still in the round bottom flask, was frozen and was thawed for 5 cycles by placing it in liquid nitrogen and 40 °C water bath respectively.

A deformable polyethylene container was made by heat-sealing the ends of a short segment cut from a disposable polyethylene pipette. Finally, about 200 μL of sample was transferred to the polyethylene container which was then sealed with a Clamco heat sealer. Samples were placed in a freezer at about −18 °C overnight. The samples were placed in the probe when they were below room temperature.

Samples of DMPC-d_{54}/DMPG/DHPC (3:1:1) were prepared by following the same protocols but with 25 % of the DMPC-d_{54} replaced by the anionic lipid DMPG. Samples of DMPC/DMPG-d_{54}/DHPC (3:1:1) were also prepared in the same way.

For comparison, one sample of DMPC-d_{54}/DMPG/DHPC (3:1:1) was also prepared with the sonication and freeze-thaw steps omitted.

3.2 NMR spectrometers

In this work, wideline deuterium NMR observations were performed using locally-built spectrometers with either a 3.5 T or a 9.4 T superconducting magnet.

3.2.1 3.5 T variable-pressure deuterium NMR spectrometer

For the purpose of variable-pressure NMR spectroscopy, which was the main part of this work, the locally-constructed solid state spectrometer was used [76] in conjunction with a 3.5 T superconducting solenoid (Nalorac Cryogenics, Ca) corresponding to a deuterium resonance frequency of 23.2 MHz. The spectrometer consisted of a computer for data acquisition, storage, and initial pulse sequence programming, a 1 kW radio transmitter, and a quadrature detection section with a 12 bit digitizing oscilloscope. The sample capsule and the cylindrical coil were inserted into a high pressure beryllium-copper cell which may be pressurized with hydraulic oil (AW ISO grade32). For this purpose, the NMR probe was connected to a manual oil pump. The schematic picture of the variable pressure probe [54] is shown in Fig. 3.1. Two gauges which were calibrated against a dead-weight gauge were employed to measure pressure. A

microprocessor-based proportional-integral-diffrencial controller (PID controller) in conjunction with a thermocouple sensor embedded around the pressure cell was used to control the temperature with an accuracy of $0.1\,°C$. Samples were held at each temperature for at least 20 minutes to equilibrate before the start of data acquisition.

Spectra were obtained by applying a quadrupole echo pulse sequence [71] with a $\frac{\pi}{2}$ pulse length of 3.5 μs. The pulse separation was 35 μs. Each spectrum was obtained by averaging 2,000 to 40,000 transients prior to Fourier transformation. Quadrature detection with repetition time of 0.8 s was employed for this purpose. Oversampling [75] was used to obtain effective dwell times of 4 μs in the free induction decays. Echo amplitudes were measured with typical pulse separations of 35, 50, 75, 100, 150, 200 μs for echo decay measurements.

3.2.2   9.4 T deuterium NMR spectrometer

For comparison, one sample was studied using a 9.4 T superconducting magnet in which the ^{2}H Larmor frequency is 61.4 MHz. This setup also uses a locally assembled spectrometer. Spectra were acquired using a quadrupole echo sequence [71] with $\frac{\pi}{2}$ pulses of length from 4.25 to 4.5 μs. The separation time (τ) between $\frac{\pi}{2}$ pulses in the quadrupole echo sequence was 35 μs, and 2000 to 4000 transients were averaged for each free induction decay. For quadrupole echo decay measurements, 400 to 1000 transients were averaged. The repetition time for acquisition was 0.9 s. Oversampling [75] was used to obtain effective dwell times of 4 μs in the free induction decays. Echo amplitudes were measured with typical pulse separations of 35, 75, 100, 150, 200, 300 and 400 μs for echo decay measurements.

3.2.3 High pressure probe

A locally built high-pressure probe was used to apply pressure [53]. This probe is designed to sustain pressures up to 270 MPa and temperatures between $-30\,°C$ and $70\,°C$ [53]. A schematic representation of this probe is shown in Figure 3.1. This schematic diagram is adapted from an article by Bonev and Morrow and more detail can be found there [53].

Schematic drawing of the high pressure deuterium NMR probe.
1) High pressure chamber
2) sample/coil module
3) thin walled stainless steel support tubes
4) suspension plate
5) brass suspension rods
6) top plate
7) top plate bolts
8) threaded brass anchor ring
9) outer aluminum tube
10) upper positioning ring
11) positioning studs
12) lower positioning ring
13) magnet and dewar
14) rf connecting wire
15) rf feed through
16) coupling capacitor
17) tuning capacitor
18) and 19) top and bottom insulating capacitor support plates
20) capacitor adjustment rods
21) styrofoam insulation
A) Stainless steel pressurizing tube
B) and C) cooling gas outlet and inlet tubes.

Figure 3.1: A schematic representation of the variable pressure NMR probe. Reprinted with permission from [53]. ©1997, American Institute of Physics.

The interior of the probe is separated from the magnet wall by an aluminium tube. Supports (5-12) can be adjusted to allow the sample to be located in the region with the highest magnetic field. The high pressure chamber (1) is suspended on three thin

walled stainless steel tubes (3). These tubes provide thermal insulation between the pressure chamber and the support. A schematic drawing of the high pressure chamber is shown in Figure 3.2.

High pressure chamber.

1) The beryllium–copper chamber body
2) rf feed through
3) rf connecting pin
4) rf connecting wire
5) PTFE antiarcing insulator cap
6) sample capsule
7) cooling gas channels
8) heater wire
9) beryllium–copper plug
10) quenched copper gaskets
11) PTFE gasket washer
12) beryllium–copper spacer
13) beryllium–copper support nut
14) washer
15) nut
A) Thin walled stainless steel support tubes
B) and C) coolant outlet and inlet tubes
D) heater connecting wire
E) thermocouple connecting wire.

Figure 3.2: A schematic representation of the high-pressure chamber. Reprinted with permission from [53]. ©1997, American Institute of Physics.

All the components of this probe are attached to the top plate (6) in Figure 3.1 except the external aluminium tube and the Styrofoam insulation (21). The brass rods (5) are used for this purpose. The sample is placed in a coil mounted in a removal teflon plug. This coil assembly is shown in Figure 3.3.
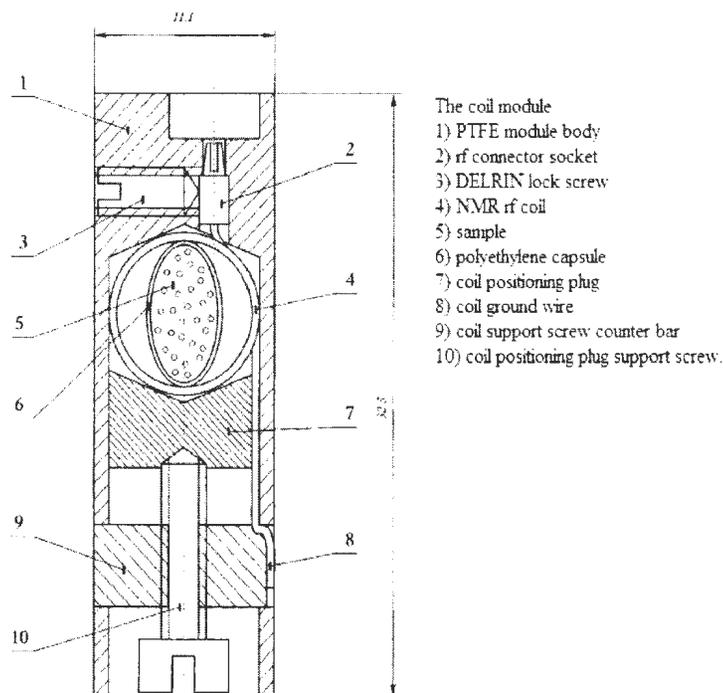
Figure 3.3: A schematic representation of the removable coil assembly. Reprinted with permission from [53]. ©1997, American Institute of Physics.

3.3 Experimental details

Every sample was stored in a freezer at $-18\,°C$ for between 8 and 48 hours prior to being placed in the NMR probe. The temperature of sample and probe were decreased to $8\,°C$ by air circulating through a liquid nitrogen heat exchanger. The samples were held at $8\,°C$ for at least one hour to equilibrate in the isotropic bicellar phase. Spectra were obtained over a series of temperatures between $4\,°C$ and $65\,°C$. After ambient pressure runs, samples were recooled to $8\,°C$ before increasing the pressure. Data were obtained at ambient pressure, 41.4 MPa and 82.7 MPa . Depending on the type of data required, temperature was raised in steps of 2 to $10\,°C$.

3.4   Probe adjustment

Over the course of the experiments, it was necessary to perform some repairs on the high pressure probe. At one point it was found that the range of adjustment on the probe capacitors was insufficient to achieve the required 50 Ω probe input impedance. It was found that both the tuning capacitor (17) and coupling capacitor (16) were moving non-axially. The coaxial teflon walled pistons, which are designed to work as the dielectric, had loosened over time. Teflon tape was used to fix these pistons to the insulating capacitor support plate (19). The teflon tubes surround brass cylinders which are connected to nylon rods (20) by a long screw made of brass. The capacitor brass cylinders were originally made with holes to hold small spacers. These holes were filled with soldered brass plugs which were filed to make a smooth, uniform surface. The rods were also found to be bent. This could cause a non-axial motion and consequently the tuning issue. These rods were straightened. To open the rods and capacitors, all of the insulation around the cooling gas outlet and inlet tubes was unwrapped. This insulation was replaced by new thermal insulating foam layers. The probe was found to tune more easily after these repairs.

Prior to acquisition of transients, spectrometer frequency and other parameters were carefully adjusted to maximize the signal-to-noise ratio.

Chapter 4

Results and Discussion

Variable pressure ^{2}H NMR experiments were performed on DMPC-d_{54}/DHPC (4:1), DMPC-d_{54}/DMPG/DHPC (3:1:1) and DMPC/DMPG-d_{54}/DHPC (3:1:1) lipid mixture dispersions in order to study the effects of pressure on lipid chain order and bilayer orientation in bicellar mixtures containing anionic lipids. Mixtures were prepared as described in Chapter 3. These molar ratios were chosen in order to match those used in previously reported observations of bicellar mixtures at either ambient pressure [23] or high pressure [63].

Spectra were acquired over different ranges of temperature depending on the applied hydrostatic pressure which was held constant as detailed below. These samples were studied at ambient pressure, 41.4 MPa and 82.7 MPa. In this thesis, 41.4 MPa is referred to as intermediate pressure and 82.7 MPa is referred to as high pressure. The upper limit pressure of 82.7 MPa was chosen because it is higher than the lowest pressure at which lipid mixtures containing one single anionic lipid species (DPPG) display interdigitation [17] and lower than the pressure at which interdigitation occurs for DPPC. After evidence of an interdigitated phase was first observed at 82.7 MPa,

subsequent anionic bicellar mixtures were studied at the intermediate pressure to determine if interdigitation occurs at lower pressure for the anionic bicellar mixtures. For some samples, the procedure for increasing the pressure from ambient or intermediate pressure to high pressure was to cycle the pressure to 110 MPa a few times before setting the sample pressure to 82.7 MPa. The details of the pressurization procedure will be explained for each sample while discussing the result for that particular sample.

Data acquisitions started from a temperature lower than the main transition temperature for DMPC and DMPG which is $\sim 23\,°C$. If a specific initial temperature is not mentioned, the initial temperature for that experiment is $8\,°C$. This procedure ensured that every temperature series started with the sample in the same state (i.e. isotropically reorienting bicelles). As detailed below, additional steps were taken to match thermal histories for some samples studied at different pressures. The temperature ranges at which data were acquired were chosen such that transitions from isotropic to nematic and from nematic to lamellar phase were observed, if present, for each pressure.

4.1 Zwitterionic bicellar mixtures (DMPC-d_{54}/ DHPC)

4.1.1 DMPC-d_{54}/DHPC(4:1) at ambient pressure

In order to establish a basis for comparison, experiments were also performed on bicellar mixtures containing no anionic lipid. Spectra were collected over a range of temperature at ambient pressure for a DMPC-d_{54}/DHPC (4:1) mixture by us-

ing both the 9.4 T and 3.5 T magnets. Spectra at selected temperatures are shown in Figure 4.1. The complete set of spectra can be found in appendix A as Figure A.1. One mixture, denoted as AR01, was cooled to 12 °C and equilibrated at this temperature for one hour. At 12 °C, the spectrum displays a narrow peak which is characteristic of isotropic reorientation on the quadrupole echo experiment time scale ($\sim 10^{-5}$). Small angle neutron scattering and pulsed field gradient NMR studies [46], and time-resolved synchrotron X-ray diffraction studies [45] suggest that the isotropically reorienting particles are disks with DMPC headgroups on the planar surfaces and DHPC molecules on highly curved edges.

The main gel to liquid crystal phase transition for DMPC is ~ 23 °C. Full chain deuteration is known to lower this temperature by a few degrees [60]. Based on the picture that has been suggested in some studies, upon increasing temperature of DMPC-d_{54}/DHPC (4:1) mixture, the small isotropically reorienting disks might fuse and form nematic ribbon-like or worm-like micelles, presumably with short chain lipids at the edges and long chain lipids on the planar surfaces [35, 37]. At 15 °C, in the series of spectra collected at 3.5 T, most of the sample is still undergoing isotropic reorientation but a small fraction gives rise to a broader spectrum which indicates partial orientational order and thus incomplete averaging of the quadrupole interaction. At 22 °C, the spectra for DMPC-d_{54}/DHPC (4:1) obtained in both magnets indicate orientational ordering of molecules with respect to the bilayer normal. The spectra at 22 °C, particularly at 9.4 T, though, do not display the sharp edge features characteristic of the Pake doublet spectra seen for axially symmetric molecular reorientation about the bilayer normal. The rounding of shoulders in these spectra indicates that molecular reorientation is not axially symmetric on the ^{2}H NMR timescale ($\sim 10^{-5}$s).
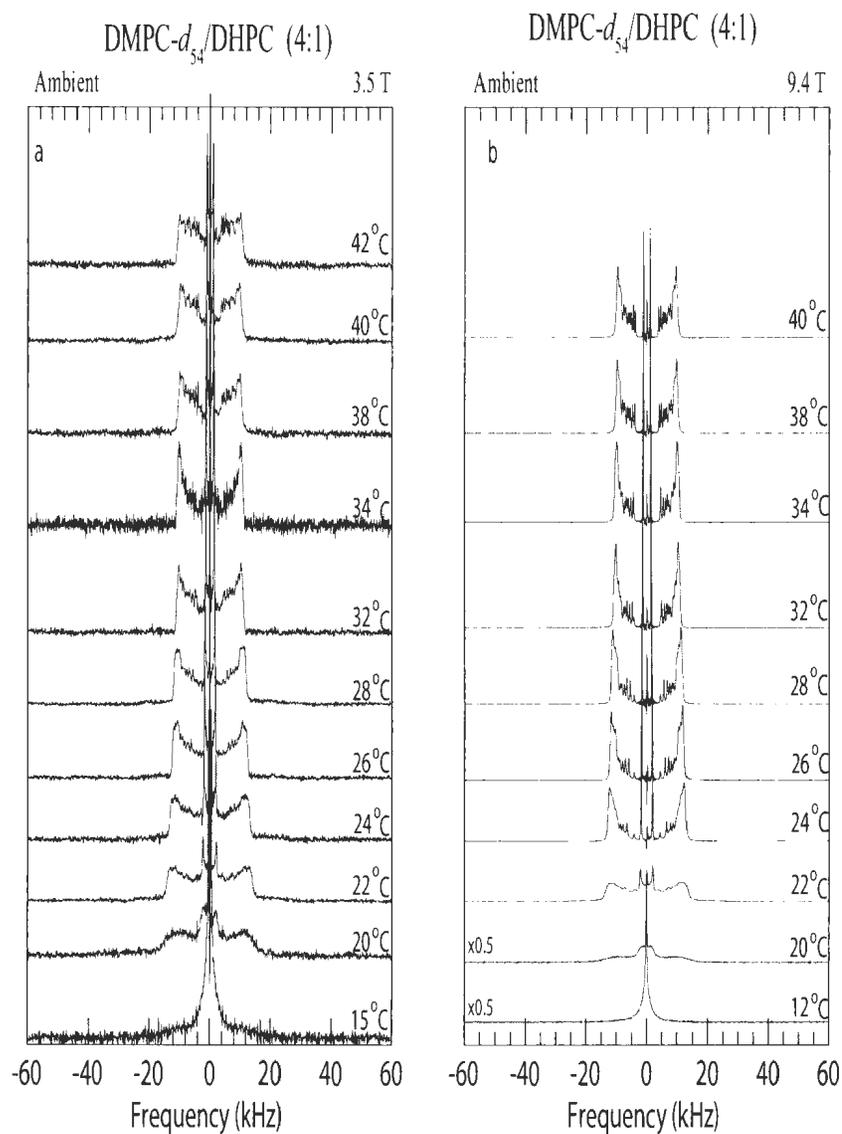
Figure 4.1: Deuterium NMR spectra for DMPC-d_{54}/DHPC (4:1) obtained with (a) the 3.5 T superconductive magnet and (b) the 9.4 T magnet at ambient pressure for a range of temperatures. The sample is denoted as AR01. The noisy baseline for the spectrum at 34 °C comes from a technical issue related to ampifier which resulted a lower number of effective scans.

At 24 °C, the spectrum in Figure 4.1b, which was collected in the 9.4 T magnet, shows characteristics of bilayer orientation, particularly the approximately zero intensity in the centre of the spectrum as well as sharp splitting. However, the spectrum collected in the 3.5 T magnet at 24 °C, as shown in Figure 4.1a, is more characteristic of lipids undergoing axially symmetric reorientation about a randomly oriented distribution of bilayer normal directions.

As can be seen from Figure 4.1b, the ambient pressure spectra of DMPC-d_{54}/DHPC (4:1) obtained in the 9.4 T magnet show characteristics of bilayer orientation from 26 °C to 40 °C. Within this range of temperature, the spectra shown in Figure 4.1b display characteristics of complete bilayer orientation with respect to the applied magnetic field. The bilayer normals are perpendicular to magnetic field in this phase and the sharp doublets corresponding to $\beta = 90°$ are characteristic of axially symmetric chain reorientation about the bilayer normal. As shown in Figure 4.1a, though, the ambient pressure spectrum of DMPC-d_{54}/DHPC (4:1) collected in the 3.5 T magnet at 34 °C shows bilayer normal orientation but the other spectra between 28 °C and 40 °C are more characteristic of partial, but not complete, bilayer orientation. This lack of complete orientation at 3.5 T is consistent with an earlier variable pressure deuterium NMR study of DMPC-d_{54}/DHPC (4:1) done at 3.5 T [63]. It was suggested in that work that the incomplete orientation observed was a result of the low magnetic field or an orientational metastability in the highly viscous worm-like micelle phase [63]. By comparing the spectra collected in this work using the 3.5 T and the 9.4 T magnets, it can be concluded that the lack of complete orientation at 3.5 T is due to the weak magnetic field.

On increasing temperature, the sample at 3.5 T begins to form vesicles around 42 °C

as can be seen, in Figure 4.1a, from the change of the observed spectrum from a superposition of sharp doublets to a superposition of Pake or powder pattern doublets. Examples of these two spectra are shown in Figure 2.6 and Figure 2.8. The doublet splitting also decreases slightly with increasing temperature, as seen in Figure 4.1a. At temperatures higher than 42 °C, the bilayers are likely closed into vesicles with DHPC molecules forming the edges of pores distributed over the vesicle surfaces. It has been reported that DHPC molecules begin to interact with DMPC molecules at about 30 °C and continue to mix more completely with increasing temperature [63, 81].

4.1.2   DMPC-d_{54}/DHPC(4:1) at 82.7 MPa

For the purpose of comparing with observations on bicellar mixtures containing anionic lipids, the same mixture of DMPC-d_{54}/DHPC(4:1) was also studied at 82.7 MPa. After obtaining data during the first cycle of heating, this mixture was cooled at ambient pressure. The process of decreasing temperature took few hours. This sample was then pressurized to 82.7 MPa while in the low temperature, isotropically reorienting disk-like phase. A set of selected spectra for DMPC-d_{54}/DHPC at ambient pressure and at 82.7 MPa is shown in Figure 4.2.

On warming at ambient pressure, DMPC-d_{54}/DHPC follows the expected pattern [35, 37] of an isotropic phase, consisting of disks with fast isotropical thermal reorientation, a magnetically alignable (nematic) worm-like micelle phase and multilamellar bilayer vesicles. At high pressure its phase transitions are shifted. However, it still shows the characteristic of isotropic reorientation at temperatures below the main transition temperature of DMPC.
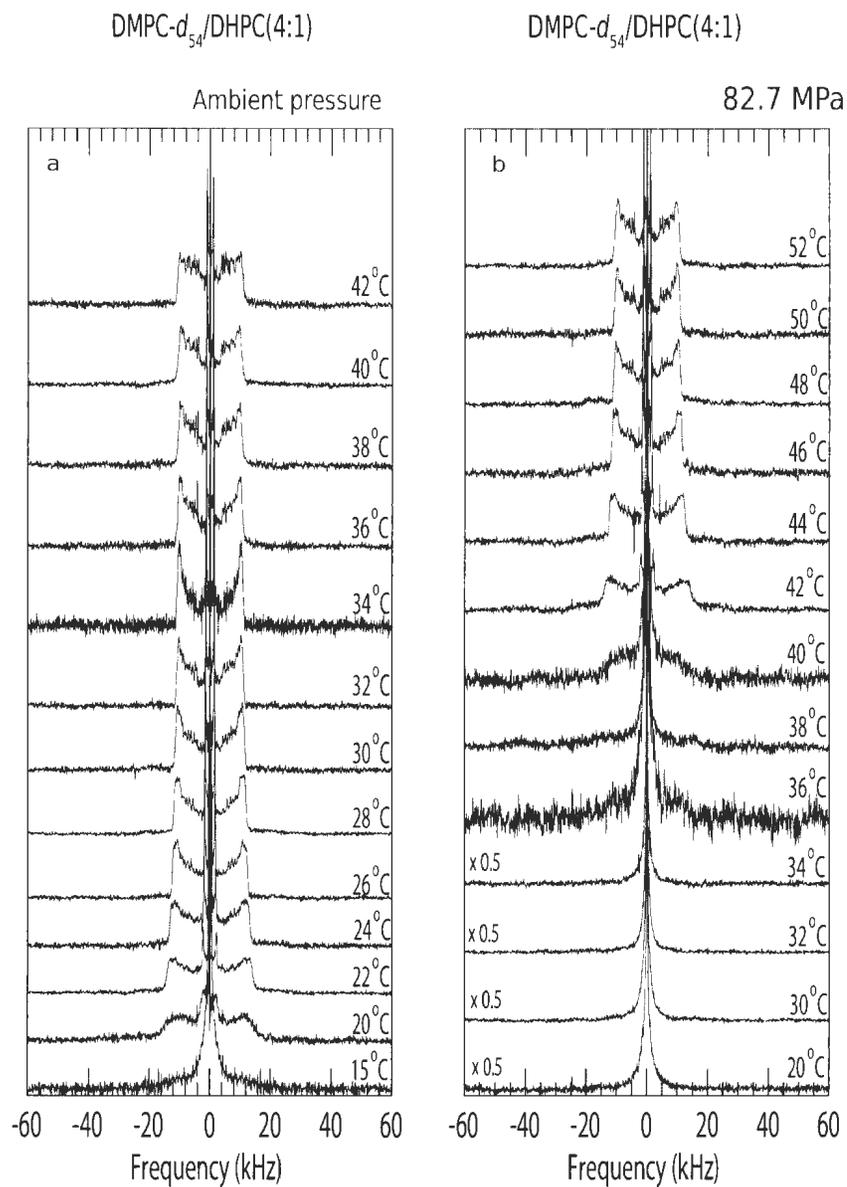
Figure 4.2: Deuterium NMR selected spectra at 3.5 T for DMPC-d_{54}/DHPC at (a) ambient pressure and (b) at 82.7 MPa for a range of temperatures. Spectra were collected from low to high temperature.

The transition from disks with isotropical reorientation to worm-like or ribbon-like micelles increases by $\sim 17\,^\circ$C at 82.7 MPa relative to ambient pressure. The pressure sensitivity of the isotropic-nematic transition temperature is thus $\frac{dT}{dP} \simeq 0.21\,^\circ$C/MPa. This value is in agreement with previous results from ^{2}H NMR studies for DMPC-d_{54}/DHPC mixtures [63] and is comparable to the value that can be inferred from the pressure-temperature phase diagram obtained by using small angle X-ray scattering (SAXS) which is $0.19\,^\circ$C/MPa [45].

Figure 4.2b shows spectra for DMPC-d_{54}/DHPC (4:1) at 82.7 MPa in the 3.5 T magnet. Based on the lower intensity of sharp double edges observed in the oriented phase spectrum observed for this sample at 82.7 MPa, it appears that applying hydrostatic pressure decrease the proportion of DMPC-d_{54} molecules that align with respect to the magnetic field. Although this makes it difficult to determine the precise temperature at which the 82.7 MPa spectra are most characteristic of bilayer orientation. This appears to be about $46\,^\circ$C based on the sharpness of the spectrum edges as can be seen in Figure 4.2b.

As will be discussed below, the formation of an interdigitated gel phase, identified by the larger quadrupole splittings resulting from the high degree of chain order in that phase, was observed on cooling some DMPC-d_{54}/DMPG/DHPC (3:1:1) samples from high temperature at 82.7 MPa. In some cases, formation of the interdigitated gel phase was seen only on cooling the DMPG-containing bicellar mixture for a second time. In order to determine whether the same behavior could be seen in the absence of DMPG, a second series of experiments were performed on the DMPC-d_{54}/DHPC (4:1) sample. In this set of experiments, spectra were collected through warming and cooling cycles at both ambient pressure and at 82.7 MPa. For this series of experi-

ments, the DMPC-d_{54}/DHPC (4:1) sample was designated as ARM1 for the ambient pressure observations and ARMB1 for the observations at 82.7 MPa. The ambient pressure spectra for this experiment are shown in the Appendix (Figures A.3 and A.4). ^{2}H NMR spectra obtained from this sample during the warming and cooling cycle at 82.7 MPa are in Figure 4.3.

Because this experiment was primarily intended to test for the formation of the highly ordered gel phase under specific conditions, spectra were collected at selected temperatures only. While no evidence of interdigitation, which would be characterized by specific spectral features as discussed in Chapter 2, was observed in this experiment, additional experiments would be needed before the possibility of interdigitation at 82.7 MPa in DMPC-d_{54}/DHPC (4:1) could be conclusively ruled out.
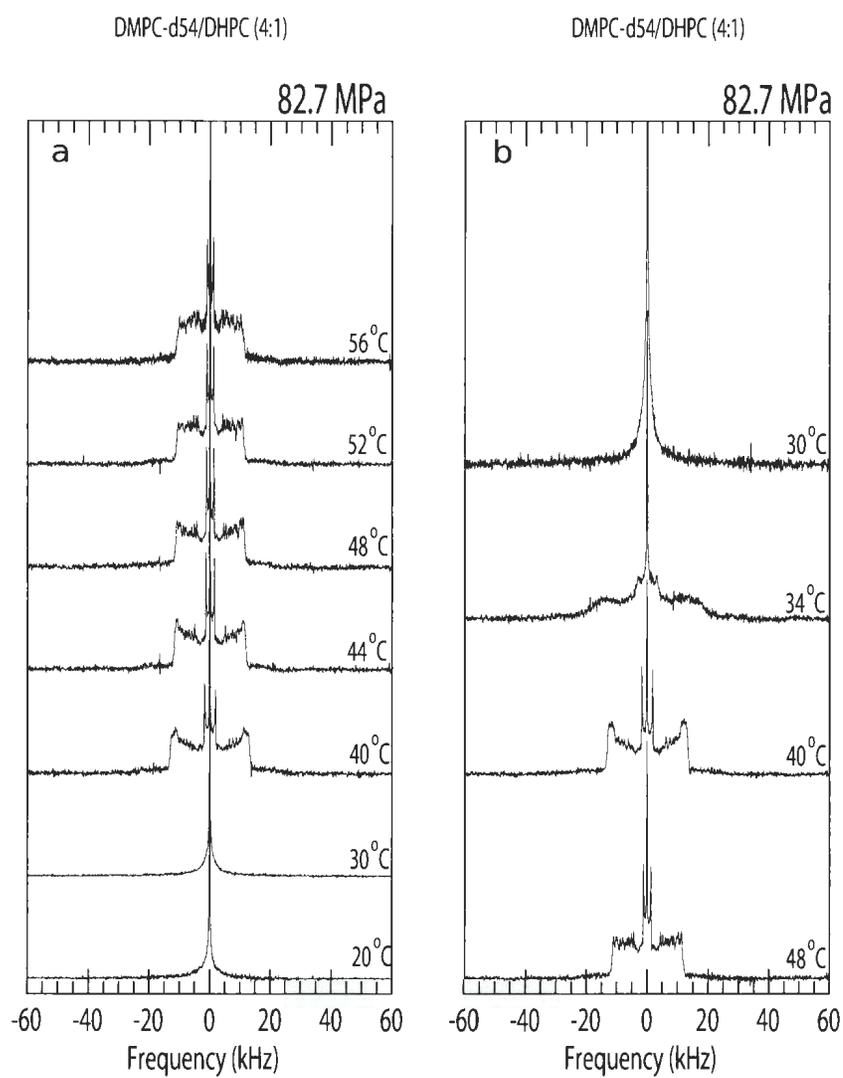
Figure 4.3: Deuterium NMR selected spectra for DMPC-d_{54}/DHPC collected during the second cycle of (a) warming and (b) cooling for a range of temperatures at 82.7 MPa. This sample was labeled ARMB1.

4.2 Anionic bicellar mixture with chain perdeuterated DMPC

In order to study the influence of anionic lipids on the phase behavior and morphologies of bicellar mixtures at ambient pressure and their response to hydrostatic pressure, variable pressure ^{2}H NMR experiments were performed on bicellar mixtures containing anionic lipid components by using the 3.5 T magnet. The molar ratio of long chain lipids to short chain lipid was kept constant at about 4, but 25% of the DMPC-d_{54} was substituted with DMPG. DMPC-d_{54}/DMPG/DHPC(3:1:1) mixtures were prepared as described in chapter 3.

Multiple samples of DMPC-d_{54}/DMPG/DHPC (3:1:1) were prepared. While each sample was prepared following the same protocol as closely as possible, minor differences in the sample preparation process can influence phase behavior of bicellar mixtures. For the initial DMPC-d_{54}/DMPG/DHPC(3:1:1) samples prepared, the approach was to collect data, sequentially, at ambient pressure, 41.4 MPa, and then at 82.7 MPa. In some cases, pressure was changed at high temperature prior to equilibration at low temperature and in some cases the sample was cooled back to 8 °C prior to the pressure being changed. Spectra obtained from these samples are shown in the appendix and referred to, as needed, in the text.

To eliminate the effect of minor differences in preparation process, another sample was prepared which was four times larger in quantity than the previous samples and portions of it were used for experiments at different pressures. This sample was divided and packed in four high pressure polyethylene containers each containing approximately 200 μL of mixture. After each portion of this sample was placed in the probe,

the coil and the high-pressure chamber were cooled to 8 °C before the initial pressure was set for that series of experiments. Figures 4.4, 4.5 and 4.6 show spectra for portions of this sample at different pressures but with the same thermal history in the sense that the series of spectra for each pressure were collected on the first run from 8 °C for that portion of the sample. After the initial heating run at a specific temperature, the first two portions of this sample were also used for additional observations at higher pressure. Spectra from these additional runs are included in the Appendix and noted, as needed, in the text.

4.2.1 DMPC-d_{54}/DMPG/DHPC (3:1:1) at ambient pressure

Figure 4.4 shows a set of spectra at selected temperatures for DMPC-d_{54}/DMPG/DHPC (3:1:1) at ambient pressure. The complete corresponding set of spectra can be found in Appendix A as Figure A.16. This sample was labeled as AR11. This mixture was cooled to 8 °C and equilibrated at this temperature for one hour. At 8 °C, the spectrum displays a narrow peak which is characteristic of small disks undergoing isotropic reorientation on the quadrupole echo experiment time scale ($\sim 10^{-5}$ s) as mentioned previously. Upon increasing the temperature of the DMPC-d_{54}/DMPG/DHPC (3:1:1) mixture, the small disks start to fuse and form nematic ribbon-like or worm-like micelles, presumably with short chain lipids at the edges and long chain lipids on the planar surfaces [45, 46]. At 18 °C the spectrum indicates that most of the DMPC-d_{54} molecules are arranged with partial orientational order but a small fraction is still undergoing isotropic reorientation. At 22 °C in Figure 4.4a, the spectrum for DMPC-d_{54}/DMPG/DHPC (3:1:1) indicates orientational ordering of molecules with respect to the bilayer normal but reorientation about the bilayer normal is not fully axially symmetric on the experimental time scale. The spectrum at 24 °C, is becoming more

characteristic of lipids undergoing axially symmetric reorientation about a randomly oriented distribution of bilayer normal directions.

At 28 °C and 29 °C, the spectra in Figure 4.4a show characteristics of complete bilayer orientation with respect to the magnetic field. The bilayer normals are perpendicular to the magnetic field at this temperature. At 32 °C, the spectrum shows the superposition of two different phases. The presence of sharp edges, the low intensity in the centre and the doublets within suggest that oriented nematic phase and lamellar vesicles coexist at this temperature. Therefore, this spectrum suggests that this transition is first order and it provides a good indication of the nematic-to-lamellar transition temperature for DMPC-d_{54}/DMPG/DHPC (3:1:1) at ambient pressure.

From studies using per-deuterated DHPC, it has been suggested that DHPC molecules begin to move from edges to planar regions above the oriented nematic-to-lamellar vesicle transition temperature [63]. Worm-like micelle edges become unstable near the upper end of nematic phase temperature range. Studies suggest that around this temperature, individual ribbons begin to fuse and form extended lamellar sheets [46]. These bilayered sheets fold into multilamellar vesicles as temperature increases [46]. The transition from magnetically alignable phase to lamellar phase is demonstrated by the 32 °C spectrum in Figure 4.4a which shows a superposition of spectral components characteristic of both phases.

At temperatures higher than 34 °C, the DMPC-d_{54} molecules begin to form vesicles as can be seen, in Figure 4.4a, from the change of the observed spectrum from a superposition of narrow doublets to a superposition of Pake or powder pattern doublets.
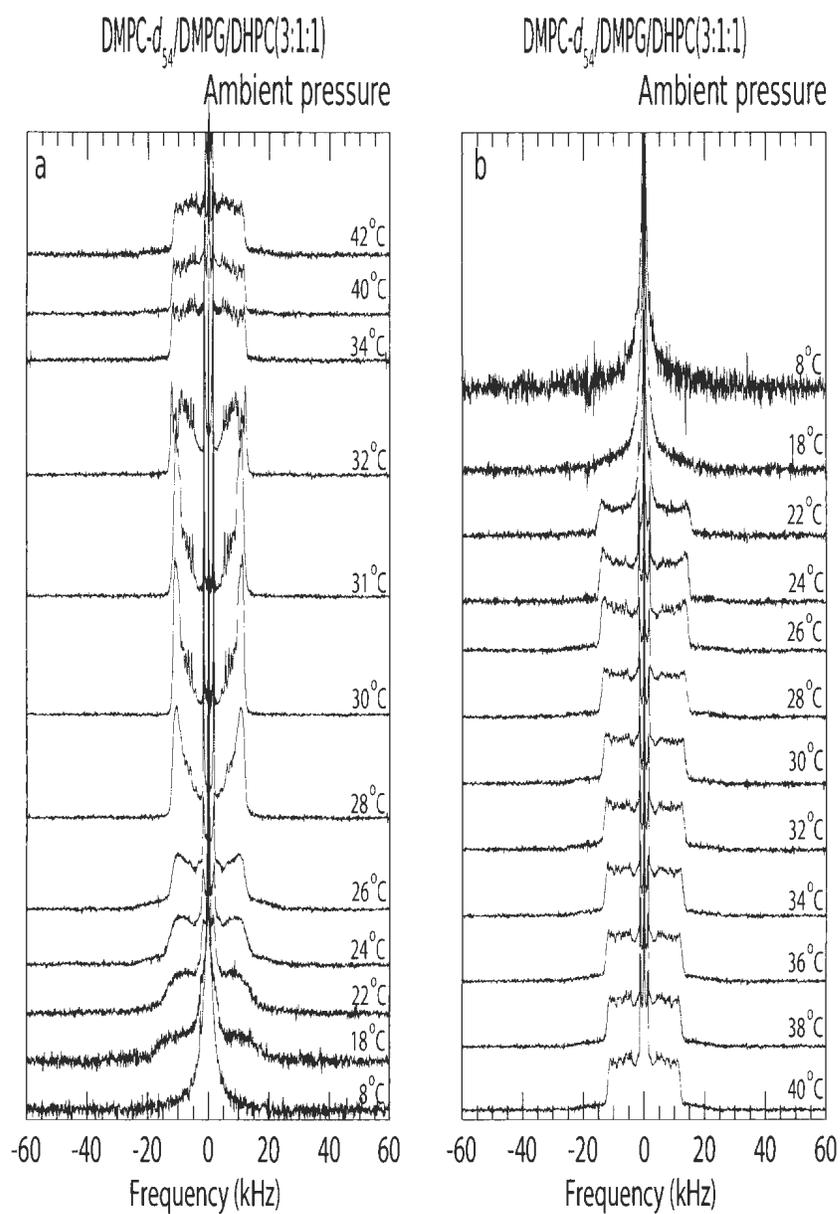
Figure 4.4: Deuterium NMR selected spectra for DMPC-d_{54}/DMPG/DHPC (3:1:1) collected during the cycle of (a) warming and (b) cooling for a range of temperatures at ambient pressure. Spectra in (a) and (b) were collected in order from the bottom to the top of each stack. This sample was labeled AR11.

On decreasing the temperature from 40 °C, the spectra for this sample, shown in Figure 4.4b, are characteristic of axially symmetric reorientation about bilayer normals with a spherical distribution of directions. This indicates persistence of the lamellar vesicle phase over a wide temperature range ($\sim$ 22 °C) on cooling. The doublet splitting increases slightly with decreasing temperature. This is due to the rise in chain order with decreasing temperature which causes S_{CD} to increase. At 18 °C, a sharp transition from lamellar vesicle state to the isotropic reorientation state causes the spectrum obtained at that temperature to display a narrow peak in the centre.

One significant observation about the influence of anionic lipids on bicellar mixtures is that DMPC-d_{54}/DMPG/DHPC(3:1:1) mixtures display bilayer orientation over a range of temperatures at 3.5 T while bilayer orientation is more difficult to observe for DMPC-d_{54}/DHPC (4:1) at 3.5 T. DMPC-d_{54}/DHPC (4:1) mixtures do display bilayer orientation in higher magnetic fields as shown in Figure 4.1b. The significant orientation shown, in Figure 4.4a, by DMPC-d_{54}/DMPG/DHPC (3:1:1) at 3.5 T suggests that anionic lipid, particularly DMPG, facilitates bilayer orientation under conditions where bilayer orientation may be more difficult to observe in the absence of DMPG.

4.2.2   DMPC-d_{54}/DMPG/DHPC (3:1:1) at high pressure

In order to study the response of the anionic bicellar mixture to hydrostatic pressure and to compare that response to the response of DMPC-d_{54}/DHPC (4:1), a portion of the sample with the same preparation and thermal history as the one shown in Figure 4.4 was studied at 41.4 MPa while warming and cooling. After equilibrating at 8 °C for one hour, the sample was pressurized to 41.4 MPa. The corresponding set
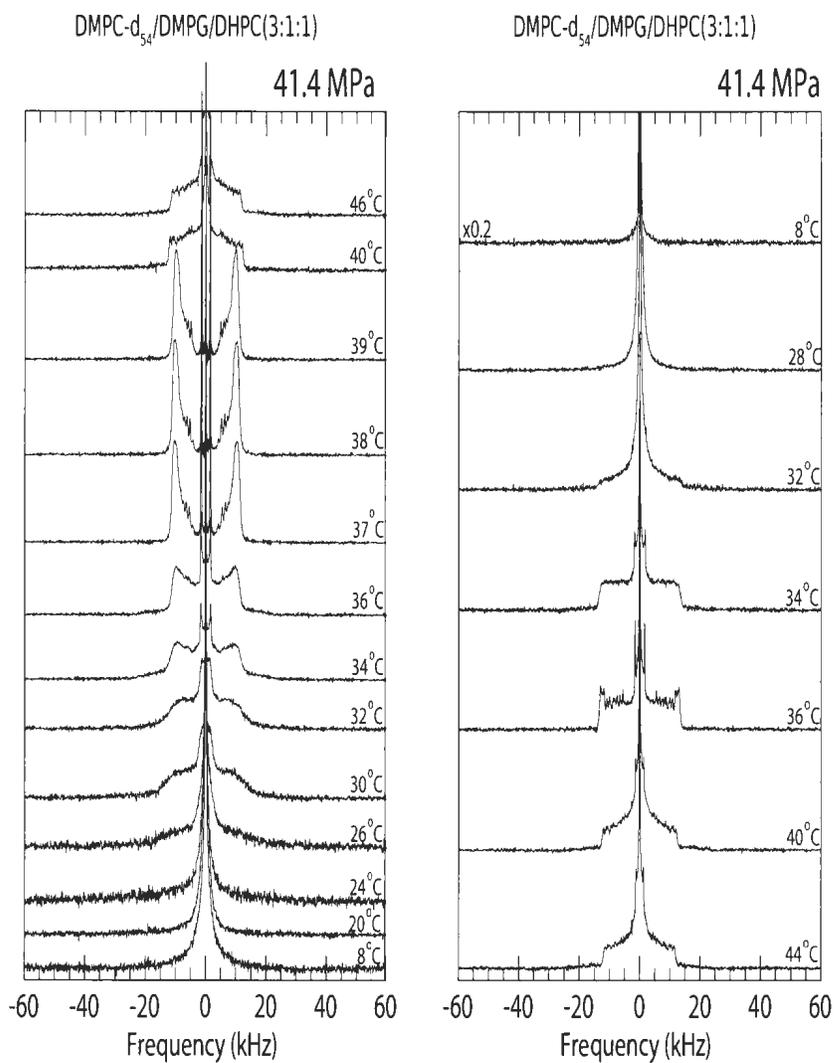
Figure 4.5: Deuterium NMR selected spectra for DMPC-d_{54}/DMPG/DHPC (3:1:1) collected during the cycle of (a) warming and (b) cooling for a range of temperatures at 41.4 MPa. Spectra in (a) and (b) were collected in order from the bottom to the top of each stack. This sample was labeled ARA11.

of spectra obtained while warming is shown in Figure 4.5a.

From 8 °C to 28 °C, the narrow central peak in the spectra of Figure 4.5 indicates the presence of bilayered disks undergoing isotropic reorientation on the quadrupole echo timescale. From 26 °C to 32 °C, the spectra in Figure 4.5a show that the amount of orientationally ordered lipid increases but reorientation about the bilayer normal is not axially symmetric. The spectrum at 34 °C displays more vertical edges around ± 12 kHz and thus does indicate axially symmetric reorientation about the bilayer normal but without complete orientation with respect to the magnetic field. At 37 °C, bilayer normals are mostly oriented with respect to the magnetic field. This temperature is about 9 °C higher than the onset of complete orientation at ambient pressure which corresponds to a $\frac{dT}{dP}$ of ∼ 0.21 °C/MPa for the onset of orientation in DMPC-d_{54}/DMPG/DHPC (3:1:1). This is a slightly higher sensitivity to pressure than displayed by the corresponding behaviour in DMPC-d_{54}/DHPC (4:1) in previous studies[63, 45].

The sharp transition from oriented bilayers to multilamellar vesicles at 41.4 MPa occurs at ∼ 40 °C as seen in Figure 4.5a. This is ∼ 8 °C higher than the nematic-vesicle transition seen in Figure 4.4a at ambient pressure. Based on the comparison of the ambient pressure and 41.4 MPa values of this transition temperature, the pressure sensitivity of the nematic-vesicle transition for DMPC-d_{54}/DMPG/DHPC (3:1:1) can thus be estimated to be ∼ 0.19 °C/MPa.

From the comments above, it can be seen that DMPC-d_{54}/DMPG/DHPC mixtures show the expected sequence of phases on warming namely an isotropic phase, consisting of disks with fast isotropically thermal reorientation, a magnetically alignable

worm-like micelle phase and multilamellar bilayer vesicles. The transitions, though, occur at higher temperatures as mentioned above.

The set of spectra for DMPC-d_{54}/DMPG/DHPC (3:1:1) recorded while cooling at 41.4 MPa is shown in Figure 4.5b. At 44 °C and 40 °C, the spectra are typical of vesicles at high pressure. The increase in intensity toward the centre of the spectrum may reflect a slight difference in the dependence of orientational order parameter on position along the chain at high pressure compared to the case for ambient pressure. At 36 °C, the spectrum in Figure 4.5b appears to be a superposition of oriented nematic and lamellar vesicle spectral components. Partial or complete orientation, though, has not been observed while cooling at DMPC-d_{54}/DMPG/DHPC (3:1:1) at high pressure.

Upon cooling to 32 °C, the narrow spectral components in Figure 4.5b show that, most of the sample is undergoing isotropic reorientation but with a small fraction still giving rise to a broader spectrum which indicates partial orientational order and thus incomplete averaging of the quadrupole interaction. At 28 °C, the narrow peak indicates that the sample is in a state with complete isotropic reorientation and this phase continues to exist until 8 °C.

A fresh portion of the commonly prepared DMPC-d_{54}/DMPG/DHPC (3:1:1) sample was then placed in the probe and cooled to 8 °C. After equilibrating for one hour, this sample was pressurized to 82.7 MPa while in the isotropically reorienting disk-like phase. Spectra obtained while warming this sample at 82.7 MPa are shown in Figure 4.6a.
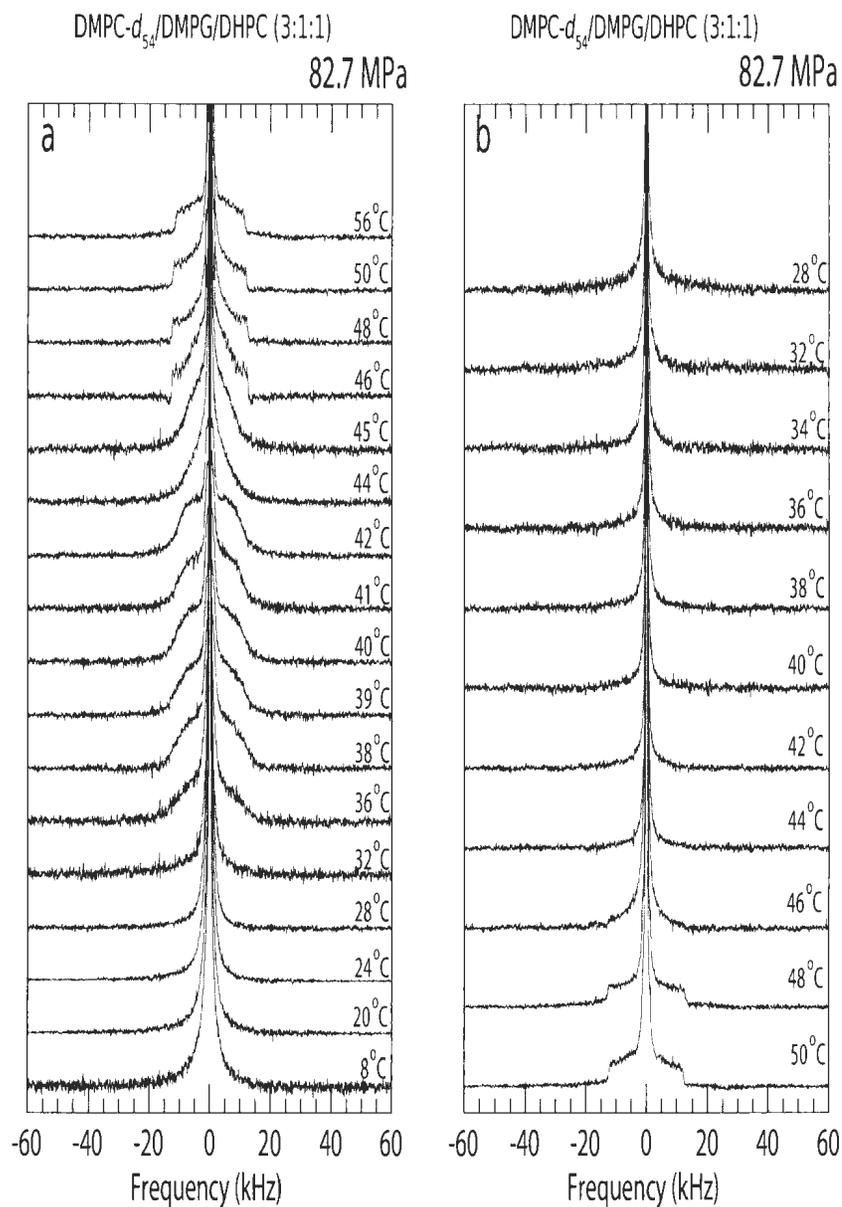
Figure 4.6: Deuterium NMR selected spectra for DMPC-d_{54}/DMPG/DHPC (3:1:1) collected during the first cycle of (a) warming and (b) cooling for a range of temperatures at 82.7 MPa. This sample was labeled ARB11.

As was the case for all other anionic bicelle samples observed in this study (see Figures A.4b, A.8a, A.11a, A.14b and A.22a in the Appendix A), this sample did not enter an oriented nematic phase at 82.7 MPa. Between 38 °C to 42 °C, the spectra in Figure 4.6a are characteristic of lipids with some orientational order but not undergoing axially symmetric reorientation about the bilayer normal. For some samples, this partially ordered nematic phase was not observed and the transition occurred directly from the isotropic orientation phase to the lamellar vesicle phase.

Figures 4.6a and 4.6b show that this sample of DMPC-d_{54}/DMPG/DHPC (3:1:1) did not display clear evidence for an oriented nematic phase on either warming or cooling. This was typical of other DMPC-d_{54}/DMPG/DHPC (3:1:1) samples studied (see Figures A.4b, A.8a, A.11a, A.14b and A.22a in the Appendix A) and some samples even showed a direct transition from isotropic reorientation to lamellar vesicle. For this reason it was not possible to include 82.7 MPa observations in an estimate of the sensitivity to pressure of the oriented nematic to lamellar vesicle transition. However, if a linear dependence of transition temperature on pressure is assumed, extrapolating from the ambient pressure and 41.4 MPa nematic-to-vesicle transition temperatures suggests that the onset of the vesicle phase should be around 48 °C at 82.7 MPa. The spectra in Figure 4.6a and 4.6b do show changes between 45 °C and 46 °C on warming (Figure 4.6a) and between 48 °C and 46 °C on cooling (4.6 b) that may indicate this transition.
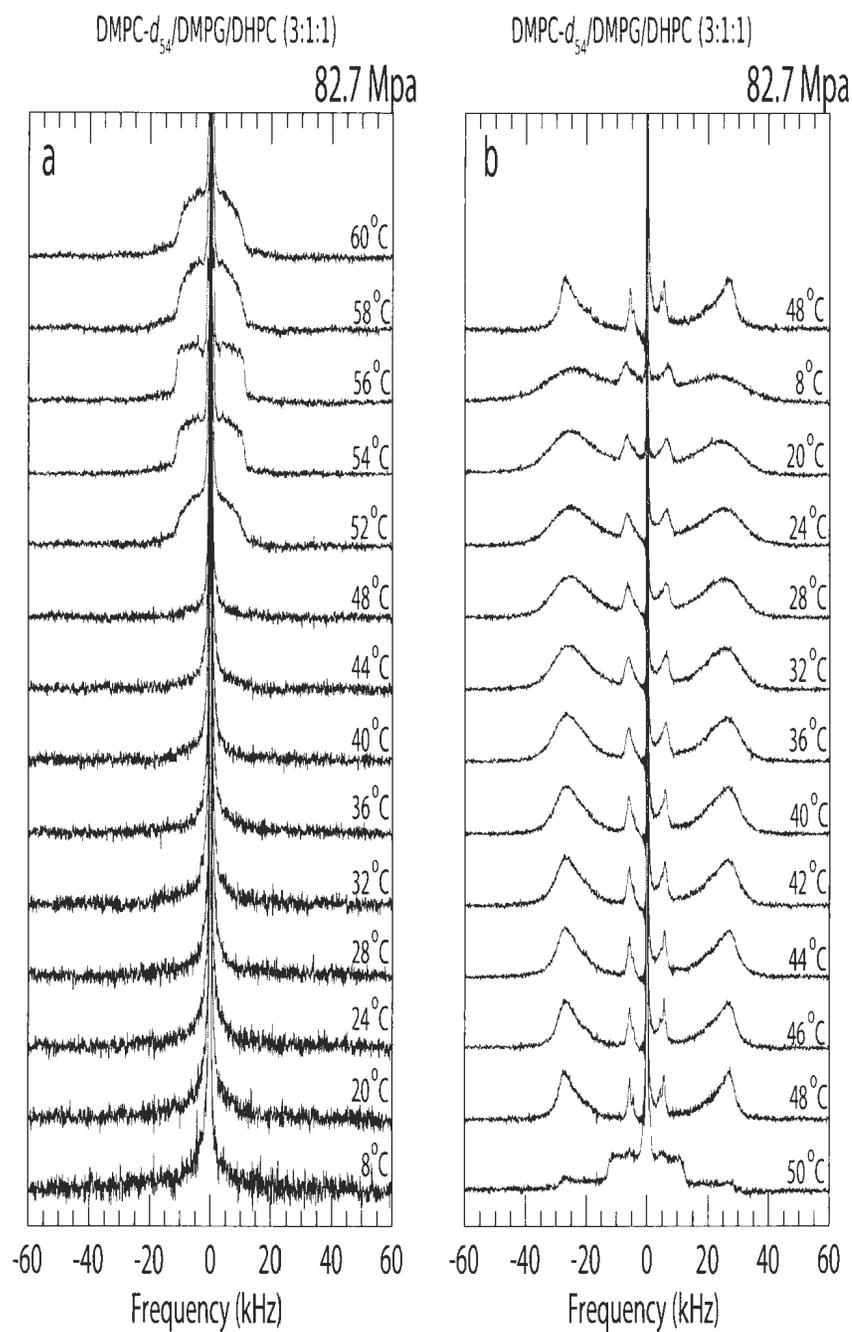
Figure 4.7: Deuterium NMR selected spectra for DMPC-d_{54}/DMPG/DHPC (3:1:1) collected during the second cycle of (a) warming and (b) cooling for a range of temperatures at 82.7 Mpa.

4.2.3 Thermal history dependence of bicellar mixture behaviour and observation of interdigitated gel phase

In this work and in previous studies [24, 63], it has been observed that the occurrence of bilayer orientation, the temperature at which transitions occur, and observation of specific phases can be sensitive to the mixture's thermal history. Figure 4.7 shows spectra obtained during a second warming and cooling cycle, at 82.7 MPa, of the sample from which the spectra of Figure 4.6a were obtained. Figure 4.7a shows that on warming for the second time, the isotropic phase persists to 52 °C. For example, Figure 4.8 compares the spectra obtained at 40 °C on the first and second warming cycle for this sample at 82.7 MPa. When the mixture, at 82.7 MPa, was warmed through 40 °C for the first time, a fraction of DMPC-d_{54} molecules formed nematic worm-like micelles without magnetic alignment. When it passed through 40 °C for the second time, however, the spectrum was dominated by a narrow central peak characteristic of bilayered disks undergoing isotropic reorientation. This suggests that cycling the sample temperature while holding it at high pressure changed some property of the sample that affected its equilibrium morphology at high temperature and high pressure. One possibility is that this cycling affected the size of particles into which the bilayers disintegrate on cooling back to the isotropic phase.

In Figure 4.7a, some inconsistencies in spectral shape were observed between 52 °C and 60 °C. The similarity of the shapes at 52 °C and 60 °C, and their difference from the shapes at 54 °C and 56 °C suggests that this inconsistency may reflect difficulties with probe tuning at high pressure and high temperature.
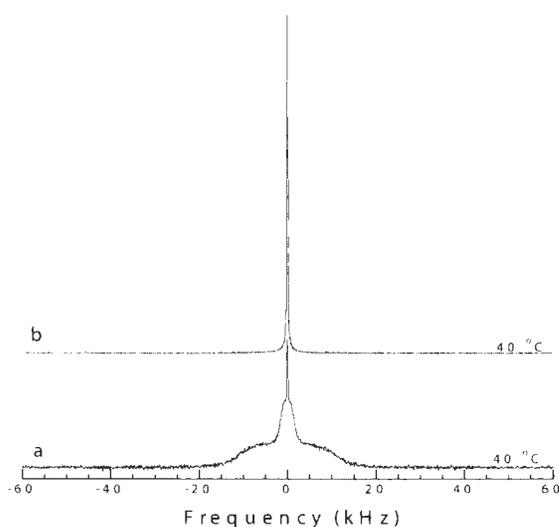
Figure 4.8: Deuterium NMR selected spectra for DMPC-d_{54}/DMPG/DHPC (3:1:1) collected at 40 °C during of (a) first cycle of and (b) second cycle of warming at 82.7 MPa.

Spectra obtained while cooling this sample of DMPC-d_{54}/DMPG/DHPC (3:1:1) for the first and second time, at 82.7 MPa, are shown in Figure 4.6b and 4.7 b respectively. This sample was cooled from 60 °C to 50 °C in few steps without data acquisition. At 50 °C, the spectra for both runs are mostly characteristic of the lamellar vesicle phase but there is also a broad component present in the 50 °C spectrum for the second cooling run (Figure 4.7b). From 48 °C, the spectra observed during the second cooling cycle are very different for those seen during the first cooling cycle.

The spectral component with a splitting of about 54 kHz is attributed to an interdigitated gel phase as described in Chapter 2. The doublet with a splitting of about 12 kHz is due to the methyl groups at the chain ends in this phase. The asymmetry in

the spectra shown in 4.7b is because of the difficulty in adjusting a single phase appropriate for both broad component and narrow component. As mentioned in Chapter 2, the large splitting in the interdigitated gel phase is seen because overlap of chains from opposite sides of the bilayer reduces the available area per lipid acyl chain by a factor of about a half. Evidence for an interdigitated phase with a similar doublet splitting was seen previously in DPPC-d_{62} and DPPG-d_{62} at high pressure [17].

Although this wide component persists over a wide range of temperature, the doublet splitting increases slightly as temperature is reduced. This is due to the increase in chain orientational order with decreasing temperature. In Figure 4.7b, the doublet is much sharper at 48 °C than at lower temperatures and intensity is concentrated at ±27 kHz rather than being spread into a Pake doublet. This doublet is also sharper than that attributed to the interdigitated phase in DPPC-d_{62} and DPPG-d_{62} [17]. This suggests that the acyl chains, while very highly ordered, are still able to undergo axially symmetric reorientation in the interdigitated phase at higher temperatures. The concentration of intensity at ± 27 kHz may indicate that the interdigitated bilayers are also partially oriented in the magnetic field.

It should be noted that the DMPC-d_{54}/DMPG/DHPC (3:1:1) mixtures in this work have not been seen to return to a non-interdigitated lipid structure at lower temperatures after undergoing the transition into the interdigitated gel phase. Previous studies showed that DPPG bilayers and DPPC bilayers pass from an interdigitated gel phase at high temperature, through a non-interdigitated gel phase at intermediate temperature and to a chain-immobilized ordered phase at low temperature [17]. In contrast, DMPC-d_{54}/DMPG/DHPC (3:1:1) mixtures show characteristics of an interdigitated gel phase over a wide range of temperatures after entering this phase.

Examples are shown in the Appendix A (Figures A.5, A.11, A.17, A.18, A.22, A.24 and A.26). It has been observed that spectral features characteristic of the interdigitated gel phase disappear at high temperatures and that the DMPC-d_{54}/DMPG/DHPC (3:1:1) mixture can display spectra characteristic of a multilamellar vesicle phase at high temperature after having been in the interdigitated gel phase. However, these samples consistently return to the interdigitated gel phase on cooling either at ambient pressure or at high pressure as detailed below. There have also been some indications that entry into the interdigitated gel phase at high pressure may also alter the observed phase behaviour at ambient pressure but further experiments are required to fully characterize this behaviour (see Figures A.6b, A.11 and A.12 in the Appendix A).

The observed interdigitated gel phase for anionic bicellar mixtures exhibits metastability. After cooling the mixture down to 8 °C, which is much lower than the gel-liquid crystal transition temperature for DMPC-d_{54} and DMPG, and allowing two hours for equilibration, the spectra obtained are still characteristic of interdigitated gel phase at high pressure as shown in appendix A (Figures A.6b, A.12a, A.17a and A.17b, A.18, A.24b). Mixtures of DMPC-d_{54}/DMPG/DHPC (3:1:1) which had entered the interdigitated gel phase were also placed in a freezer at −18 °C for several days. The mixture was then returned to the NMR probe and data were acquired for a range of temperatures at ambient pressure and high pressure. The resultant spectra still showed evidence of chain interdigitation. These spectra are shown in Figure A.6b of the Appendix A. This mixture was also sonicated and subjected to freeze/thaw cycles after interdigitation. This treatment was not found to break the altered dispersion into small bicellar disks. The corresponding set of spectra after sonication and freeze-thaw can be found in Appendix A in Figures A.6b and A.18.

4.2.4 Non-sonicated DMPC-d_{54}/DMPG/DHPC (3:1:1) mixtures

As described in Chapter 3, most of the lipid mixtures in this study were sonicated for 15 minutes and subjected to five freeze-thaw cycles before they were transferred to polyethylene NMR sample containers. The sonication and freeze-thaw cycles are intended to shear larger structures into smaller fragments. Sonication at temperatures lower than the main gel to liquid crystalline transition temperature of DMPC followed by 5 cycles of freeze-thaw, performed as the last step in the sample preparation protocol, was used in this work to produce small bicelles with long-chain lipids on the planar regions and short-chain lipids on the edges.

The observation of an interdigitated gel phase only on cooling of the anionic bicellar mixture at 82.7 MPa and the persistence of that phase once encountered led to questions regarding the possible effect of initial particle size on whether or not the sample was likely to display interdigitation at high pressure. In order to determine the influence of initial bicelle size on the phase behaviour of the anionic bicellar mixtures, a DMPC-d_{54}/DMPG/DHPC (3:1:1) mixture was prepared following the same preparation protocol as for other samples but with the sonication and freeze-thaw steps omitted. Spectra obtained in the first cycle of warming and cooling of this sample at ambient pressure are shown in Figure 4.9a.

The spectra obtained indicate that the non-sonicated mixture displays the same sequence of isotropic-nematic-lamellar phases as that displayed by mixtures prepared in the normal way using sonication and freeze-thaw cycling.
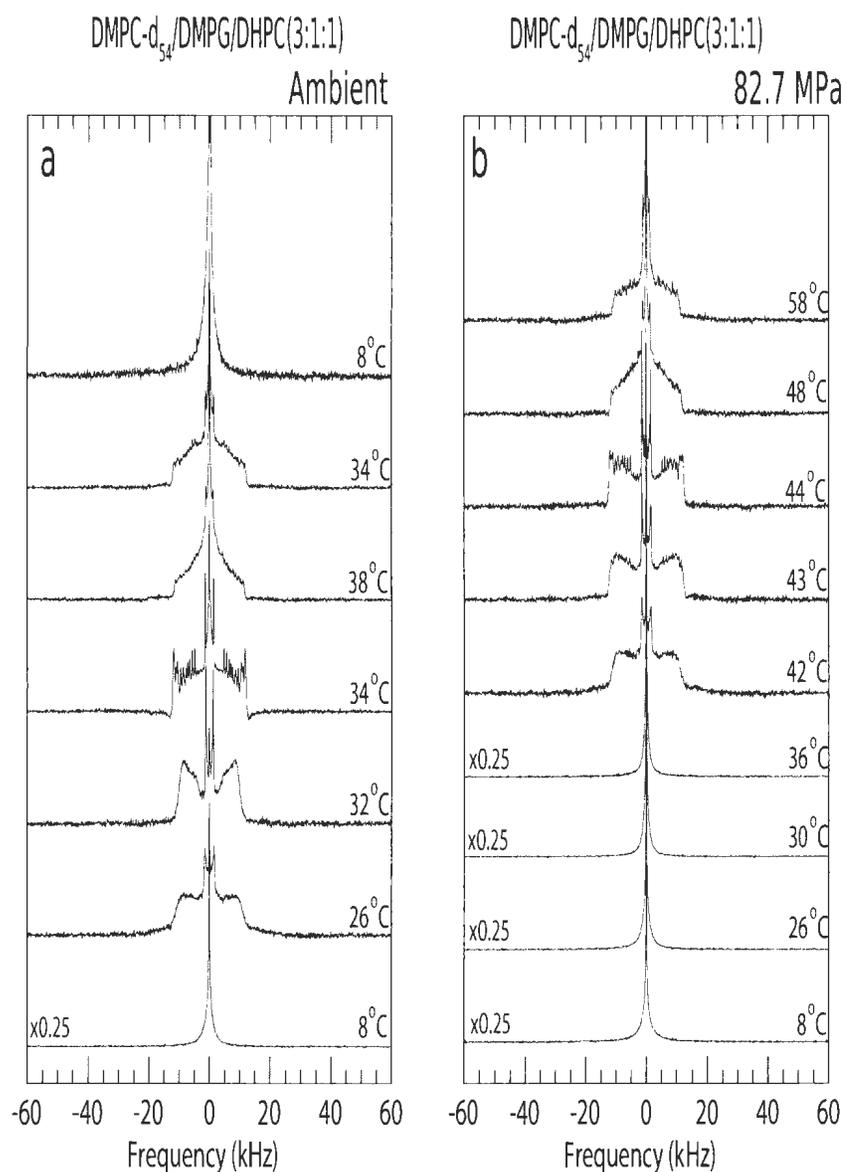
Figure 4.9: Deuterium NMR spectra of non-sonicated DMPC-d_{54}/DMPG/DHPC (3:1:1) for selected temperatures while increasing temperature at (a) ambient pressure and (b) 82.7 MPa. The sample used for these experiments was designated as AR13 at ambient pressure and ARA13 at high pressure.

The spectrum at 8 °C in Figure 4.9a displays a narrow peak which is characteristic of disks undergoing isotropic reorientation. At 32 °C, the bilayered particles are partially aligned with respect to the magnetic field. At 34 °C, the spectrum is a superposition of partially oriented and lamellar vesicle phases spectral components indicating the nematic-to-lamellar transition. At 38 °C, the spectrum is characteristic of lamellar vesicles. Spectra for this sample obtained during cooling at ambient pressure are shown as the two upper spectra in Figure 4.9a. The spectrum for this mixture is characteristic of isotropic reorientation when the sample is re-cooled to 8 °C. It should be noted that the small negative intensity in the baseline of the spectrum at 34 °C is due to a spectrometer tuning problem during the acquisition of this spectrum. It does not alter the conclusion that this sample displays the typical bicellar mixture sequence of phases on warming.

The spectra obtained when this sample is first warmed at 82.7 MPa are shown in Figure 4.9b. The isotropic-nematic transition temperature is raised as expected. The nematic-lamellar transition at 82.7 MPa occurs about 10 °C higher than the corresponding transition at ambient pressure. Although the temperature resolution of this experiment is low, the sensitivity of the oriented to lamellar vesicle transition to pressure appears to be roughly consistent with that seen for the sonicated anionic bicellar mixtures.

Figure 4.10 displays a set of spectra obtained during a cycle of cooling, warming, and then cooling from the non-sonicated DMPC-d_{54}/DMPG/DHPC (3:1:1) mixture at 82.7 MPa. The spectra are characteristic of lamellar vesicles at high temperatures. Starting from the bottom of the stack of spectra, the first four spectra were obtained on the first cycle of cooling at 82.7 MPa (second cycle of cooling overall).

As shown in Figure 4.10, these spectra are characteristic of the lamellar vesicle phase at temperatures between 52 °C and 40 °C. At 34 °C, the spectrum is characteristic of isotropically reorienting disks.

After the initial cooling to 34 °C, the mixture was warmed to 60 °C in steps of a few degrees with adequate time to equilibrate at each temperature. Spectra were obtained at 54 °C and 60 °C during this warming process. These spectra were again typical of the lamellar vesicle phase.

Finally, spectra were obtained at 50 °C, 40 °C, and 30 °C as the temperature was decreased for the second time. As shown in Figure 4.10, no evidence of a broad spectral component, characteristic of the interdigitated gel phase, was observed. At 30 °C, the spectrum was again characteristic of isotropically reorienting disks. This suggests that the initial size of the lipid particles does not change the observed morphologies of the anionic bicellar mixtures significantly. It also suggests that the appearance of the interdigitated gel phase on cooling from high temperature at 82.7 MPa is not simply a result of the sample having "forgotten" the effects of sonication and freeze-thaw cycling as a result of cooling from high temperature at high pressure.
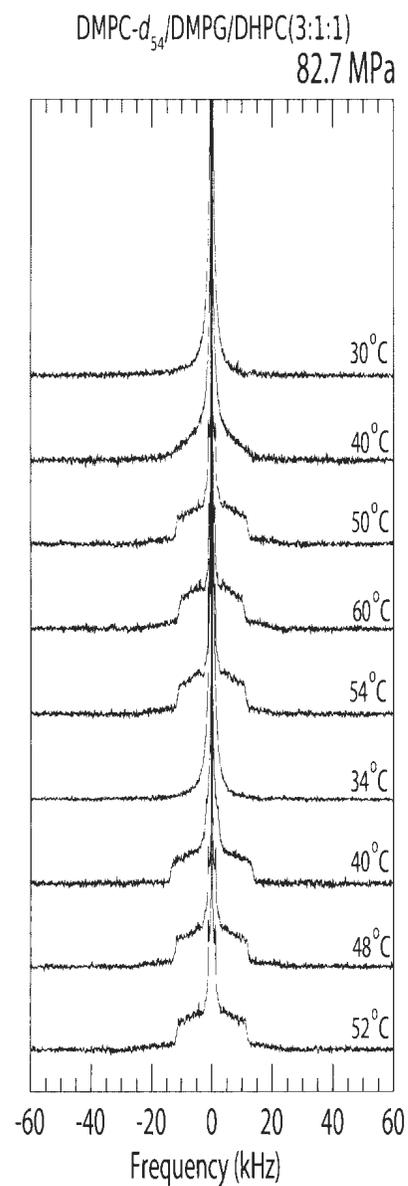
Figure 4.10: Deuterium NMR spectra of non-sonicated DMPC-d_{54}/DMPG/DHPC (3:1:1) for selected temperatures at 82.7 MPa. This sample is designated as ARA13.

4.3 Anionic bicellar mixture with chain perdeuterated DMPG

Previous studies have characterized the morphologies and phase behaviour of bicellar mixtures containing DMPC and DHPC. These studies have suggested that long chain lipid, such as DMPC, molecules occupy planar areas in either disks or sheets whereas short chain lipid molecules (i.e. DHPC) preferentially locate at edges preferabley [45, 46]. This picture has been suggested for the mixtures containing one long chain species (DMPC) and one short chain lipid (DHPC). In order to examine if DMPG molecules locate in the same environment as DMPC molecules in anionic bicellar mixtures at both ambient and high pressure, a mixture of DMPC/DMPG-d_{54}/DHPC (3:1:1) was prepared. The deuterated lipid component constitutes 25% of lipid content whereas 60% of the lipid component is deuterated in DMPC-d_{54}/DMPG/DHPC (3:1:1). The lower abundance of deuterated lipid component in DMPC/DMPG-d_{54}/DHPC (3:1:1) mixture significantly reduces the signal to noise ratio. To obtain high resolution spectra, 20000 to 40000 transients were averaged at each temperature.

4.3.1 DMPC/DMPG-d_{54}/DHPC(3:1:1) at ambient pressure

The spectra obtained at selected temperatures for DMPC/DMPG-d_{54}/DHPC (3:1:1) are shown in Figure 4.11a. For comparison, selected spectra for DMPC-d_{54}/DMPG/DHPC (3:1:1) from the same series of spectra as used to construct Figure 4.4a are shown in Figure 4.11b. The complete sets of spectra for DMPC/DMPG-d_{54}/DHPC (3:1:1) and DMPC-d_{54}/DMPG/DHPC (3:1:1) can be found in appendix A as Figures A.25, A.26, and A.19-23 respectively. Comparison of Figures 4.11a and 4.11 b shows that DMPC/DMPG-d_{54}/DHPC (3:1:1) passes through specific transitions at higher
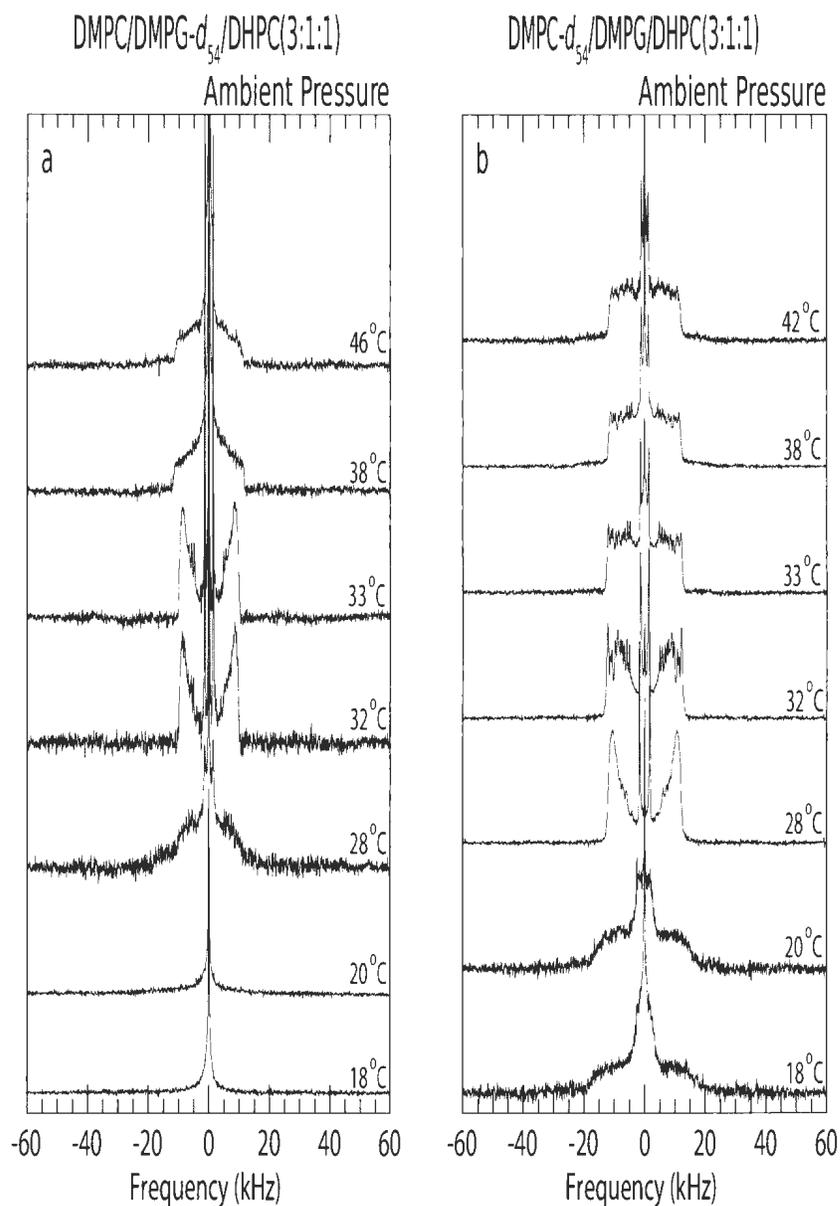
Figure 4.11: selected deuterium NMR spectra for (a) DMPC/DMPG-d_{54}/DHPC (3:1:1) and (b) DMPC-d_{54}/DMPG/DHPC (3:1:1) at ambient while increasing the temperature. The DMPC/DMPG-d_{54}/DHPC (3:1:1) sample used here (panel a) is designated as AR12. The DMPC-d_{54}/DMPG/DHPC (3:1:1) spectra used here are selected from the same series of spectra as those used in Figure 4.4a. The corresponding DMPC-d_{54}/DMPG/DHPC (3:1:1) sample is designated as AR11.

temperatures than DMPC-d_{54}/DMPG/DHPC (3:1:1). This is expected due to the lowering effect of deuteration on bilayer phase transition temperatures [60] and the lower level of sample deuteration in the DMPC/DMPG-d_{54}/DHPC (3:1:1) mixture in comparison to the mixture with per-deuterated DMPC.

Both samples start from a state with isotropically orienting disks at low temperatures. At 18 °C, the spectrum for the mixture containing DMPG-d_{54} is characteristic of isotropic reorientation whereas the sample containing DMPC-d_{54} is partially ordered but undergoing reorientation that is not axially symmetric with respect to the bilayer normal.

The nematic-lamellar phase transition occurs ~ 4 °C higher in the sample containing DMPG-d_{54} compared to the sample containing DMPC-d_{54}. As shown in Figure 4.11, the nematic-lamellar phase transition is sharp for both mixtures. The lamellar spectra for these two samples are slightly different. The high temperature spectra for the sample containing DMPG-d_{54} show a higher intensity at the centre than those for the sample containing DMPC-d_{54}.

4.3.2   DMPC/DMPG-d_{54}/DHPC (3:1:1) at 82.7 MPa

The spectra obtained from DMPC/DMPG-d_{54}/DHPC (3:1:1) at 82.7 MPa for selected temperature while warming and cooling are shown in Figure 4.12a and b respectively. DMPC/DMPG-d_{54}/DHPC (3:1:1) shows the same spectral characteristic as DMPC-d_{54}/DMPG/DHPC (3:1:1). This implies that the DMPG-d_{54} molecules participate in phase behavior and morphologies of anionic bicellar mixtures in the same way as DMPC-d_{54} and that both long chain lipids are in the same environment in the bicellar

dispersions. The high pressure transition from isotropically reorienting disks to the lamellar phase is a sharp transition and occurs at high temperature.

During the cooling process, the sample containing DMPG-d_{54} molecules starts in the lamellar vesicle phase at high temperature and undergoes a transition into the inter-digitated gel phase cooling through $50\,^{\circ}$C. The observations made for DMPC/DMPG-d_{54}/DHPC (3:1:1) mixture are consistent with the ones made for DMPC-d_{54}/ DMPG/ DHPC (3:1:1). It can be concluded that DMPG and DMPC molecules participate equally in phase behavior and morphologies. It is significant that both long chain lipids are in the same environment in the interdigitated gel phase. This demonstrates that interdigitation is not the result of the two long chain components becoming sep-arated as a result of temperature cycling at high pressure.

The observations made for DMPC/DMPG-d_{54}/DHPC (3:1:1) mixture are consistent with the ones made for DMPC-d_{54}/DMPG/DHPC (3:1:1). It can be concluded that DMPG and DMPC molecules participate equally in phase behavior and morphologies.
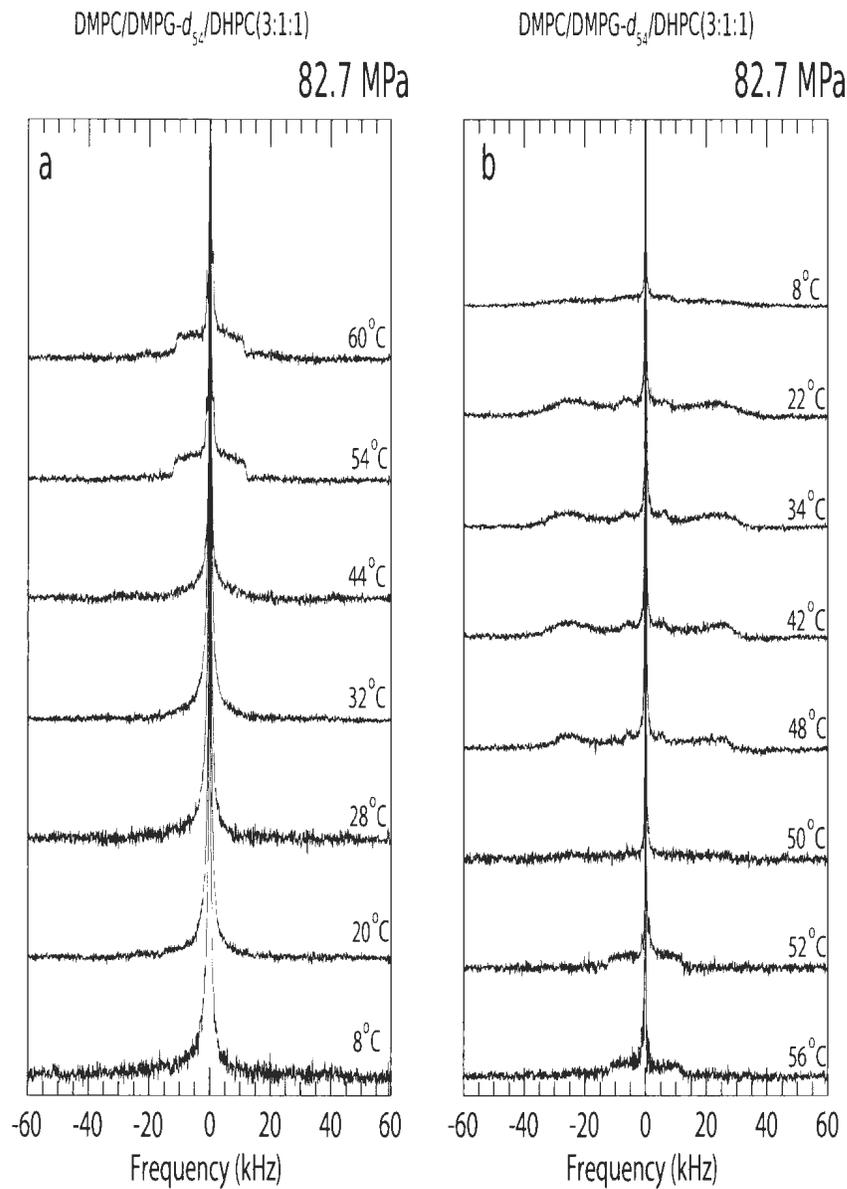
Figure 4.12: selected deuterium NMR spectra for DMPC/DMPG-d_{54}/DHPC (3:1:1) while warming (left) and cooling (right) at 82.7 MPa

4.4 Summary of observations on the interdigitated gel phase in DMPC/DMPG/DHPC

This section includes a summary of the observations done in this work about the interdigitated gel phase. It has been observed that both DMPC-d_{54}/DMPG/DHPC (3:1:1) and DMPC/DMPG-d_{54}/DHPC (3:1:1) may form an interdigitated gel phase at 82.7 MPa on cooling. This indicates that an anionic bicellar mixture in an interdigitated gel phase contains both DMPC molecules and DMPG molecules. In other words, the interdigitated gel phase is not formed as the result of a separation of DMPC and DMPG molecules (Compare Figures A.22 and A.24 to A.26 in Appendix A).

It has been found that after the interdigitated gel phase is formed at 82.7 MPa on cooling, it can be observed under other experimental conditions. The conditions under which the interdigitated gel phase has been observed in this work include a wide range of temperatures at either ambient pressure or 41.4 MPa, and subsequent treatment by of freezing, sonication, and cycles of freeze-thaw. See Figures A.5, A.11, A.17, A.18, A.22, A.24, A.26 for additional observations of the interdigitated gel phase. Figure A.6a contains a set of spectra obtained after freezing the interdigitated gel mixture, and sets of spectra obtained after freezing, sonication and cycles of freeze-thaw are shown in Appendix A, Figures A.6b and A.18. It should be noted that the presence of an interdigitated gel phase has not been observed under these conditions for DMPC/DHPC (4:1).

Applying hydrostatic pressure to bilayers in multilamellar vesicle samples generally increases chain order [56] which causes bilayer thickness to increases slightly [31]. However, the volume per lipid must decrease in response to increased pressure [58].

In effect, bilayers respond anisotropically to hydrostatic pressure. Interdigitation must also reduce the volume per lipid but involves a different balance between changes in the plane of the bilayer and in the direction of the bilayer normal.

Formation of the interdigitated gel phase appears to be facilitated by presence of a charged (anionic) lipid component. Interdigitation requires a slightly higher separation among headgroups to accommodate the overlap of chains. This may be promoted by interactions between charged headgroups. Previous studies showed that the mixtures of DPPG form an interdigitated gel phase at a lower pressure than those of DPPC [17].

In this work, it has been observed that interdigitation in DMPC-d_{54}/DMPG/DHPC (3:1:1) occurs predominantly after cycling to high temperature and then starting to cool at high pressure. This suggests that it may reflect the increased mixing of DHPC with the long chain lipids which has been reported to be an important aspect of bicellar mixture behaviour at high temperatures [81, 63]. Interdigitation at low pressures is known to be promoted by the presence of small molecules at the bilayer surface such as methanol and ethanol [13, 16].

It is possible that cycling to high temperature at high pressure modifies the distribution of DHPC in the lamellae such that a decrease in volume per lipid can be accommodated by interdigitation rather than by reversing the structural changes that occurred on warming. Further experiments, at different compositions and under different conditions, may help to clarify the details of interdigitation in these samples.

4.5 Quadrupole echo decay time measurement

The echo decay time can be determined by measuring echo amplitudes while varying the delay between the first and second pulse in the quadrupole echo sequence. As described in Section 2.3, the echo decay time at any given temperature provides helpful information about the motions of the deuterated molecules that modulate the orientation-dependent quadrupole interactions. Measured quadrupole echo decay times are plotted against temperature and shown in Figure 4.13. The black triangles represent the quadrupole echo decay times at ambient pressure. The quadrupole echo decay time was not obtained when the mixture was in the isotropic phase. Therefore, the echo decay time measurement, shown in Figure 4.13, was started from the temperature at which the sample is partially ordered. All fittings were done using Origin. The error bars were also calculated with Origin.

As shown in Figure 4.13, DMPC-d_{54}/DMPG/DHPC (3:1:1) displays echo decay times of approximately 150 μs to 200 μs at low temperatures, with a sudden increase beginning around 26 °C. T_2^{qe} passes through a minimum while the mixture experiences a transition from oriented nematic phase to lamellar phase at 30 °C. There is then a sharp increase at approximately 38 °C corresponding to the transition from the oriented nematic phase to the lamellar vesicle phase.

For the mixture at high pressure identified as being in the interdigitated gel phase, on the basis of the large doublet splittings observed, the echo decay times are very short as shown in Figure 4.13. The echo decay times are between 150 μs and 250 μs over the range of temperatures from 50 °C to 64 °C.

The measured echo decay times for another sample of DMPC-d_{54}/DMPG/DHPC
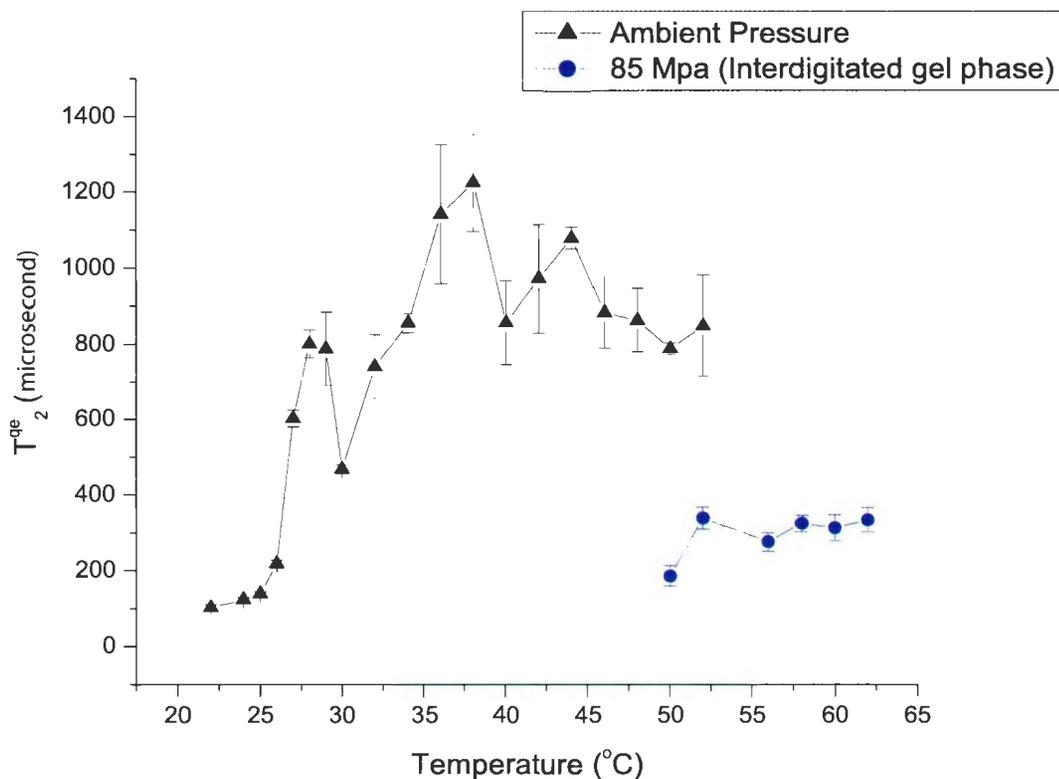
Figure 4.13: The quadrupole echo decay time for DMPC-d_{54}/DMPG/DHPC (3:1:1) at ambient (black triangles) and at 82.7 MPa while warming (blue circles). It should be noted that the echo decay times at 82.7 MPa were collected while the sample was in the interdigitated gel phase. The corresponding set of spectra can be found in appendix A as Figure A.5a and Figure A.5b.

(3:1:1) are shown in Figure 4.14. The black triangles indicate the echo decay time at ambient pressure whereas the red squares represent the echo decay times at 41.4 MPa. The corresponding spectra can be found in appendix A as A.16 and A.18. At ambient pressure, this sample of DMPC-d_{54}/DMPG/DHPC (3:1:1) also displays short echo decay times at low temperatures, with a sudden increase beginning around 29 °C. the temperature at which the corresponding spectra (Figure 4.4a) show characteristic of the oriented nematic phase. T_2^{qe} passes through a minimum at 32 °C. the temperature at which the sample spectrum is a superposition of oriented nematic and

lamellar phase components. This is the temperature at which the mixture undergoes a transition from the oriented nematic phase to the lamellar phase. The echo decay time increases with increasing the temperature up to 800 μs at 42 °C.

As shown by red squares in Figure 4.14, this sample of DMPC-d_{54}/DMPG/DHPC (3:1:1) at 41.4 MPa displays short echo decay times at temperatures for which the spectra are characteristic of partial orientational order. The echo decay time gradually increases until it reaches a maximum at 39 °C. The corresponding spectrum is characteristic of oriented nematic phase at this temperature. This maximum is about 600 μs whereas it is $\sim$ 950 μs for the oriented nematic phase at ambient pressure. The echo decay time decreases until 46 °C. The echo decay times at 41.4 MPa are generally smaller than the ones at ambient pressure.

The echo decay times in the magnetically-oriented temperature range for DMPC-d_{54}/DMPG/DHPC (3:1:1) found in this work are smaller than those previously observed for DMPC-d_{54}/DHPC (4:1) [77]. Those values are larger than the echo decay times observed for DMPC-d_{54} [77]. This might suggest that the presence of DMPG can decrease the mechanical effect of DHPC which has been reported to increase echo decay times in the lamellar vesicle phase [77]. It has also been reported that by increasing the ratio of DMPG in the bicellar mixtures, ^{2}H NMR spectra at high temperature become similar to those for the multilamellar dispersion of DMPC-d_{54} in the liquid crystalline phase [77].
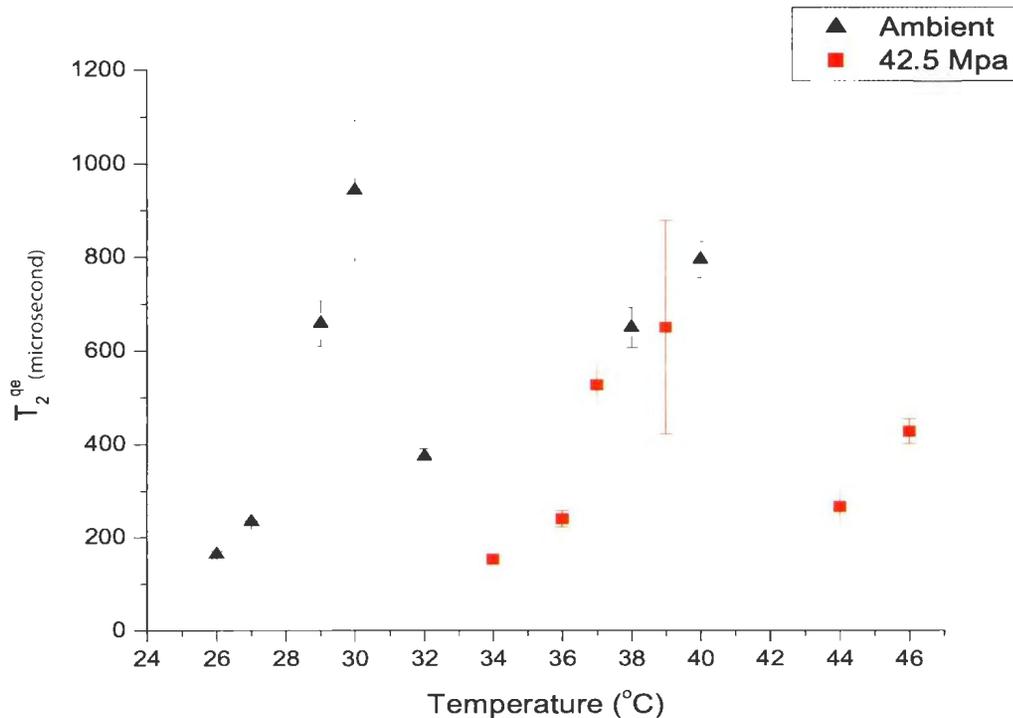
Figure 4.14: The quadrupole echo decay time for DMPC-d_{54}/DMPG/DHPC (3:1:1) at ambient (black triangles) and at 41.4 MPa while warming (red squares). The corresponding spectra can be found in 4.4 a and 4.5 b. This sample is designated as AR11 at ambient pressure and ARA11 at 41.4 MPa.

4.6 Phase diagram

Temperature-composition phase diagrams have been previously reported for bicellar mixtures [24, 78, 79, 80]. Based on ^{31}P NMR studies of DMPC/DHPC mixtures in 80 wt% D_2O, it was reported that for DMPC concentrations lower than ~70%, the only observed phase is isotropic. If DMPG and DMPC are considered together as the long chain component, the mixture at Q=4 and 10% lipid by weight is expected to be in the isotropic, oriented, or lamellar vesicles phases, depending on temperature, at ambient pressure [79]. This is consistent with the ambient pressure observations made here.

Temperature-pressure phase diagrams for bicellar mixtures with different molar ratios, obtained using ^{2}H NMR spectroscopy, have been reported [63]. The nematic phase has been observed for bicellar mixtures with Q=3 and Q=4.4 between 23 °C to 52 °C at different ranges of pressures from ambient to 135 MPa.

Figure 4.15 shows a temperature-pressure phase diagram derived from inspection of the spectra obtained from DMPC-d_{54}/DMPG/DHPC (3:1:1) at ambient, 41.4 MPa and 82.7 MPa. This sample was denoted as AR11, at ambient pressure, ARA11 at 41.4 MPa, and ARB11 at 82.7 MPa. As mentioned earlier, differences in sample preparation, concentration, and thermal history can influence the temperatures at which the DMPC-d_{54}/DMPG/DHPC (3:1:1) mixture undergoes transitions. This may have contributed to some variation in the temperature ranges within which the spectra are characteristic of specific phases. Thus, the perimeter of each phase region shown in Figure 4.15 could vary by a few degrees.

The black squares represent temperatures at which the spectra are characteristic of the isotropic phase. Although spectra were obtained at many temperatures within the observed temperature range, not all are shown in Figure 4.15 to avoid clutter. The temperatures for the upper and bottom limits of each phase are shown.

The red circles denote the phase in which bicellar disks have fused and formed worm-like micelles showing either partial orientational order or partial orientation as shown in Figure 4.15. The green triangles represent the temperatures at which complete bilayer orientation is observed. The olive star denotes the temperature at which oriented bilayers and lamellar vesicles coexist. It should be noted that this superposition was
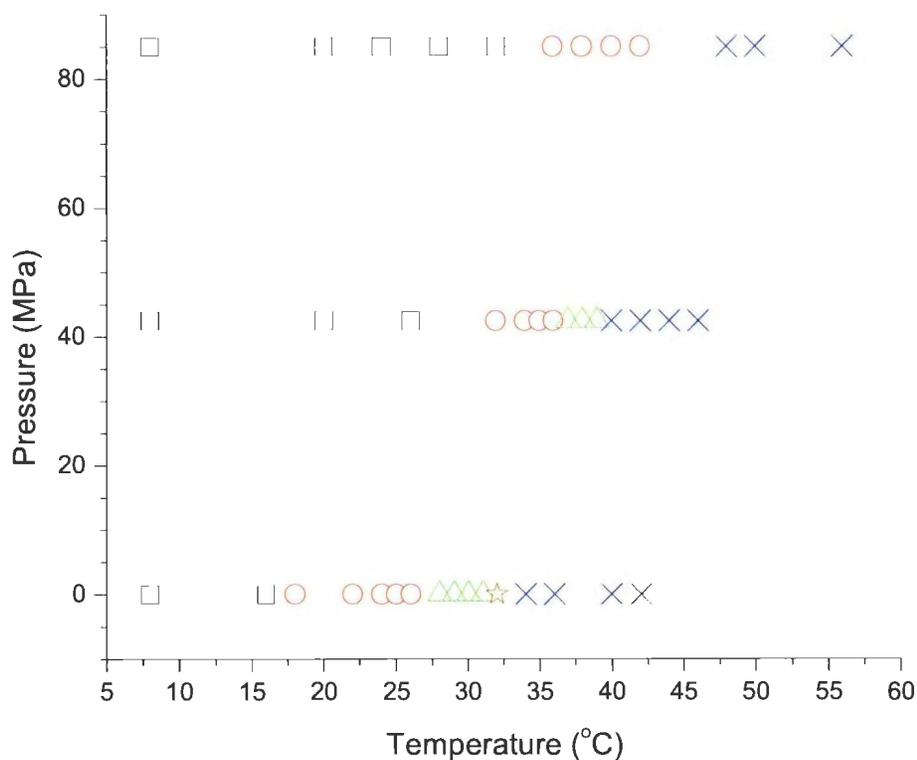
Figure 4.15: Phase diagrams based on the spectra obtained for DMPC/DMPG-d_{54}/DHPC (3:1:1) at ambient, 41.4 MPa and 82.7 MPa. ($\square$) represents the isotropic phase. Circles ($\bigcirc$) indicate the temperatures at which the corresponding spectra were typical of either partially ordered phase or partially oriented phase while ($\triangle$) represents completely oriented phase. The temperature at which the spectrum was characteristic of a superposition of oriented and lamellar vesicle spectra is shown with a non-solid star. The lamellar vesicle phase is shown with ($\times$).

observed at 41.4 MPa a few times (See Figures A.7b, A.8a and A.10b in Appendix A). However, the spectral features of this superposition were not observed at 41.4 MPa for the sample on which this phase diagram is based.

The lamellar vesicle phase is represented with blue ($\times$) symbols. It should be noted that over the second cycle of warming at 82.7 MPa, the narrow peak which indicates the presence of the isotropically reorienting disks was observed up to 46 °C. As can be

seen the corresponding spectra of Figure 4.7, the anionic bicellar mixture underwent a sharp transition from the isotropic phase to the lamellar vesicle phase in this case.

Chapter 5

Summary

Experiments were performed in order to study the phase behavior and morphologies of bicellar mixtures containing a lipid component with a negatively charged headgroup and the response of such anionic bicellar mixtures to hydrostatic pressure. Variable-pressure ^{2}H NMR spectroscopy provided information about the behavior of the long chain and the short chain lipid components in the presence of the acidic lipid component at ambient and high pressure in comparison to bicellar mixtures.

Phase behavior was studied by comparing DMPC-d_{54}/DHPC (4:1) to DMPC-d_{54}/DMPG/DHPC (3:1:1) either at ambient or high pressure, DMPC-d_{54}/DMPG/DHPC (3:1:1) to DMPC/ DMPG-d_{54}/DHPC at either ambient or high pressure and DMPC-d_{54}/DMPG/DHPC phase behavior at ambient pressure to its phase behaviors at 41.4 MPa and 82.7 MPa. These observations, in conjunction with previous studies provide some insight into the influence of acidic lipid components in bicellar mixtures morphologies at ambient and high pressure.

The DMPC-d_{54}/DHPC (4:1) mixture was not found to enter an interdigitated gel

phase at 82.7 MPa while cooling. This result is in consistent with previous ^{2}H NMR studies of bicellar mixtures at high pressure [63]. The reason that the phase behavior of DMPC-d_{54}/DHPC (4:1) was re-examined at this specific pressure (82.7 MPa) and under specific conditions of thermal cycling was to compare its behaviour with that of the anionic mixture, DMPC-d_{54}/DMPG/DHPC (3:1:1), which did show evidence for interdigitation under some conditions.

^{2}H NMR spectra shown in Fig. 4.3 indicate that DMPC-d_{54}/DMPG/DHPC (3:1:1) mixtures show the same sequence of phase morphologies as DMPC-d_{54}/DHPC (4:1) at ambient pressure. The anionic bicellar mixtures were found to form bilayered disks with isotropic reorientation at temperatures lower than the gel-liquid transition temperature of the long chain lipid component, nematic worm-like or ribbon-like micelles at intermediate temperatures, and lamellar vesicles at high temperatures [24, 46]. The isotropic-nematic and nematic-lamellar transition temperatures are higher for DMPC-d_{54}/DMPG/DHPC (3:1:1) than for DMPC-d_{54}/DHPC (4:1) by few degrees which may be partly due to the lower fraction of deuterated lipid in DMPC-d_{54}/DMPG/DHPC (3:1:1) mixtures[60]. Furthermore, it was observed that the presence of DMPG facilitates the magnetic orientation of bicellar assemblies. This can be concluded by comparing the spectra obtained at low magnetic field for DMPC-d_{54}/DHPC (Figure 4.1) to those obtained under the same conditions for DMPC-d_{54}/DMPG/DHPC (Figure 4.4).

The phase transition temperatures have been observed to rise with increasing pressure for the anionic bicellar mixture. The magnetically completely oriented nematic worm-like micelle phase has not been observed at 82.7 MPa. At this pressure, DMPC-d_{54}/DMPG/DHPC (3:1:1) samples sometimes displayed a transition directly from the

isotropic phase to the lamellar vesicle phase at high temperature (for example, Figure 4.8a which shows the second warming of the ARB11 sample at 82.7 MPa) and sometimes displayed a transition from the isotropic phase to an unoriented, anisotropic phase at intermediate temperature and then a second transition to the lamellar vesicle phase at higher temperature (for example, Figure 4.6a which shows the initial warming of the ARB11 sample at 82.7 MPa). This suggests that phases of the anionic bicellar mixture may display metastability under some conditions, particularly at high pressure.

Using just the results from ambient pressure and 41.4 MPa (Figures 4.1-4.5), the temperature at which orientation of the DMPC-d_{54}/DMPG/DHPC (3:1:1) nematic phase appeared on warming was found to increase with pressure at a rate of $\sim 0.21\,^{\circ}\mathrm{C/MPa}$. The temperature at which the vesicle phase of this mixture appeared increased with pressure at a rate of $\sim 0.19\,^{\circ}\mathrm{C/MPa}$. These are similar to the pressure sensitivities of the transitions observed for DMPC-d_{54}/DHPC (4:1).

As shown in Fig. 4.8, spectra for DMPC-d_{54}/DMPG/DHPC (3:1:1) were collected at 82.7 MPa, while warming and cooling, which indicate the occurrence of a transition into an interdigitated gel phase on cooling at 82.7 MPa. The interdigitated gel phase can be characterized by a doublet with a large splitting. Within this doublet, it is not possible to resolve distinct splittings for deuterons on specific chain segments. This suggests that the chains in the interdigitated phase are very straight with little dependence of orientational order parameters on position along the chain. This interdigitated gel phase has been observed under different experimental circumstances which could indicate that its occurrence is sensitive to experimental parameters that may not yet be consistently controlled. However, cooling at 82.7 MPa has been found

to consistently result in formation of the interdigitated gel phase in the anionic bicellar mixtures studied here. It also has been observed that once the interdigitated gel phase was formed, it can be observed under other conditions such as ambient pressure, 41.4 MPa, after freezing, and being subjected to the sonication and cycles of freeze-thaw.

Mixtures with chain pre-deuterated DMPG molecules were prepared to determine the involvement of DMPG molecules in different morphologies and phases and whether the DMPG and DMPC components were in the same environments in these mixtures. DMPC/DMPG-d_{54}/DHPC (3:1:1) shows spectral characteristics that are qualitatively similar to those of DMPC-d_{54}/DMPG/DHPC (3:1:1). DMPG-d_{54} molecules undergo isotropic-nematic and nematic-lamellar transitions at ambient at higher temperatures than DMPC-d_{54}/DMPG/DHPC (3:1:1), likely due to the lower fraction of chain deuterated component. It is shown in Fig. 4.9 that DMPG-d_{54} molecules are in effectively the same environment as DMPC-d_{54} within the interdigitated gel phase for anionic bicellar mixtures. This confirms that interdigitation, as observed here, is not the result of DMPG being separated from DMPC as a result of temperature or pressure cycling.

The observations of DMPC-d_{54}/DMPG/DHPC (3:1:1) without sonication and freeze-thaw cycling confirm that interdigitation is also not a result of lipid particle sizes relaxing to a "pre-sonication" state as a result of temperature or pressure cycling. The DMPC-d_{54}/DMPG/DHPC particles with, presumably, a larger initial size due to the absence of sonication and freeze-thaw cycling isotropic-nematic-lamellar phases at ambient pressure. The interdigitated gel phase has not been observed for this non-sonicated mixture. This may have been due to lack of sonication or the highest temperature to which the non-sonicated sample was warmed.

Bibliography

[1] Alberts B., *Molecular Biology of the Cell*, **5th Ed.**, (2008)

[2] Bax A., Grishaev A., "Weak Alignment NMR: A Hawk-eyed View Of Biomolecular Structure.", *Curr. Opin. Struct. Biol.*, **15(5)**, 563-570, 2005.

[3] Ceve G., Marsh D., *Phospholipid Bilayers*, John Wiley & Sons Inc., New York (1987)

[4] Bloom M., Evans E., Mouritsen O.G., "Physical properties of the fluid lipidbilayer component of cell membranes: a perspective.", *Q. Rev. Biophys.*, **24** 293-397, 1991.

[5] Lehninger A. L. , Nelson, D. L., Cox M. M., *Principles of Biochemistry.*, **5**th ed., New York, (2008)

[6] Yeagle P. L., *The structure of biological membranes*, CRC press,**2nd Ed.**,54. (2005)

[7] Heimburg T., *Thermal Biophysics of membrane*, Wiley-VCH verlag GmbH and co. 16. (2007)

[8] Arora A., Tamm L. K., "Biophysical approaches to membrane protein structure determination.", *Curr. Opin. Struct. Biol.*, 11 Issue 5, 540-547, 2001.

[9] Strenk L. M., Westerman P. W. , and Doane J. W. . "A model of orientational ordering in phosphatidylcholine bilayers based on conformational analysis of the glycerol backbone region.", *Biophysics Journal*, **48(5)**, 765-773, 1985.

[10] Luzzati V., *Biological membrane*, **V.1**, Edited bu Chapman, Academic press, London. (1968)

[11] Hauser H., "Shortchain Phospholipids as detergents", *Biochem. Biophys. Acta*, **1508**, 164-181, 2000.

[12] Kleinschmidt J.H., Tamm L.K, "Structural transitions in shortchain lipid assemblies studied by (31)PNMR spectroscopy.", *Biophys. J.*, **83(2)**, 994-1003, 2002.

[13] Simon S.A., MacIntosh Y.J., "Interdigitated hydrocarbon chain packing causes the biphasic transition behavior in lipid/alcohol suspensions.", *Biochim. Biophys. Acta, Biomembr.* **773(1)**, 169, 1984.

[14] Boggs, J.M., and Mason J.T., "Calorimetric and fatty acid spin label study of subgel and interdigitated gel phases formed by asymmetric phosphatidylcholines.",*Biochim. Biophys. Acta.*,**863(2)** , 231-242, 1986.

[15] Hui, S.W., and Huang C., "Xray diffraction evidence for fully interdigitated bilayers of 1stearoyllysophosphatidylcholine.",*Biochemistry (Easton)*, **25(6)**, 1330, 1986.

[16] Adachi, T., H. Takahashi, K. Ohki, Hatta I., "Interdigitated Structure of PhospholipidAlcohol Systems Studied by XRay Diffraction.", *Biophys. J.*, **68(5)**, 1850-1885, 1995.

[17] Singh, H., and Morrow M.R., "Pressure induces interdigitation differently in DPPC and DPPG.", *Eur. Biophys. J.*, **37(6)**, 783, 2008.

[18] Sandres C. R., Schwonk J. P., "Characterization of magnetically orientable bilayers in mixtures if dihexanoylphosphatidylcholine and dimyristoylphosphatidylcholine by solid state NMR", *Biochemistry*, **31** 8898-8905. 1992.

[19] Nieh, M. P., Raghunathan, V. A. Wang, H., Katsaras, J., "Highly aligned lamellar lipid domains induced by macroscopic confinement." *Langmuir*, **19**, 6936-6941, 2003.

[20] Davis, J. H., "Deuterium Magnetic Resonance Study of the Gel and Liqui Crystalline Phases of the Dipalmitoyl Phosphatidylcholine." *Biophys. J.*, **27**,339-358, 1979.

[21] Struppe J., Vold R. R., "Dilute bicellar solutions for structural NMR work", *J. Magn. Reson.*, **135** 541-546. 1988.

[22] Sandres C. R., Presser R. S., "Bicelles: a model membrane system for all seasons", *Structure*,1227-1234. 1998.

[23] Prosser, R. S., J. S. Hwang,Vold R. R., "Magnetically Aligned Phospholipid Bilayers with Positive Ordering: A New Model Membrane System.", *Biophys. J.*, **74(5)**, no. 5, 2405-2418, 1998.

[24] Sterniu E., Nizza D., Gawrisch K., "Temperature Dependence of DMPC/DHPC Mixing in a Bicellar Solution and Its Structural Implications", *Langmuir*, **17**, 2610-2616. 2001.

[25] Vold, R. R., Prosser R. S., "Magnetically oriented phospholipid bilayered micelles for structural studies of polypeptides: does the ideal bicelle exist?.", *J. Magn. Reson.*, B, **113**, 267-271,1996.

[26] Vold, R. R., Prosser, R. S., Deese, A. J., "Isotropic solutions of phospholipid bicelles: A new membrane mimetic for highresolution NMR studies of polypeptides". *J. Biomol. NMR*, **9**, 329-335, 1997.

[27] Luchette, P. A., Vetman, T. N., Prosser, R. S., Hancock, R. E. W., Nieh, M. P.; Glinka, C. J., Krueger, S., Katsaras, J." Morphology of fasttumbling bicelles: a small angle neutron scattering and NMR study." *Biochim. Biophys. Acta*, 1513(2), 83-94. 2001.

[28] Stamatoff, J., D. Guillon. L. Powers, P. Cladis, Aadsen D. . "XRay Diffraction Measurements of Dipalmitoylphosphatidylcholine as a Function of Pressure.", *Biochem. Biophys. Res. Commun.*, **85 (2)**, 724-728. 1978.

[29] Choma, C.T. , Wong P.T.T. . "The Structure of Anhydrous and Hydrated Dimyristoylphosphatidyl Glycerol a Pressure Tuning Infrared Spectroscopic Study.", *Chem. Phys. Lipids*, **61 (2)**. 131-137, 1992.

[30] Ahn, T., Oh D.B., Lee B.C., Yun C.H. "Importance of Phosphatidylethanolamine for the Interaction of Apocytochrome c with Model Membranes Containing Phosphatidylserine.", *Biochemistry*, **39 (33)**, 10147-10153. 2000.

[31] Winter, R., Pilgrim W.C., "A Sans Study of High-Pressure Phase-Transitions in Model Biomembranes.", *Ber. Bunsenges. Phys. Chem.*, **93 (6)**, 708-717. 1989.

[32] Prasad S.K., Shashidhar R., Gaber B.P., Chandrasekhar S.C., "Pressure Studies on 2 Hydrated Phospholipids 1,2-DimyristoylPhosphatidylcholine and 1,2Dipalmitoyl Phosphatidylcholine.", *Chem. Phys. Lipids*, **43 (3)**, 227-235. 1987.

[33] Liu N.I.,Kay R.L., "Redetermination of PressureDependence of Lipid Bilayer PhaseTransition.", *Biochemistry*, **16 (15)**, 3484-3486. 1977.

[34] Wong, P.T.T., Mantsch H.H., "A LowTemperature Structural PhaseTransition of 1,2DipalmitoylSnGlycero3Phosphocholine Bilayers in the Gel Phase.", *Biochim. Biophys. Acta*, **732(1)**, 92-98. 1983.

[35] Harroun,T.A., Koslowsky M., Nieh M.P., de Lannoy C.F., Raghunathan V.A., Katsaras J. "Comprehensive Examination of Mesophases Formed by DMPC and DHPC Mixtures.", *Langmuir*, **21(12)**, 5356-5361. 2005.

[36] Rowe, B. A., Neal S. L., "Fluorescence probe study of bicelle structure as a function of temperature: Developing a practical bicelle structure model." *Langmuir*, **19**, 2039-2048, 2003.

[37] Nieh M.P., Raghunathan V.A., Glinka C.J., Harroun T.A., Pabst G., Katsaras J., "Magnetically Alignable Phase of Phospholipid "Bicelle" Mixtures is a Chiral Nematic made Up of Wormlike Micelles.", *Langmuir*, **20(19)**, 7893-7897. 2004.

[38] Nieh M.P., Glinka C.J., Krueger S. , Prosser R.S., Katsaras J., "SANS Study of the Structural Phases of Magnetically Alignable LanthanideDoped Phospholipid Mixtures.", *Langmuir*,**17(9)**, 2629-2638. 2001.

[39] Struppe J., Komives A., Taylor, S. S., Vold, R. R., " 2H NMR studies of a myristoylated peptide in neutral and acidic phospholipid bicelles.", *Biochemistry* ,**37** , 15523-15527.1998.

[40] Struppe, J., Whiles J. A., Vold R. R., "Acidic phospholipid bicelles: a versatile model membrane system.", *Biophys. J.*, **78**, 281-289, 2000.

[41] Palleboina D., Waring A. J., Notter R. H., Booth V., Morrow M. ,"Effects of the lung surfactant protein B construct MiniB on lipid bilayer order and topography", *Eur. Biophys. J.*, **41**, 755-767, 2012.

[42] Nieh M.P., Raghunathan V. A., Glinka C. J., Harroun T., Katsaras J., "Structural phase behavior of high concentration, alignable biomimetic bicelle mixtures.", *Macromol. Symp.*, **219**, 135-145, 2005.

[43] Soong R., Macdonald P. M., "Water Diffusion in Bicelles and the Mixed Bicelle Model.", *Langmuir*, **25(1)**, 380-390, 2009.

[44] van Dam L., Karlsson G. , Edwards K., " Direct Observation and Characterization of DMPC/DHPC Aggregates Under Conditions Relevant for Biological Solution NMR.", *Biochim. Biophys. Acta, Biomembr.*, **16(2)**, 241-256. 2004.

[45] Winter R., Jeworrek C., "Effect of Pressure on Membranes.", *Soft Matter*, **5(17)**, 3157-3173. 2009.

[46] Soong R., Nieh M.P., Nicholson E., Katsaras J., Macdonald P. M., " Bicellar Mixtures Containing Pluronic F68: Morphology And Lateral Diffusion From Combined SANS And PFG NMR Studies.", *Langmuir*, **26(4)**, 2630-2638, 2009.

[47] Winter R., *High Pressure Bioscience and Biotechnology*, **2nd ed.**, SpringerVerlag, Heidelberg, (2003)

[48] Silverman J. A., Deitcher S. R.," Marqibo (R) (Vincristine Sulfate Liposome Injection) Improves the Pharmacokinetics and Pharmacodynamics of Vincristine.", *Cancer Chemoth. Pharm.*, **71(3)**, 555-564, 2013.

[49] Dai Z. J., Li S., Gao J., Xu X.N., Lu W.F., Lin S., Wang X.S., "Sonodynamic Therapy (SDT): A Novel Treatment of Cancer Based on Sonosensitizer Liposome as a New Drug Carrier.", *Med. Hyp..*, **80(3).**, 300-302, 2013.

[50] Brown A., Skanes I., and Morrow M.R., "PressureInduced Ordering in MixedLipid Bilayers." , *Phys. Rev. E*, **69(1)**, 2004.

[51] Bonev B.B., Morrow M.R., "H2 NMR Studies of Dipalmitoylphosphatidylcholine and DipalmitoylphosphatidylcholineCholesterol Bilayers at High Pressure." , *Can. J. Chem.*, **76(11)**, 1512-1519, 1998.

[52] Bonev B.B.. Morrow M.R., "Effects of Hydrostatic Pressure on Bilayer Phase Behavior and Dynamics of Dilauroylphosphatidylcholine.", *Biophys. J.*, **70(6)**, 2727-2735, 1996.

[53] Bonev B.B., Morrow M.R., "Simple Probe For Variable Pressure Deuterium Nuclear Magnetic Resonance Studies Of Soft Materials.", *Rev. Sci. Instrum.*, **68(4)**, 1827, 1997.

[54] Bonev B.B., Morrow M.R., "Effect of Pressure on the Dimyristoylphosphatidylcholine Bilayer Main Transition.", *Phys. Rev. E*, **55(5)** : 5825-5833, 1997.

[55] Bonev B.B., Morrow M.R., "Hydrostatic PressureInduced Conformational Changes in Phosphatidylcholine Headgroups, a 2H NMR Study.", *Biophys. J.*, **69(2)**, 518-523, 1995.

[56] Driscoll D.A., Samarasinghe S., Adamy S., Jonas J., Jonas A., "Pressure Effects on Dipalmitoylphosphatidylcholine Bilayers Measured by 2 H NuclearMagneticResonance.", *Biochemistry*, **30(13)**, 3322-3327, 1991.

[57] Braganza L.F., Worcester D.L. . "HydrostaticPressure Induces Hydrocarbon Chain Interdigitation in SingleComponent PhospholipidBilayers.", *Biochemistry*, **25(9)**, 2591-2596, 1986.

[58] Utoh S., Takemura T., "PhaseTransition of Lipid Multilamellar Aqueous Suspension Under HighPressure Investigation of PhaseDiagram of Dipalmitoyl Phosphatidylcholine Bimembrane by High Pressure DTA and Pressure Dilatometry." *Jpn. J. Appl. Phys., Part 1*, **24(3)**, 356-360, 1985.

[59] Wong P.T.T., Siminovitch D.J., Mantsch H.H., "Structure and Properties of Model Membranes: New Knowledge from High Pressure Vibrational Spectroscopy." *Biochim. Biophys. Acta* ,**Acta 947(1)**, 139-171, 1988.

[60] Uddin, Md. N., "Investigation of the phase behavior of bicellar mixtures by diffrential scanning calorimetry and variable pressure by ^{2} H NMR. " MSc diss., Memorial University of Newfoundland, 2010.

[61] Tristramnagle S., " Measurement Of Chain Tilt Angle In Fully Hydrated Bilayers Of Gel Phase Lecithins." *Biophys. J.*, **64(4)**, 1097-1109, 1993.

[62] Tristramnagle S., Liu Y., Legleiter J. , Nagle J., "Structure Of Gel Phase DMPC Determined By XRay Diffraction." *Biophys. J.*, **83(6)**, 3324-3335, 2002.

[63] Uddin Md N., Morrow M.R., "Bicellar Mixture Phase Behavior Examined by VariablePressure Deuterium NMR and Ambient Pressure DSC.", *Langmuir*, **26 (14)**, 12104-12111. 2010.

[64] Kozak M., Kempka M., Szpotkowski K., Jurga S., "NMR in Soft Materials: A Study of DMPC/DHPC Bicellar System.", *J. Non-Cryst. Solids*, **353 (4751)**, 4246-4251. 2007.

[65] Seelig J., "Deuterium magnetic resonance: theory and application to lipid membranes", *Q. Rev. Biophys.*, **10(3)**, 353-418, 1977.

[66] Levitt M. H., "Magnetism", *Spin dynamics: basics of nuclear magnetic resonance.*, Chichester: John Wiley & Sons, 2001.

[67] Maraviglia, B., "NMR studies of membrane and whole cells", *Physics of NMR spectroscopy in biology and medicine*, North Holland physics publishing, Amsterdam, 121-157, (1988).

[68] Burnett L.J., Muller B.H., "Deuteron Quadrupole Coupling Constants in Three Solid Deuterated Paraffin Hydrocarbons: C2D6, C4D10, C6D14." *J. Chem. Phys.*, **55(12)**, 5829, 1971.

[69] Davis J. H., "The description of membrane lipid conformation, order and dynamics by 2H NMR.", *Biochim. Biophys. Acta.*, **737**, 117-171, 1983.

[70] Davis J.H, "Deuterium Nuclear Magnetic Resonance spectroscopy in partially ordered systems", *Isotopes in the physical and biomedical science*, **V 2**, Elsevier science publishers B. V., 99-157, 1991.

[71] Davis J. H., Jeffrey K. R., Bloom M.. Valic M. I., Higgs T. P. "Quadrupole Echo Deuteron Magnetic Resonance Spectroscopy in Ordered Hydrocarbon Chains." *Chem. Phys. Lett.*, **42:** 46874696, 1976.

[72] Kilfoil M. L., Morrow M. R., "Slow Motions in Bilayers Containing Anionic Phospholipid.", *Physica A.*, **261**, 82-94, 1998.

[73] Pauls K. P., MacKay A. L., Soderman O., Bloom M., Tanjea A. K., Hodges R. S., "Dynamic Properties of the Backbone of an Integral Membrane Polypeptide Measured by 2HNMR.", *Eur. Biophys. J.*, **12**, 1-11, 1985.

[74] Morrow M. R., Stewart J., Taneva S., Dico A., Keough K. M.W. " Perturbation of DPPC Bilayers by High Concentrations of Pulmonary Surfactant Protein SPB., *Eur. Biophys. J.*, **33**, 285-290, 2004.

[75] Prosser R. S., Davis J. H., Dahlquist F. W., Lindorfer M.A. " 2H nuclear magnetic resonance of the gramicidin A backbone in a phospholipid bilayer". *Biochemistry.* **30**, 4687-4696. 1991.

[76] Morrow, M.R.," Transverse Nuclear Spin Relaxation In Phosphatidylcholine Bilayers Containing Gramicidin." *Biochim. Biophys. Acta, Biomembr.*, **1023(2)**, 197-205, 1990.

[77] MacEachern L., Sylvester A., Flynn A., Rahmani A., Morrow M. R., " Dependence of Bicellar System Phase Behavior and Dynamics on Anionic Lipid Concentration.", *Langmuir*, **29(11)**, 3688-3699.2013

[78] Katsaras J., Harroun T. A.. Pencer J., Nieh M.P., " "Bicellar" Lipid Mixtures As Used In Biochemical And Biophysical Studies.", *Prax. Naturwiss*, **92(8)**, 355-366, 2005.

[79] Raffard G., Steinbeuckner S., Arnold A., Davis J. H, Dufourc E. J," Temperature composition diagram of dimyristoylphosphatidylcholine dicaproylphosphatidylcholine "bicells" self orienting in the magnetic field. A solid state ^{2}H NMR and ^{2}P NMR study.", *Langmuir*, **16**, 7655-7662, 2000.

[80] Nieh M.P., Glinka C., Krueger S., Prosser R., Katsaras J., "SANS Study On The Effect Of Lanthanide Ions And Charged Lipids On The Morphology Of Phospholipid Mixtures." *Biophys. J.*, **82(5)**,2487-2498, 2002.

[81] Triba M. N., Warschawski D. E., Devaux P. F., "Reinvestigation By Phosphorus NMR Of Lipid Distribution In Bicelles."*Biophys. J.*, **88(3)**, 1887-1901, 2005.

Appendix A

^{2}H NMR spectra The following Appendix includes the complete set of ^{2}H NMR spectra obtained over the course of this work.
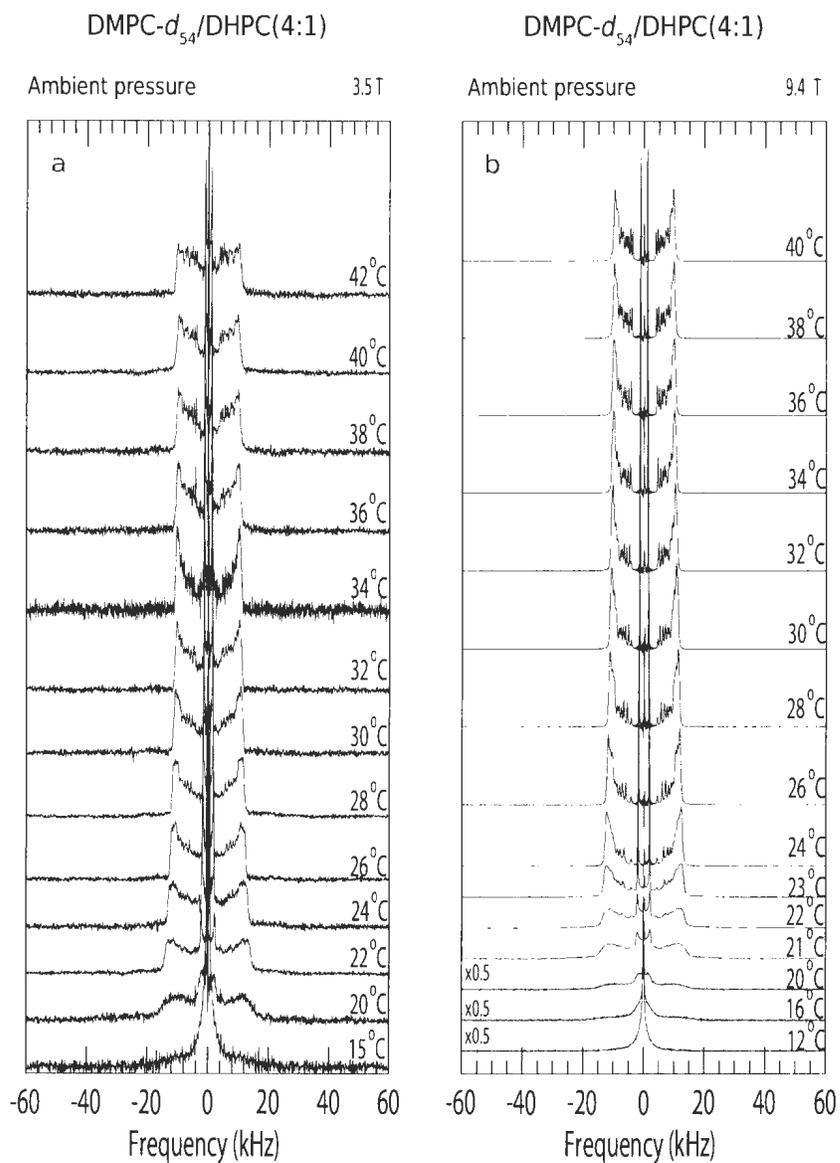
Fig. A. 1: Deuterium NMR spectra for DMPC-d_{54}/DHPC (4:1) obtained with (a) the 3.5 T superconductive magnet and (b) the 9.4 T magnet at ambient pressure for a range of temperatures. Spectra were collected from low to high temperature. The sample is denoted as AR01.
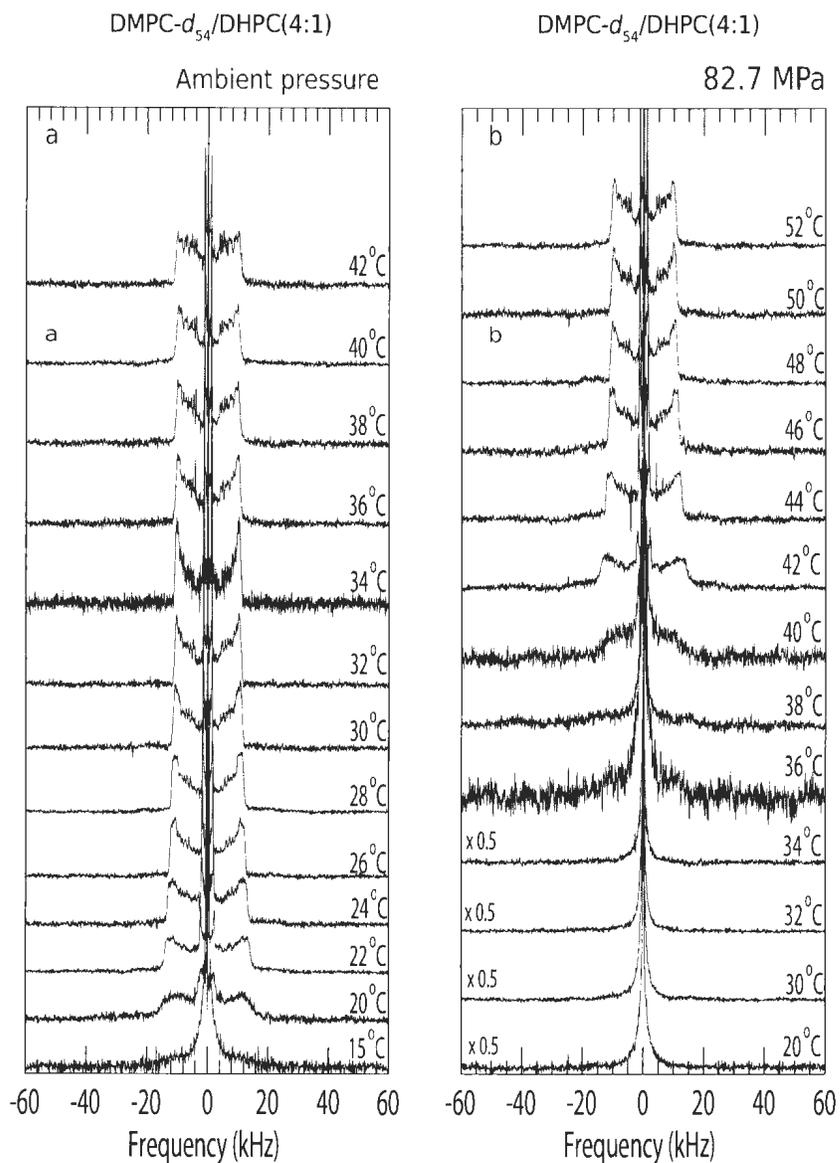
Fig. A. 2: Deuterium NMR spectra for DMPC-d_{54}/DHPC (4:1) obtained with 3.5 T superconductive magnet at (a) ambient pressure and (b) 85 MPa for a range of temperatures. Spectra were collected from low to high temperature. The sample is denoted as AR01 at ambient pressure and ARA1 at 85 MPa.

DMPC-d_{54}/DHPC (4:1)   DMPC-d_{54}/DHPC (4:1)

Ambient pressure   82.7 Mpa
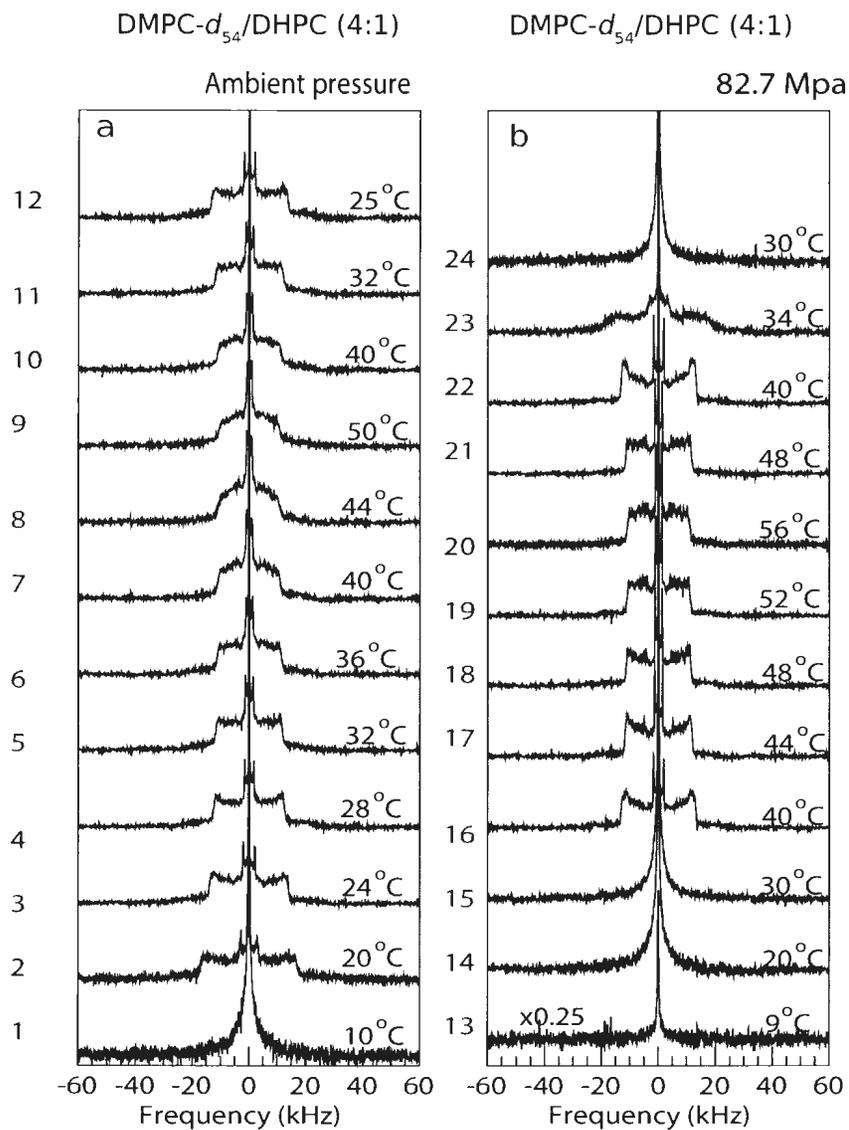
Fig. A. 3: Deuterium NMR spectra for DMPC-d_{54}/DHPC (4:1) obtained, in the order shown, with 3.5 T superconductive magnet for the second cycle of warming and cooling at (a) ambient pressure (b) 85 MPa for a range of temperatures. The sample is denoted as ARM1 at ambient pressure and ARMB1 and 85 MPa.
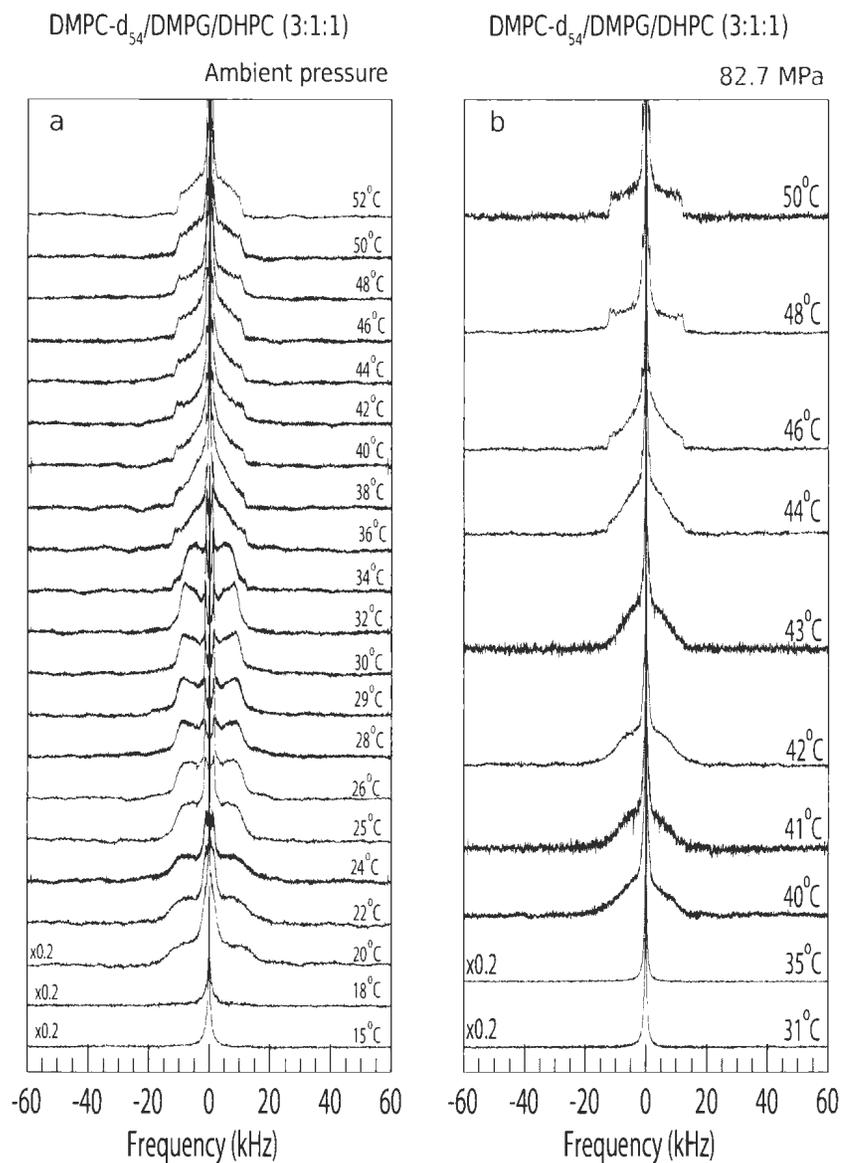
Fig. A. 4: Deuterium NMR spectra for DMPC-d_{54}/DMPG/DHPC (3:1:1) obtained with 3.5 T superconductive magnet at (a) ambient pressure and (b) 85 MPa for a range of temperatures. Panel (b) Pressure was cycled to 85 MPa five times before the pressure was raised from ambient pressure to 85 MPa at $\sim 25\,°C$. The sample is denoted as AR02 at ambient pressure and ARA2 at 85 MPa.

Figure A.5 shows the deuterium NMR spectra for DMPC-d_{54}/DMPG/DHPC (3:1:1) obtained with 3.5 T superconductive magnet at (a) ambient pressure and (b) 85 MPa for a range of temperatures. Panel (b) Pressure was cycled to 100 Mpa five times before the pressure was set to 85 MPa. The pressurization was done at high temperature ($\sim 30\,^\circ$C). Then the mixture was cooled to $10\,^\circ$C at 85 MPa without obtaining spectra. A set of spectra then were obtained while warming at high pressure. The pressurization at high temperature and cooling the mixture at that pressure might have been responsible for the observation of an interdigitated gel phase (b). The sample was denoted AR03 at ambient and ARA3 at 85 MPa.

Figure A.6 shows the spectra collected, in the order shown, for sample AR03 after acquisition of the ambient pressure and 85 MPa spectra in Figure A.5. After the mixture were displayed spectral characteristics of the interdigitated gel phase at 85 Mpa (A.5b), the mixture was frozen for 3 hours followed by being cycled to 85 MPa at $21\,^\circ$C. The pressure then was raised to 42.5 MPa. The spectra obtained during the process of warming at 42.5 MPa is shown in panel (a). As the temperature increases, the spectra seem to be characteristic of interdigitated gel phase at low temperatures ($21\,^\circ$C $\leq T \geq 38\,^\circ$C), non-interdigitated gel phase with a fraction of interdigitated gel phase component at intermediate temperatures ($42\,^\circ$C $\leq T \leq 46\,^\circ$C), and a complete non-interdigitated gel phase at high temperatures($\geq 48\,^\circ$C). The mixture was then cooled to the room temperature, depressurized and froze for 3 days. This was followed by sonication and 5 cycles of freeze-thaw. The spectra then obtained at ambient pressure, shown in (b), at $8\,^\circ$C, $12\,^\circ$C and $21\,^\circ$C. The mixture then was pressurized up to 42.5 MPa at $21\,^\circ$C after the pressure was cycled five times to 85 MPa. The spectra obtained at 42.5 MPa while warming is shown in Panel (b). The spectra are characteristic of the interdigitated gel phase over a range of temperatures. It can be seen that the doublet becomes sharper at higher temperatures. This suggests that the acyl

chains are still able to undergo axially symmetric reorientation in the interdigitated phase at higher temperatures. It is noteworthy to compare the temperatures at which the spectra are characteristic of gel phase for at 42.5 MPa and 85 MPa by comparing A.6 and A.5. This sample was labeled as ARB3 in the experiment corresponding to the panel (a) and ARC3 in the one corresponding to the panel (b).
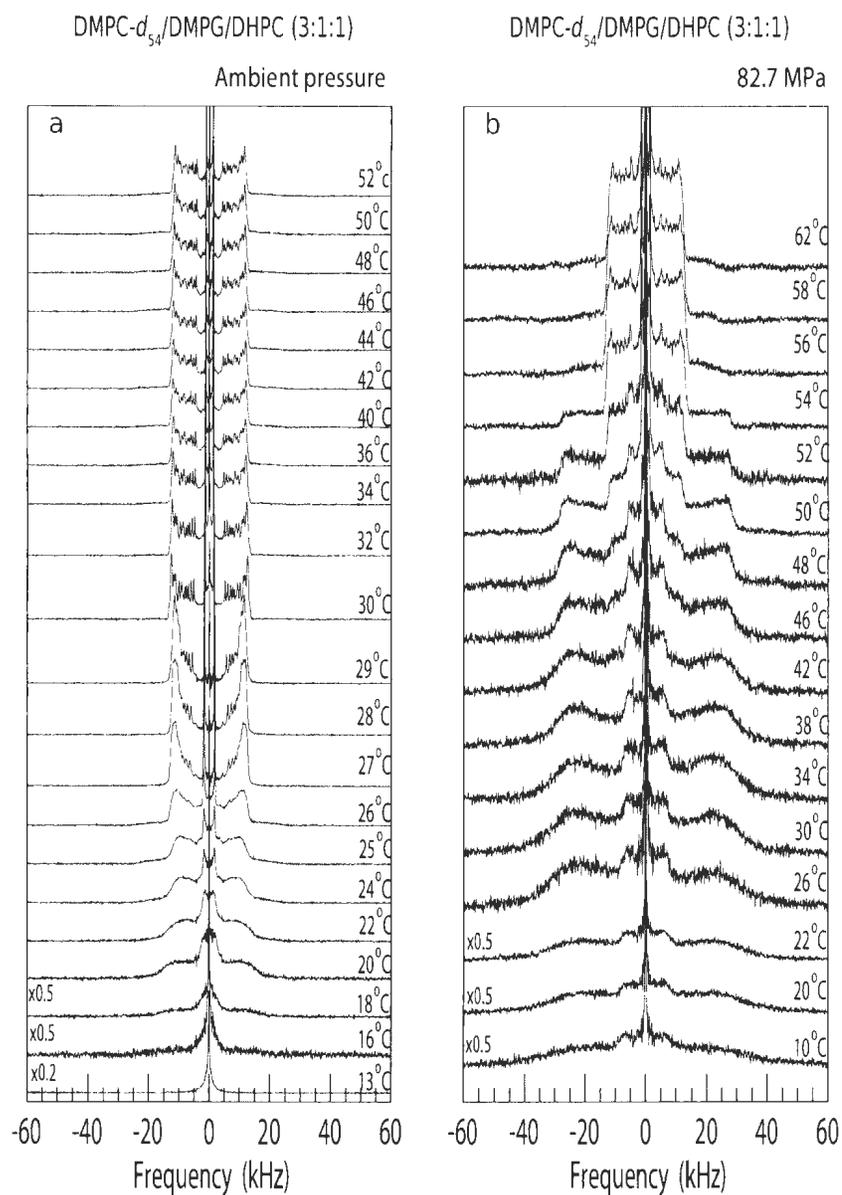
Fig. A. 5: Deuterium NMR spectra for DMPC-d_{54}/DMPG/DHPC (3:1:1) obtained with 3.5 T superconductive magnet at (a) ambient pressure and (b) 85 MPa for a range of temperatures. This sample was denoted as AR03 at ambient pressure and ARA3 at 85 MPa.

DMPC-d_{54}/DMPG/DHPC (3:1:1)   DMPC-d_{54}/DMPG/DHPC (3:1:1)

41.4 MPa
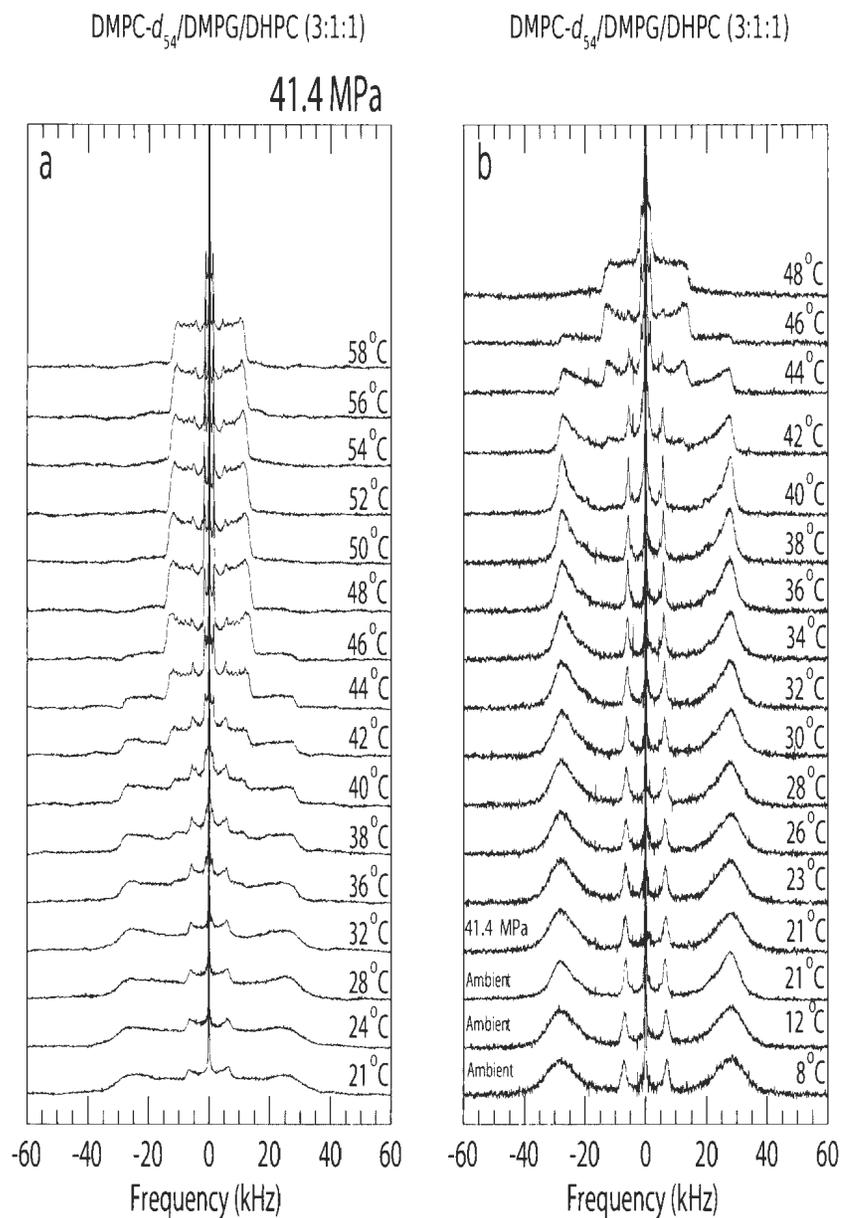
Fig. A. 6: Deuterium NMR spectra for DMPC-d_{54}/DMPG/DHPC (3:1:1) obtained with 3.5 T superconductive magnet at 42.5 MPa (a) after frozen for three hours and (b) after frozen for three days, sonicated followed by 5 cycles of freeze-thaw, for a range of temperatures. This sample was labeled as ARB3 in the experiment corresponding to the panel (a) and ARC3 in the one corresponding to the panel (b).

Figure A.7 shows Deuterium NMR spectra for DMPC-d_{54}/DMPG/DHPC (3:1:1) obtained with 3.5 T superconductive magnet at (a) ambient pressure and (b) 42.5 MPa for a range of temperatures. After the first cycle of warming, the sample cooled to 8 °C. The mixture was pressurized to 42.5 MPa, while showed spectral characteristics of the isotropic phase, at this temperature. The sample was denoted AR06 for the experiment performed at ambient and ARB6 for the one at 42.5 MPa.

Figure A.8 shows deuterium NMR spectra for DMPC-d_{54}/DMPG/DHPC (3:1:1) obtained with 3.5 T superconductive magnet at (a) 85 MPa and (b) ambient pressure using the same sample as the one used to obtain spectra shown in Figure A.7. After the first cycle of warming at ambient pressure and 42.5 MPa, as shown in Figure A.7, pressure dropped at 19 °C from 42.5 MPa to ambient pressure. The sample, then was pressurized up to 85 MPa while cooled further to 14 °C at ambient pressure. The spectra obtained while warming at 85 MPa is shown in Figure A.8a. The sample then cooled to 22 °C at 85 MPa without data acquisition. The pressure dropped to ambient pressure at this temperature. The spectra obtained while warming at ambient pressure is shown in Figure A.8 b The sample was denoted as ARB6 for the experiment performed at 85 MPa and ARC6 for the one performed at ambient pressure for the second time.
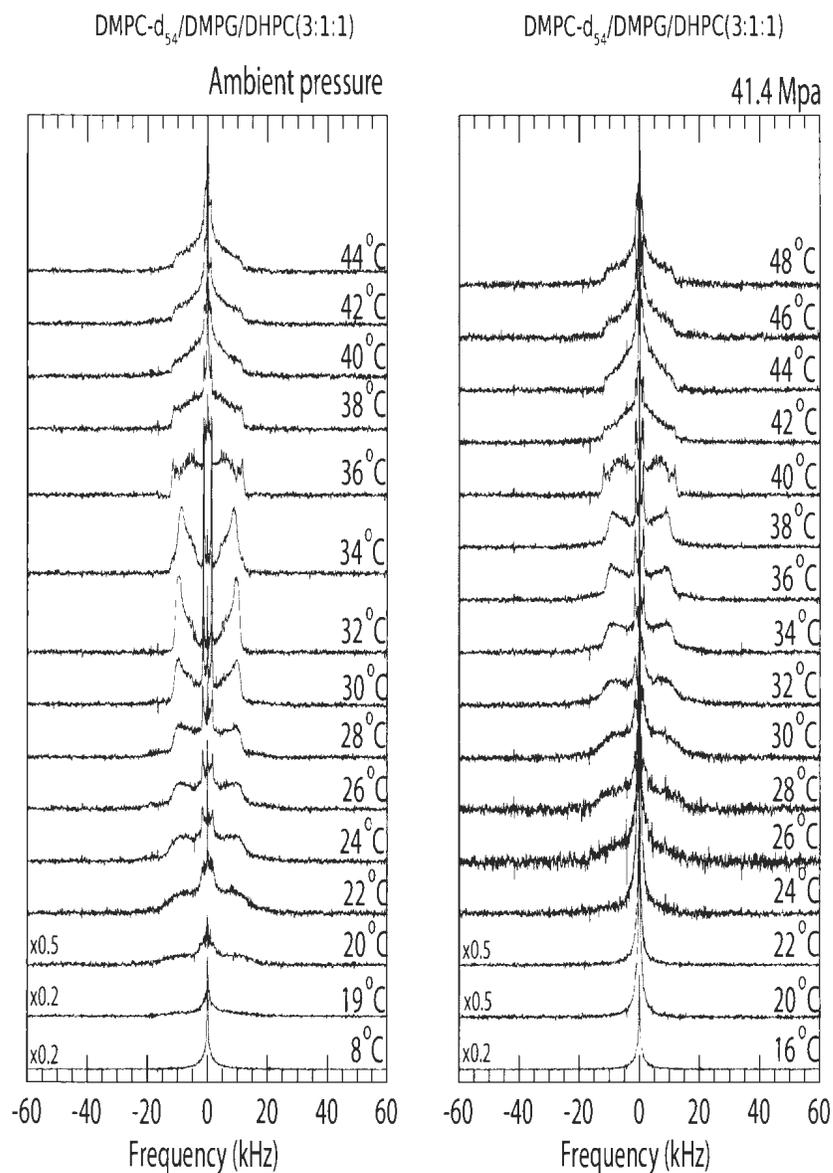
Fig. A. 7: Deuterium NMR spectra for DMPC-d_{54}/DMPG/DHPC (3:1:1) obtained with 3.5 T superconductive magnet at (a) ambient pressure and (b) 42.5 MPa for a range of temperatures. The sample was denoted AR06 for panel (a) and ARA6 for panel (b).

DMPC-d_{54}/DMPG/DHPC(3:1:1)   DMPC-d_{54}/DMPG/DHPC(3:1:1)
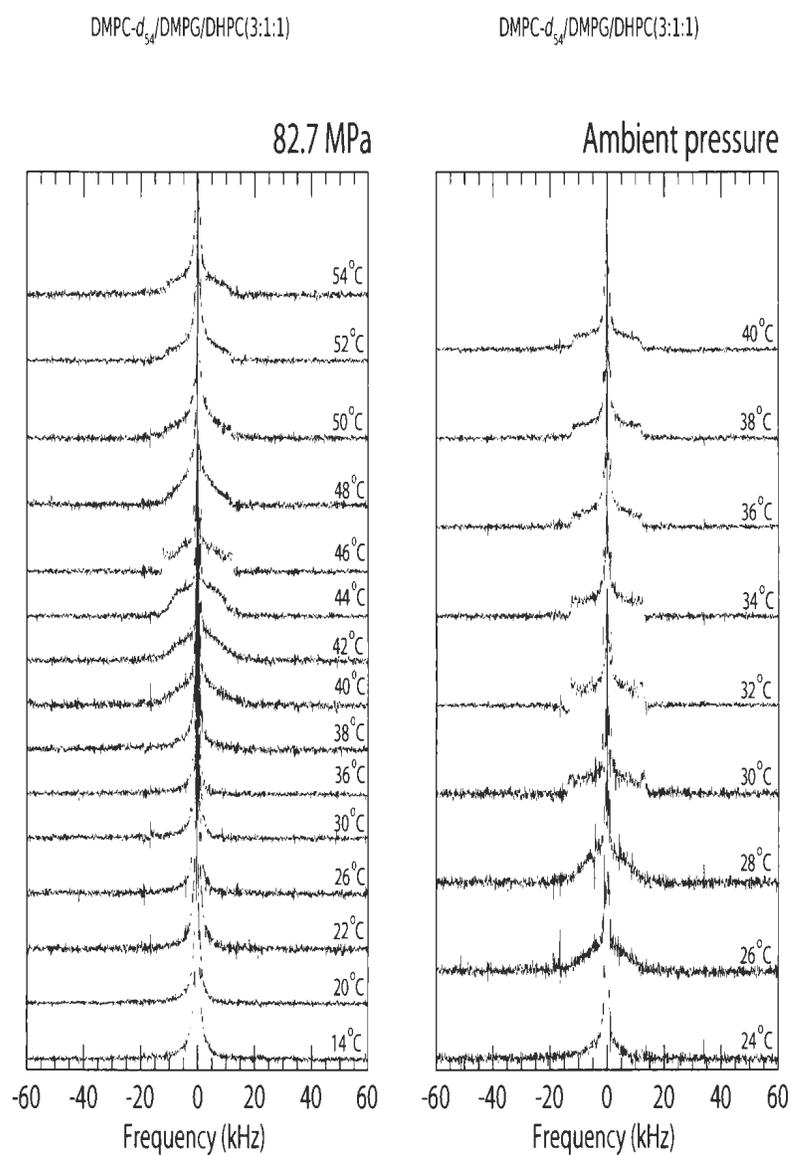
Fig. A. 8: Deuterium NMR spectra for DMPC-d_{54}/DMPG/DHPC (3:1:1) obtained with 3.5 T superconductive magnet at (a) 85 MPa and (b) ambient pressure. The sample was denoted ARB6 for panel (a) and ARC6 for panel (b).

Figure A.9 shows deuterium NMR spectra for DMPC-d_{54}/DMPG/DHPC (3:1:1) obtained with 9.4 T superconductive magnet at ambient performed by using the leftover of the AR06. The sample is denoted as AR07. It should be noted that the mixture did not equilibrate sufficiently during the course of this experiment. It might have been caused the lack of observation of oriented nematic phase over the course of this specific experiment.

DMPC-d$_{54}$/DMPG/DHPC(3:1:1)
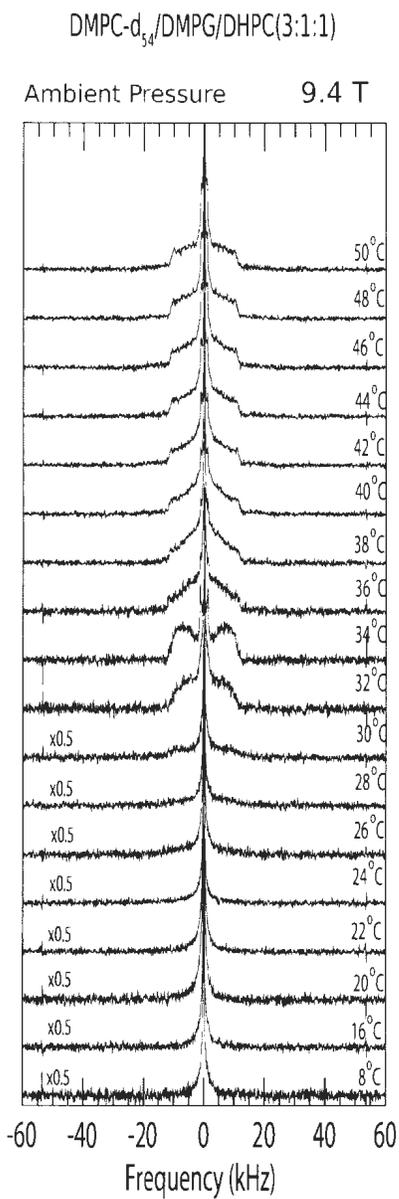
Fig. A. 9: Deuterium NMR spectra for DMPC-d_{54}/DMPG/DHPC (3:1:1) obtained with 9.4 T superconductive magnet at ambient pressure. This sample was labeled as AR07.

Figure A.10a shows deuterium NMR spectra for DMPC-d_{54}/DMPG/DHPC (3:1:1) at ambient pressure. The mixture then cooled to 8 °C and presurized up to 42.5 MPa at this temperature. The spectra obtained at 42.5 MPa while warming is shown in A.10b.

This mixture cooled to 8 °C and pressurized to 85 MPa. The spectra obtained for the cycle of warming at 85 MPa is shown in Figure A.11a. The pressure was accidentaly dopped at 48 °C and pressurized again up to 85 MPa. The spectra obtained while cooling is shown in A.10b. The mixture cooled at 85 MPa to 34 °C while the spectra obtained are characteristic of the interdigitated gel phase from 45 °C to 34 °C. The pressure then dropped to ambient pressure at 32 °C. The spectra obtained while cooling at ambient pressure, in the order shown in A.11b, are characteristic of a non-interdigitated gel phase at 32 °C. However, the spectra become more characteristic of an interdigitated gel phase on decreasing temperature. This may suggest that the temperature at which DMPC-d_{54}/DMPG/DHPC (3:1:1) mixtures with spectral characteristics of an interdigitated gel phase undergo into a phase with mostly non-interdigitated gel phase features varies by applying hydrostatic pressure. This sample was denoted as ARB8 for the experiment performed at 85 MPa while warming and ARC8 for the one performed while cooling.
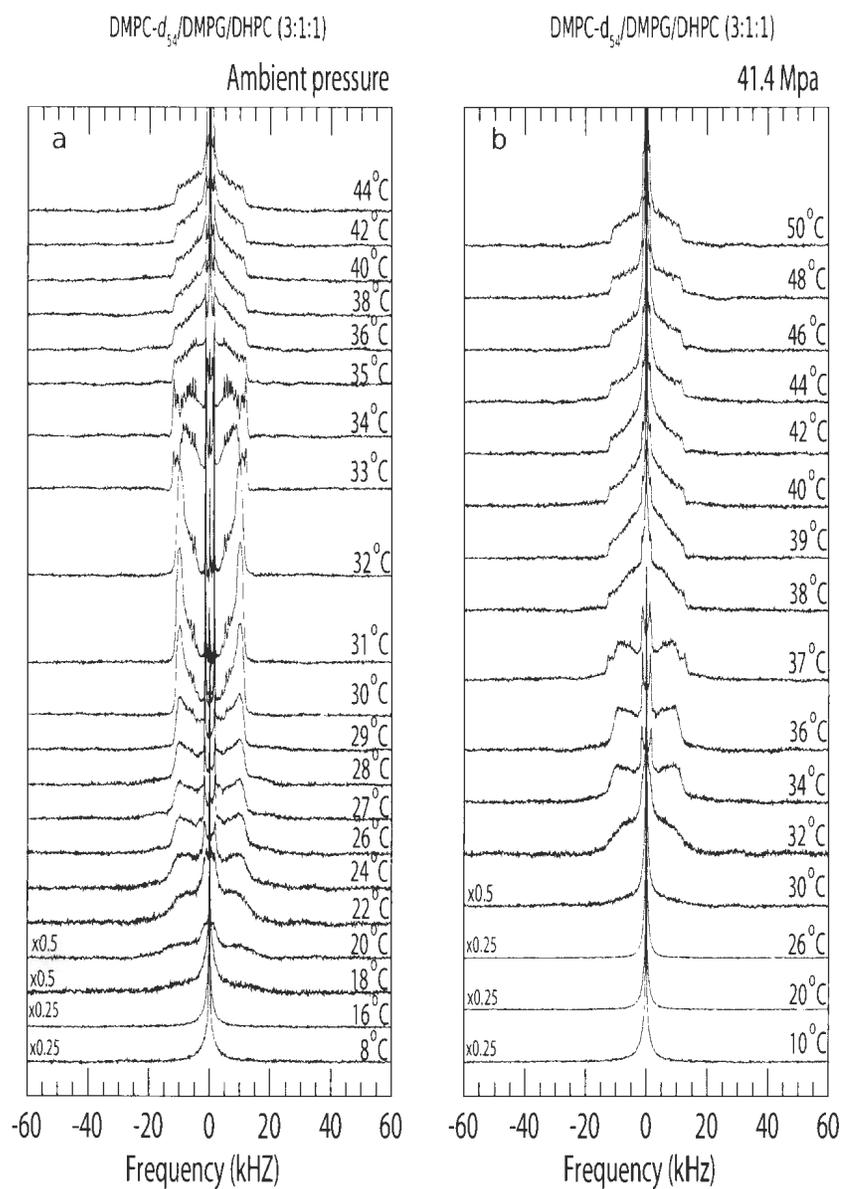
Fig. A. 10: Deuterium NMR spectra for DMPC-d_{54}/DMPG/DHPC (3:1:1) obtained with 3.5 T superconductive magnet at (a) ambient pressure and (b) 42.5 MPa. The pressure was raised at 8 °C. This sample was denoted as AR08 at ambient pressure and ARA8 at 42.5 MPa.
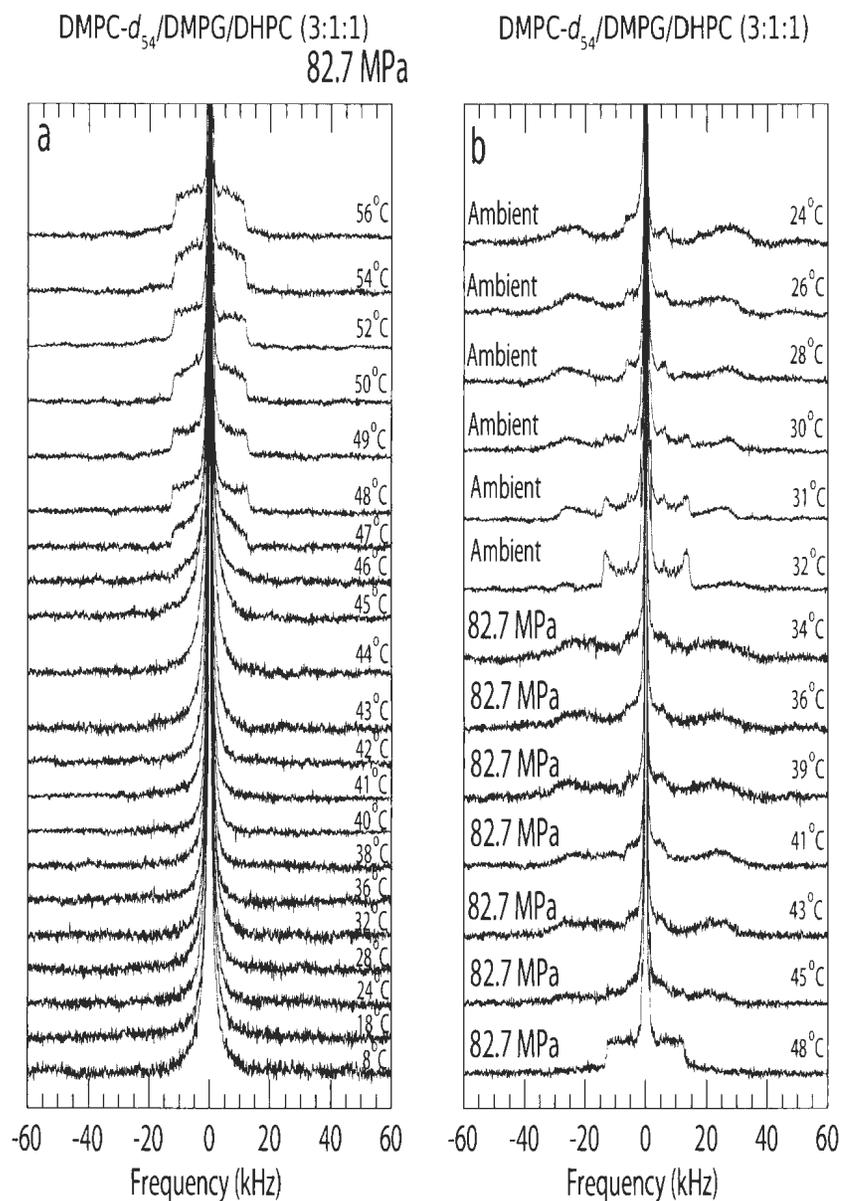
Fig. A. 11: Deuterium NMR spectra for DMPC-d_{54}/DMPG/DHPC (3:1:1) obtained with 3.5 T superconductive magnet at 85 MPa (a) while warming and (b) while cooling, in the order shown, at 85 MPa and at ambient pressure. This sample was denoted as ARB8 for the experiment performed at 85 MPa while warming and ARC8 for the one performed while cooling.

Figure A.12 shows the deuterium NMR spectra for the same sample as the one of which spectra obtained is shown in Figure A.11. After the sample underwent a transition into an interdigitated gel phase, as shown in Figure A.11, the mixture cooled to 8 °C and equilibrated for two hours at this temperature. The spectra obtained over the cycle of warming at ambient is shown in Figure A.12a. As can be seen, the spectra are characteristic of a non-interdigitated gel phase at temperature higher than 34 °C. The spectra obtained at ambient while cooling is shown in Figure A.12b. It was observed that the spectra become characteristic of the interdigitated gel phase again after passing 32 °C. For further inquiries, it is worth mentioning that the sample was denoted ARD8 during both warming and cooling process but saved with different extensions to distinguish the warming and cooling processes.
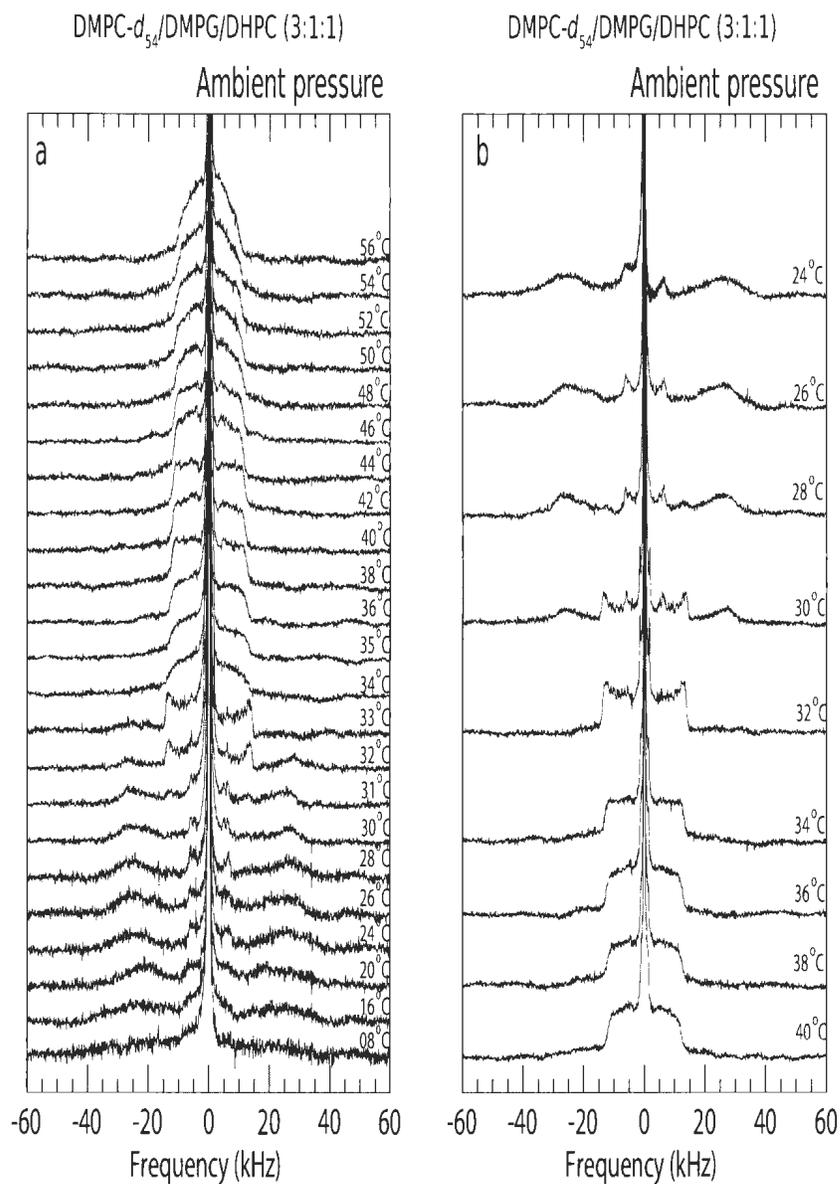
Fig. A. 12: Deuterium NMR spectra for DMPC-d_{54}/DMPG/DHPC (3:1:1) obtained, at ambient pressure while (a) warming and (b) cooling after the mixture formed an interdigitated gel phase during cooling process at high temperature as shown in Figure A11. This sample was denoted as ARD8.

Figure A.13a shows the deuterium NMR spectra for DMPC-d_{54}/DMPG/DHPC (3:1:1) obtained with the 3.5 T superconductive magnet at ambient pressure for the first cycle of warming. A.13b shows spectra for the second cycle of warming at ambient obtained within a short time after the first cycle. It should be noted that the spectra were obtained by averaging 2000 to 4000 transients at each temperature which is not adequate to obtain high resolution spectra using our setup. Furthermore, the mixture did not equilibrate adequately at each temperature. It might be helpful for further inquiries to note that the data acquired for this sample were saved under tha same name (AR09) but with different extensions.

This mixture then cooled to 8 °C and pressurized to 42.5 MPa. Figure A.14a shows the spectra obtained during the cycle of warming. This mixture cooled to 8 °C at 42.5 MPa with no spectrum obtained. The pressure was subsequently raised directly from 42.5 MPa to 85 MPa at this temperature. Figure A.14b shows the spectra obtained over increasing the temperature. The sample was labeled ARA9 for the experiment at 42.5 MPa and ARB9 for the one performed at 85 MPa.

To make the comparison easier, the same set of spectra as the one shown in A.14b is shown in Figure A.15a. The spectra obtained over the cycle of cooling at high pressure is shown in Figure A.15b. It worth mentioning that the data acquired while cooling are also saved as ARB9 but with a different extension.
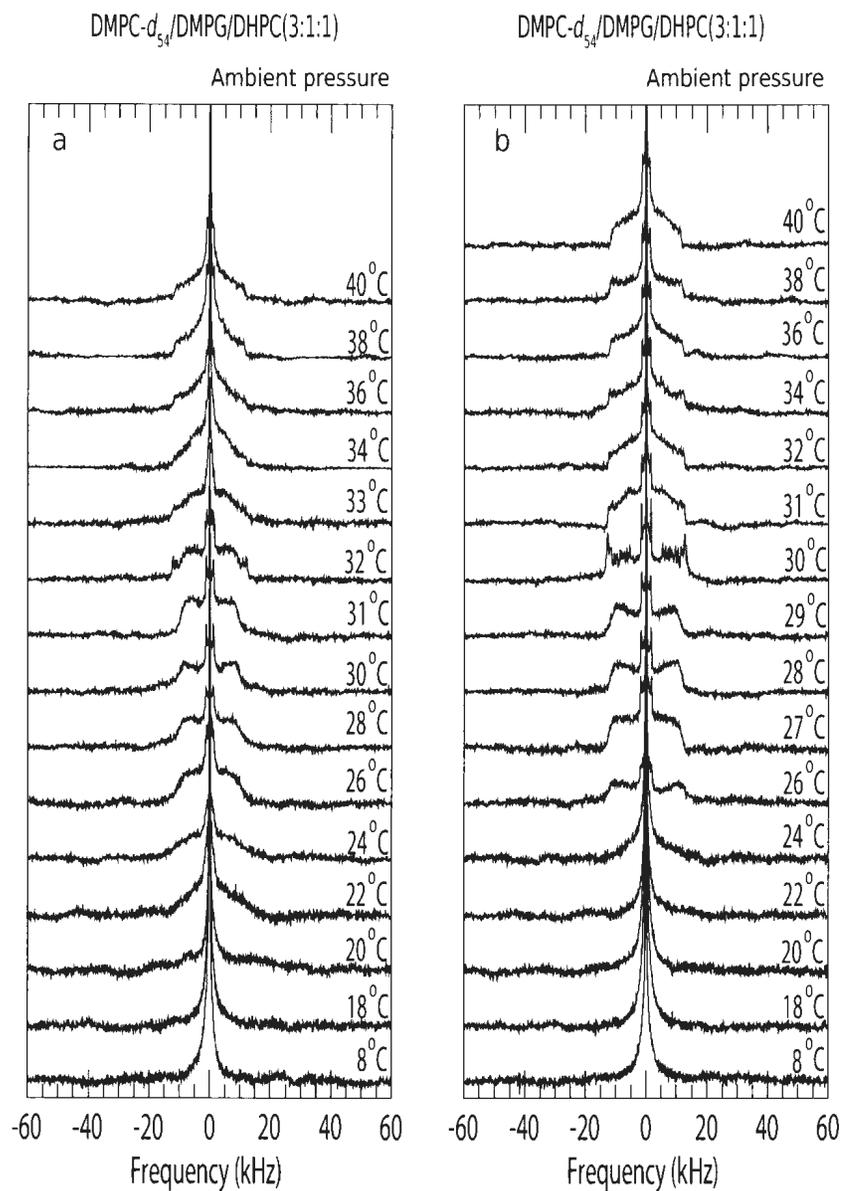
Fig. A. 13: Deuterium NMR spectra for DMPC-d_{54}/DMPG/DHPC (3:1:1) obtained with the 3.5 T superconductive magnet at ambient pressure for (a) the first cycle of warming and (b) the second cycle. This sample was denoted as AR09.
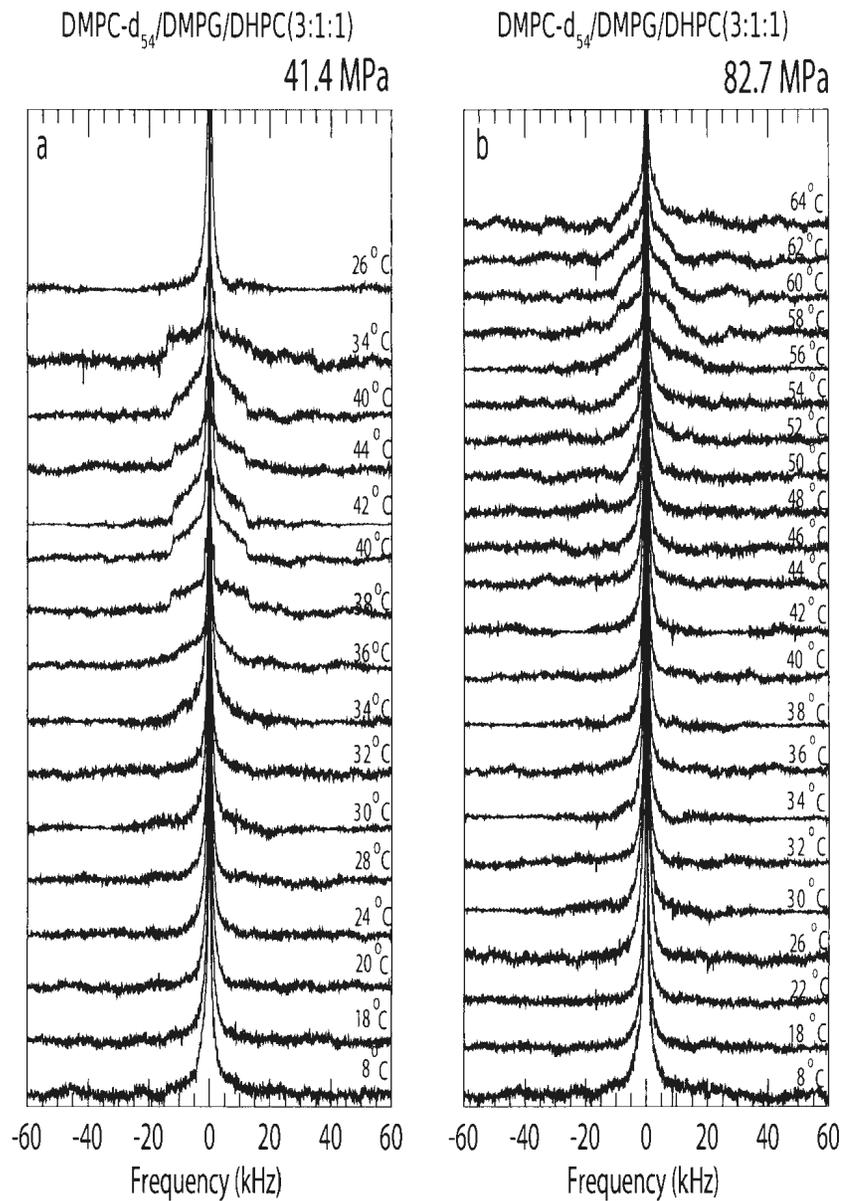
Fig. A. 14: Deuterium NMR spectra for DMPC-d_{54}/DMPG/DHPC (3:1:1) obtained with 3.5 T superconductive magnet while (a) warming and cooling at 42.5 MPa and (b) warming at 85 Mpa. This sample was labeled as (a) ARA9 and (b) ARB9.

DMPC-d_{54}/DMPG/DHPC (3:1:1)

82.7 MPa

DMPC-d_{54}/DMPG/DHPC (3:1:1)

82.7 MPa
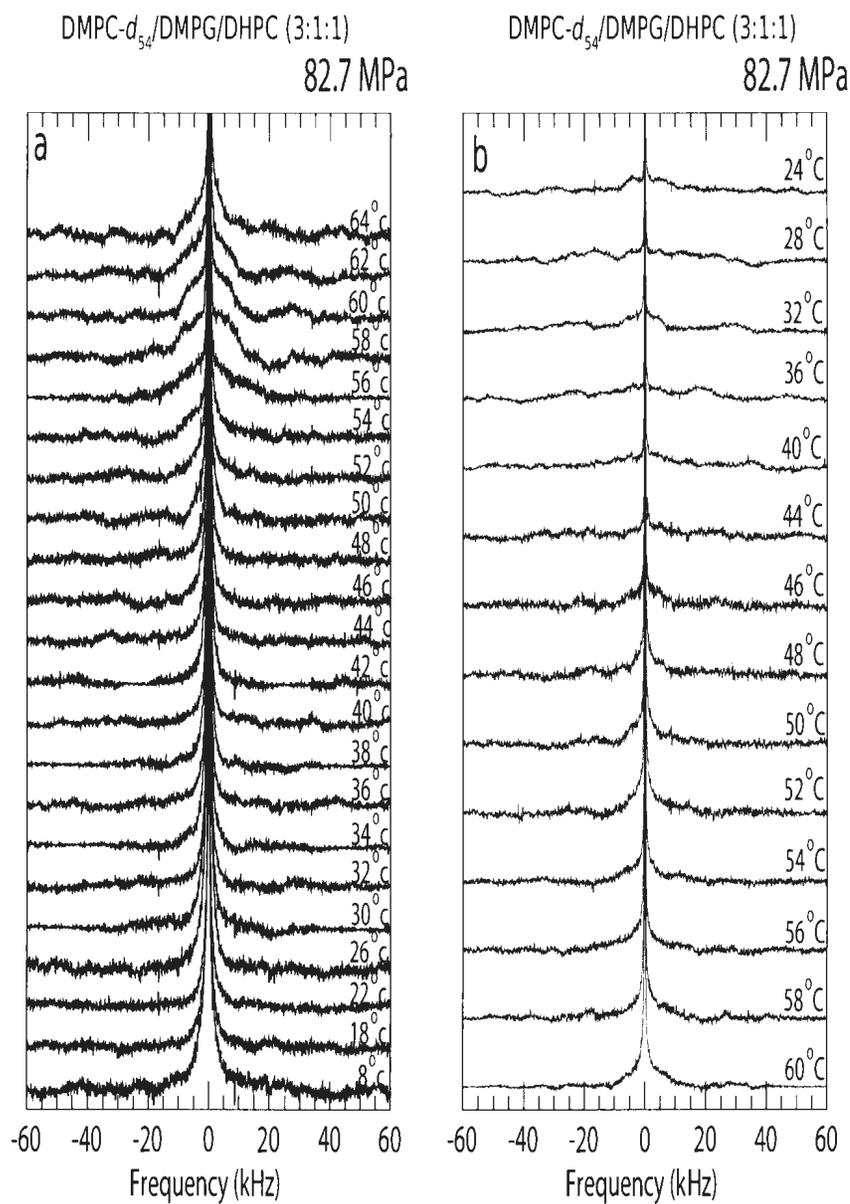
Fig. A. 15: Deuterium NMR spectra for DMPC-d_{54}/DMPG/DHPC (3:1:1) obtained with 3.5 T superconductive magnet at 85 Mpa while (a) warming and (b) cooling. The sample was denoted as ARB9.

Figure A.16a shows deuterium NMR spectra for DMPC-d_{54}/DMPG/DHPC (3:1:1) obtained with 3.5 T superconductive magnet of the first cycle of warming at ambient. It should be noted that this sample was in freezer for 30 minutes prior to data acquisition started. The mixture then cooled back to 8 °C. The first spectrum, shown in Figure A.16b, obtained when sample equilibrated one hour at 8 °C. As can be seen, the spectrum obtained is not characteristic of the complete isotropic phase. The second spectrum in Figure A.16b obtained subsequent to three hours of equilibration at 8 °C. As can be seen in Figure A.16b, the spectrum is not completely characteristic of the isotropic phase. The pressure raised to 42.5 MPa at this temperature eventhough the spectra obtained did not display characteristics of the isotropic phase. The spectra obtained while warming at 42.5 MPa are shown in Figure A.16b above the ones obtained at ambient pressure. This sample was denoted as AR010 for the experiment performed at ambient pressure and AR10 for the one performed at 42.5 MPa.
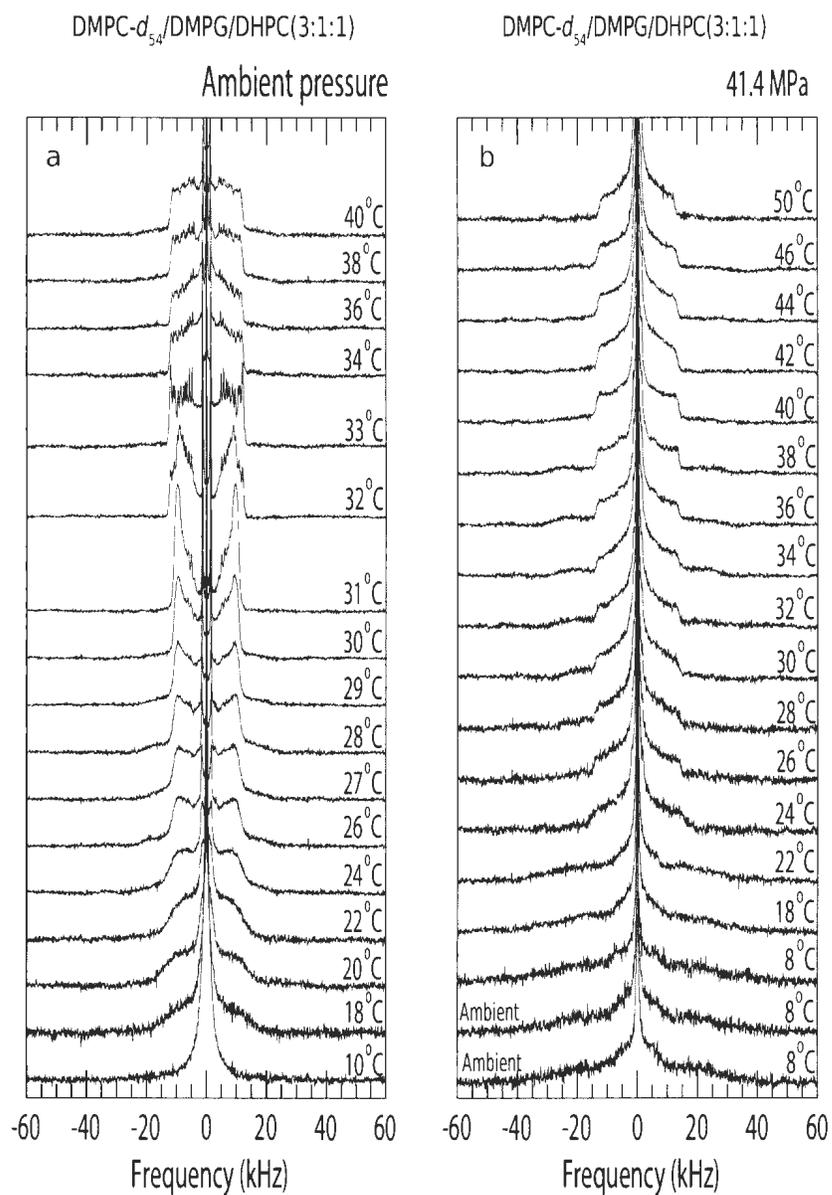
Fig. A. 16: Deuterium NMR spectra for DMPC-d_{54}/DMPG/DHPC (3:1:1) obtained with 3.5 T superconductive magnet while (a) warming at ambient pressure and (b) warming at 42.5 MPa otherwise "ambient" is mentioned. This sample was denoted as AR10 at ambient pressure and ARA10 at 42.5 MPa.

Figure A.17b shows the spectra obtained after the mixture was warmed and cooled at ambient pressure once, as shown in Figure A.16a, and warmed at 42.5 MPa, as shown in Figure A.16b and duplicated in A.17b. The spectra obtained over the cycle of cooling at 42.5 Mpa are shown in Figure A.17b with the label of "42.5 Mpa". The broad spectral component observed over this range of temperatures suggests the presence of an interdigitated gel phase in the DMPC-d_{54}/DMPG/DHPC (3:1:1) mixture. The spectrum obtained at 8 °C, which is not characteristic of the isotropic phase, was collected after the mixture equilibrated for one hour at ambient pressure. The spectrum obtained at 4 °C does not indicate the isotropic phase even though the mixture equilibrated at this temperature for $\sim$2 hours.

The mixture then warmed to 40 °C in steps of few degrees without data acquisition. The spectrum at 40 °C is characteristic of a non-interdigitated gel phase as expected. The spectra obtained during the process of cooling is shown in Figure A.17b (6 °C $\leq T \leq$ 40 °C). The sample then equilibrated at the room temperature for 2 days prior to equilibrate at 46 °C for one day. The consequent spectra obtained for cooling is shown in Figure A.17b. It should be noted that the spectra displayed in Figure A.17b are collected in the order shown. It worth mentioning for further inquiries that the data acquired, as of A.17a and A17b, were saved under the name of ARA10 but with different extensions.
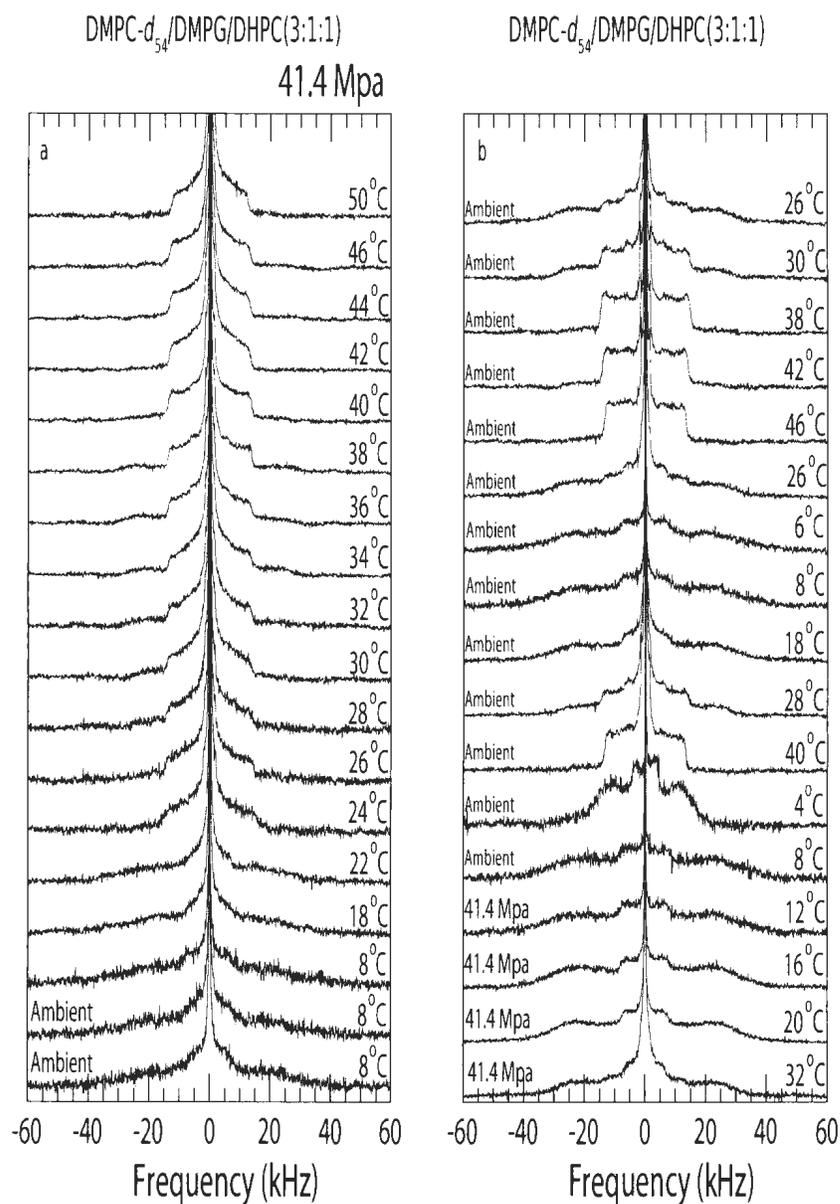
Fig. A. 17: Deuterium NMR spectra for DMPC-d_{54}/DMPG/DHPC (3:1:1) obtained with 3.5 T superconductive magnet while (a) warming at 42.5 MPa and (b) In the order shown at the pressure mentioned on the left side of the spectra. This sample was denoted as ARA10.

The same mixture as the one, the spectra of which is shown in Figure A.17, was subjected to a series of experiment in order to determine the influence of chain freeze, sonication, and cycles of freeze-thaw on the phase behaviours of DMPC-d_{54}/DMPG/DHPC (3:1:1) after the interdigitation. The details corresponding to these experiment will be described below.

The mixture was frozen three days. The spectra obtained then over a range of temperatures at ambient pressure as shown in Figure A.18. The spectra follow the sequence of an interdigitated gel phase at lower temperatures ($T \leq 26\,°\text{C}$), a coexistance of an interdigitated gel phase and a non-interdigitated gel phase at intermediat temperatures ($28\,°\text{C} \leq T \leq 32\,°\text{C}$) and a non-interdigitated gel phase in high temperatures ($T \geq 34\,°\text{C}$).

The mixture was then cooled at ambient, sonicated at $19\,°\text{C}$ for 15 minutes, and subjected to 5 cycles of freeze-thaw. The spectra obtained at $8\,°\text{C}$ and $18\,°\text{C}$ at ambient pressure, in the order shown in Figure A.18, are characteristic of an interdigitated gel phase. It should be noted that this sample was labeled as ARB10 during this experiment. It worth mentioning that the data acquired were saved with different extensions.
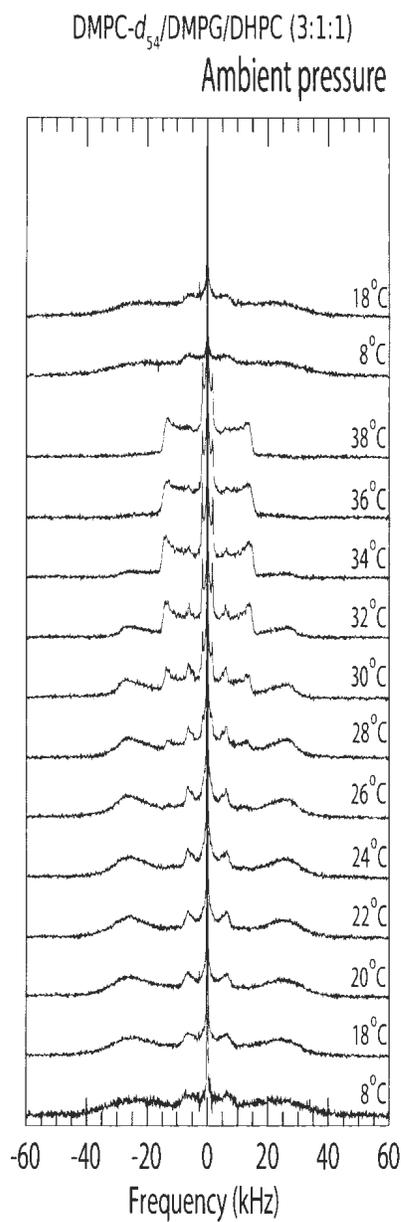
Fig. A. 18: Deuterium NMR spectra for DMPC-d_{54}/DMPG/DHPC (3:1:1) obtained with 3.5 T superconductive magnet,in the order shown, frozen for three days and then warmed up to 38 °C at ambient, then subjected to sonication and cycles of freeze-thaw prior to obtain the last two spectra. The detailed description of the process can be found in the P.126. This sample was labeled as ARB10.
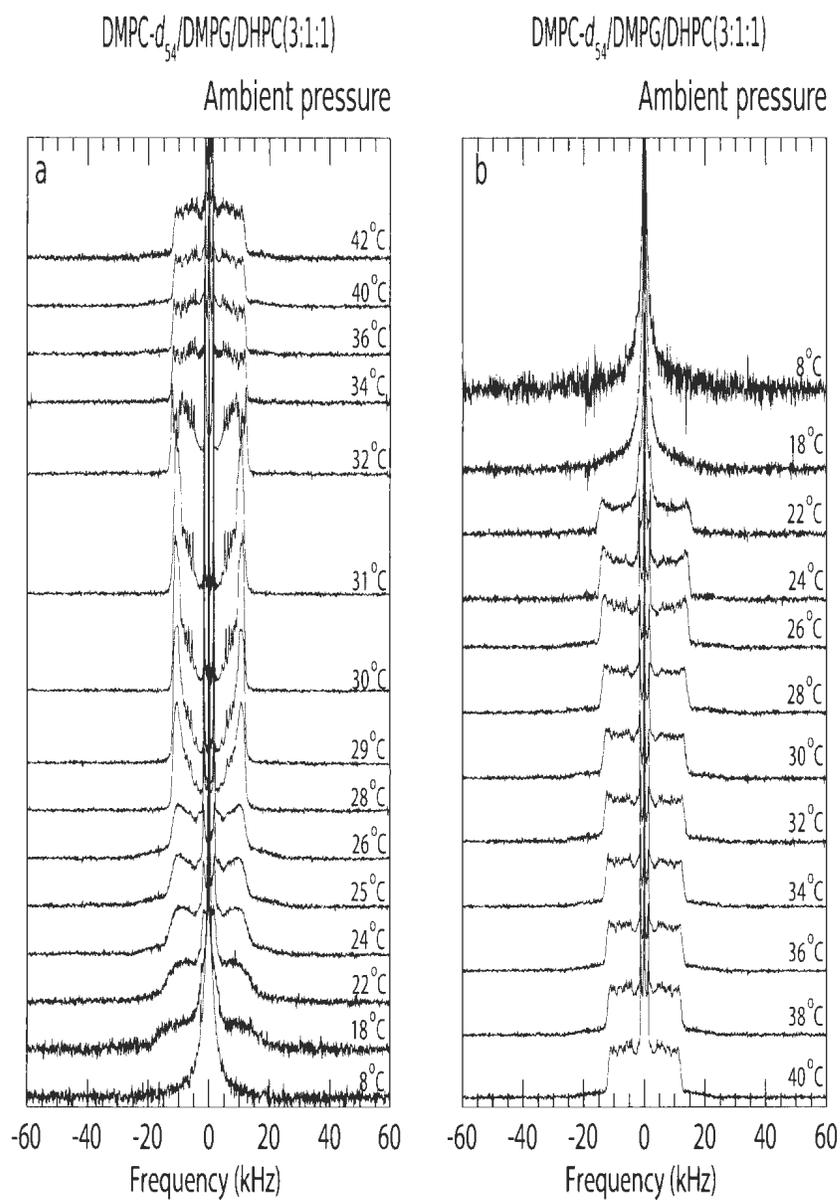
Fig. A. 19: Deuterium NMR spectra for DMPC-d_{54}/DMPG/DHPC (3:1:1) obtained with 3.5 T superconductive magnet at ambient pressure while (a) warming and (b) cooling. This sample is a part of the big batch that made to eliminate the minor differences in the sample preparation process. This sample was labeled as AR11.

The detailed description of the Figure A.19 can be found in 4.2.1. Figure A.20 a shows spectra collected, in the order shown, for sample AR11 after acquisition of the ambient pressure spectra in Figure 4.4. (a) Pressure was cycled to $\sim$ 100 MPa five times before acquisition at 8 °C. Spectra were then obtained at 26 °C and 38 °C while warming at ambient pressure. Pressure was then cycled to $\sim$100 MPa five times at 38 °C. Spectra were then collected on cooling from 38 °C to 18 °C at ambient pressure. (b) The sample was warmed to 36 °C and pressure was raised to 42.5 MPa. Spectra were obtained on cooling from 36 °C to 22 °C The sample was then held at 42.5 MPa, warmed to 38 °C, and pressurized to 85 MPa. Spectra were then obtained on cooling from 38 °C to 28 °C. The broad component ($\sim \pm 27$ kHz) in the 32 °C and 28 °C spectra at 85 MPa may indicate formation of interdigitated gel on cooling at high pressure. This sample was denoted as AR11.
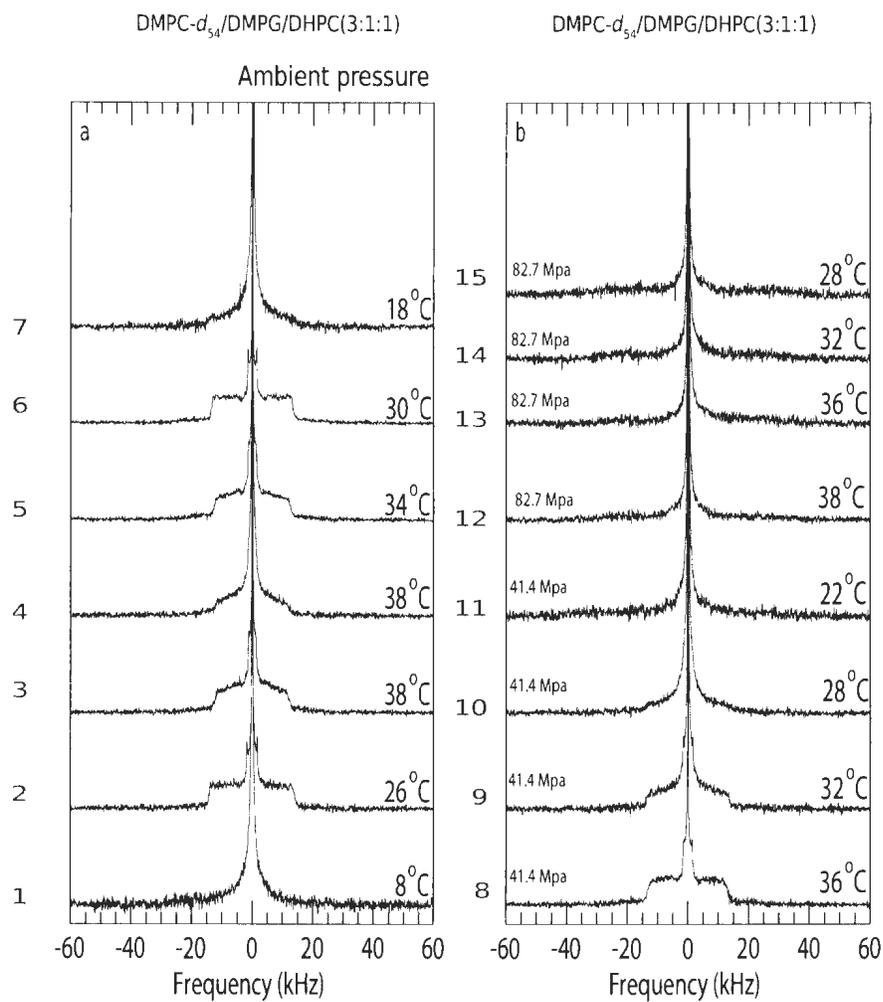
Fig. A. 20: Deuterium NMR spectra for DMPC-d_{54}/DMPG/DHPC (3:1:1) obtained with 3.5 T superconductive magnet at ambient pressure while subjected to different experimental conditions as decribed in P.129. This sample was denoted as AR11.
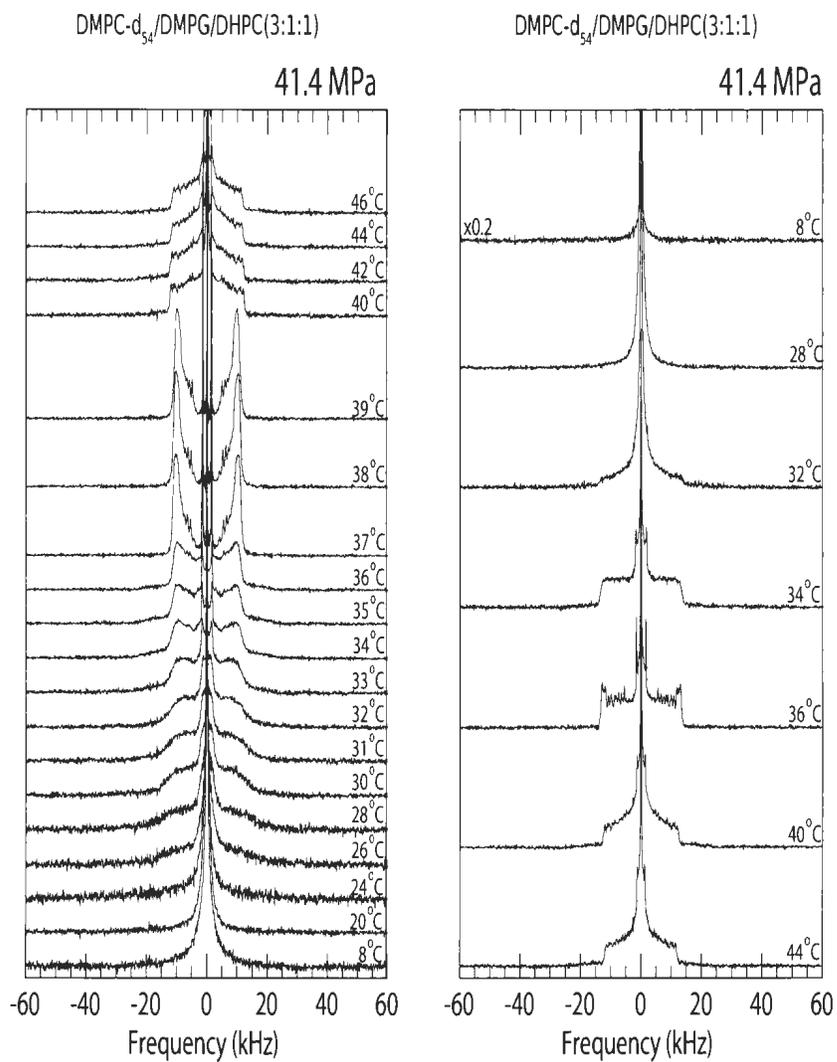
Fig. A. 21: Deuterium NMR spectra for DMPC-d_{54}/DMPG/DHPC (3:1:1) obtained with 3.5 T superconductive magnet at 42.5 MPa while (a) warming and (b) cooling. This sample was denoted as ARA11.
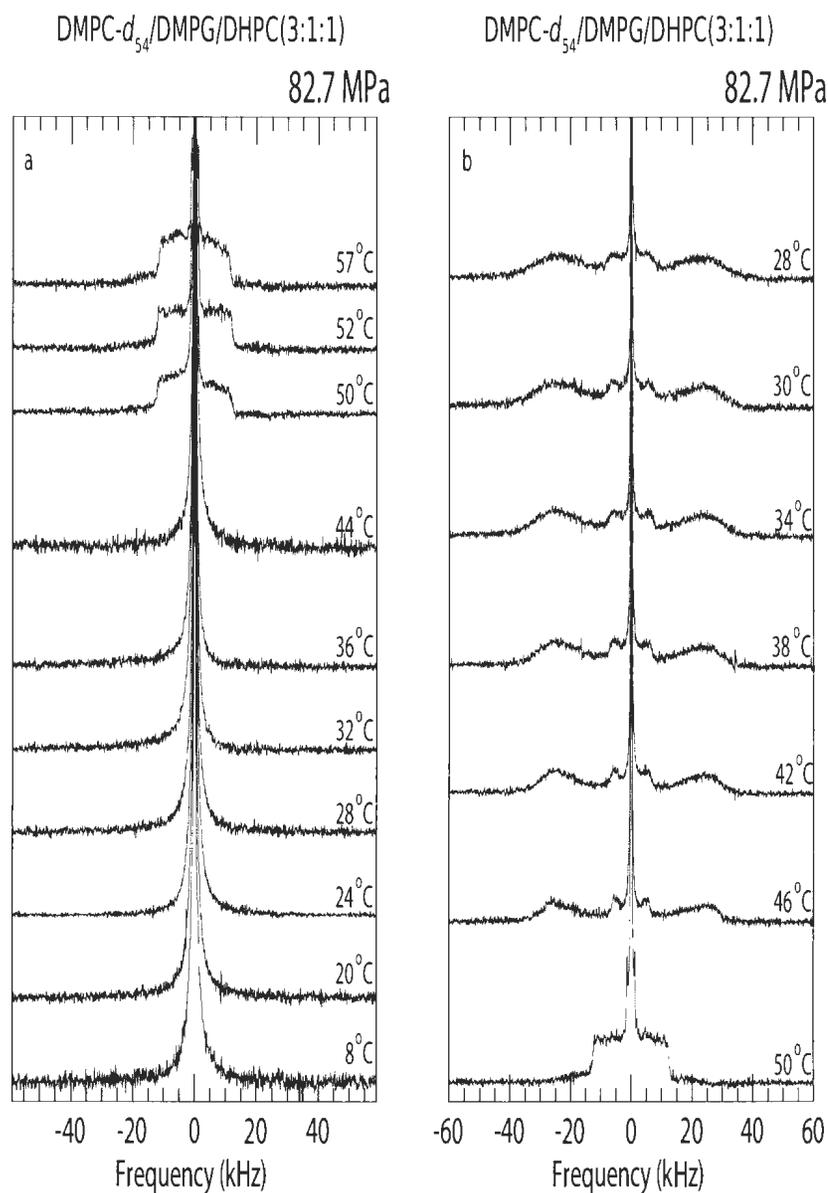
Fig. A. 22: Deuterium NMR spectra for DMPC-d_{54}/DMPG/DHPC (3:1:1) obtained with 3.5 T superconductive magnet at 85 MPa while (a) warming and (b) cooling. These sets of spectra were collected after the first cycle of warming and cooling were performed at 42.5 MPa As shown in A.21. As can be seen, The mixture undergoes into an interdigitated gel phase while cooling at 85 MPa. This sample was denoted as ARA11.
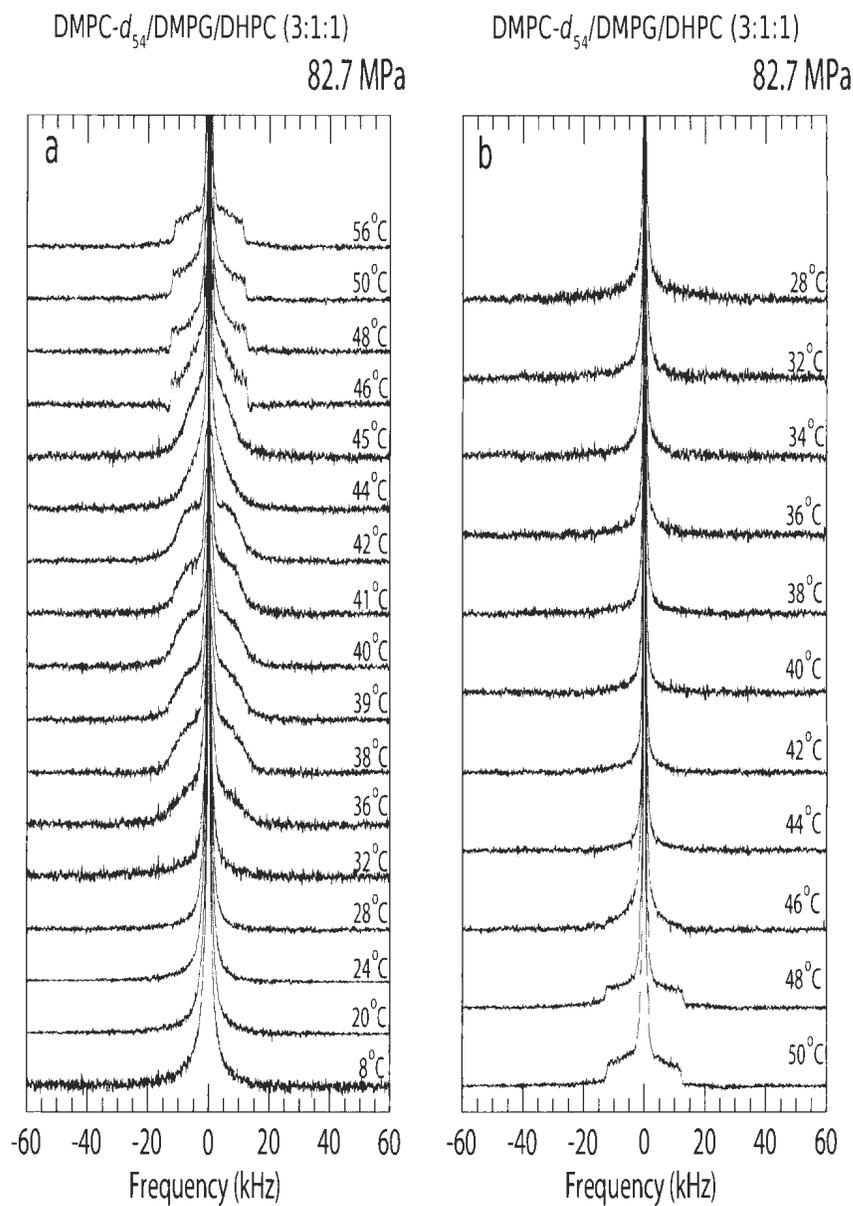
Fig. A. 23: Deuterium NMR spectra for DMPC-d_{54}/DMPG/DHPC (3:1:1) obtained with 3.5 T superconductive magnet at 85 MPa while (a) warming and (b) cooling. This sample is a part of the big batch that made to eliminate the minor differences in the sample preparation process. This sample was denoted as ARB11.
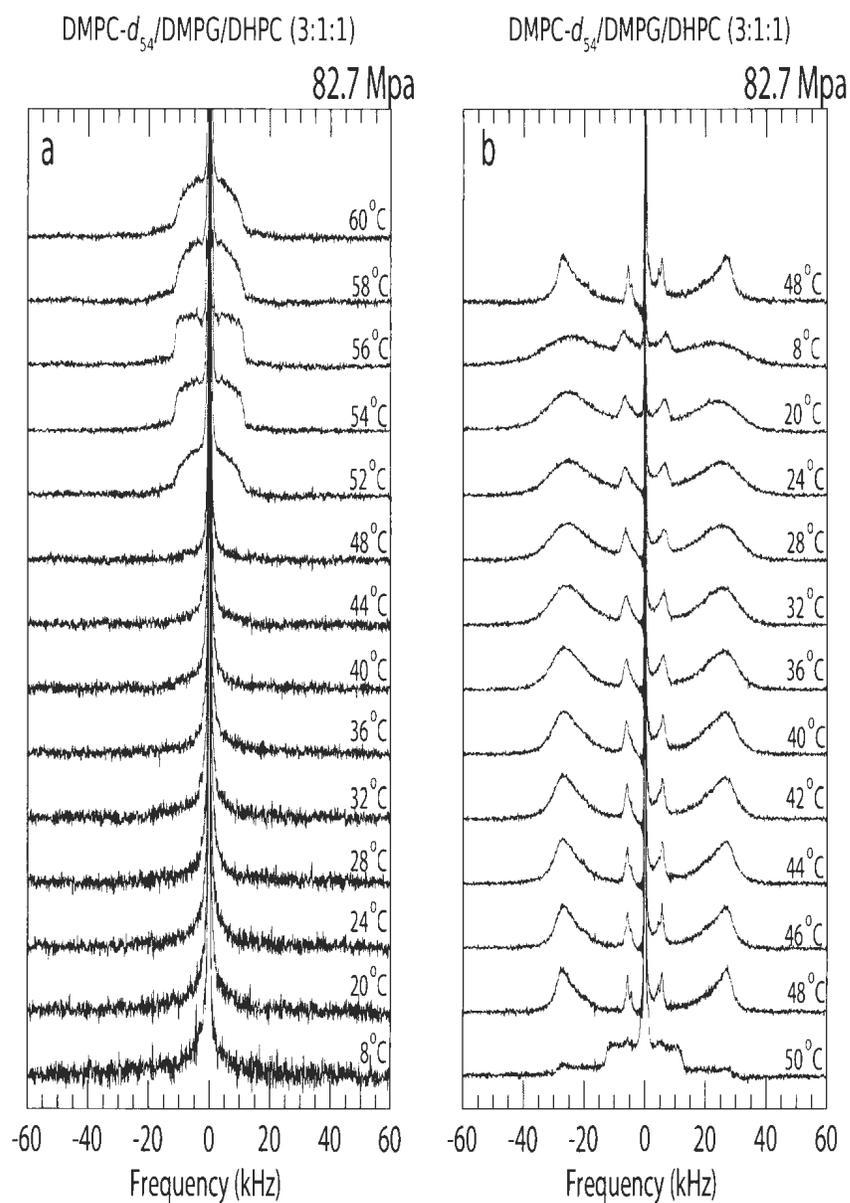
Fig. A. 24: Deuterium NMR spectra for DMPC-d_{54}/DMPG/DHPC (3:1:1) obtained with 3.5 T superconductive magnet at 85 MPa for the second cycle of (a) warming and (b) cooling. As can be seen, an interdigitated gel phase was observed while the second cycle of cooling at 85 MPa. This sample was denoted as ARB11.

Figure A.25a shows spectra obtained for DMPC-d_{54}/DMPG/DHPC (3:1:1) at ambient pressure. Figure A.25b is the spectra showed in Figure A.19a but at selected temperatures. as can be seen, the DMPC-d_{54}/DMPG/DHPC (3:1:1) mixture shows the same sequence of phase morphologies as the And DMPC/DMPG-d_{54}/DHPC (3:1:1) mixtures. However, these transitions occur at different temperatures which is expected due to the lowering effect of deuteration on bilayer phase transition temperatures [60] and the lower level of sample deuteration in the DMPC-d_{54}/DMPG/DHPC (3:1:1) mixture in comparison to the mixture with perdeuterated DMPC. It should be noted that the DMPC/DMPG-d_{54}/DHPC (3:1:1) sample was denoted as AR12 while the DMPC-d_{54}/DMPG/DHPC (3:1:1) sample was denoted as AR11.
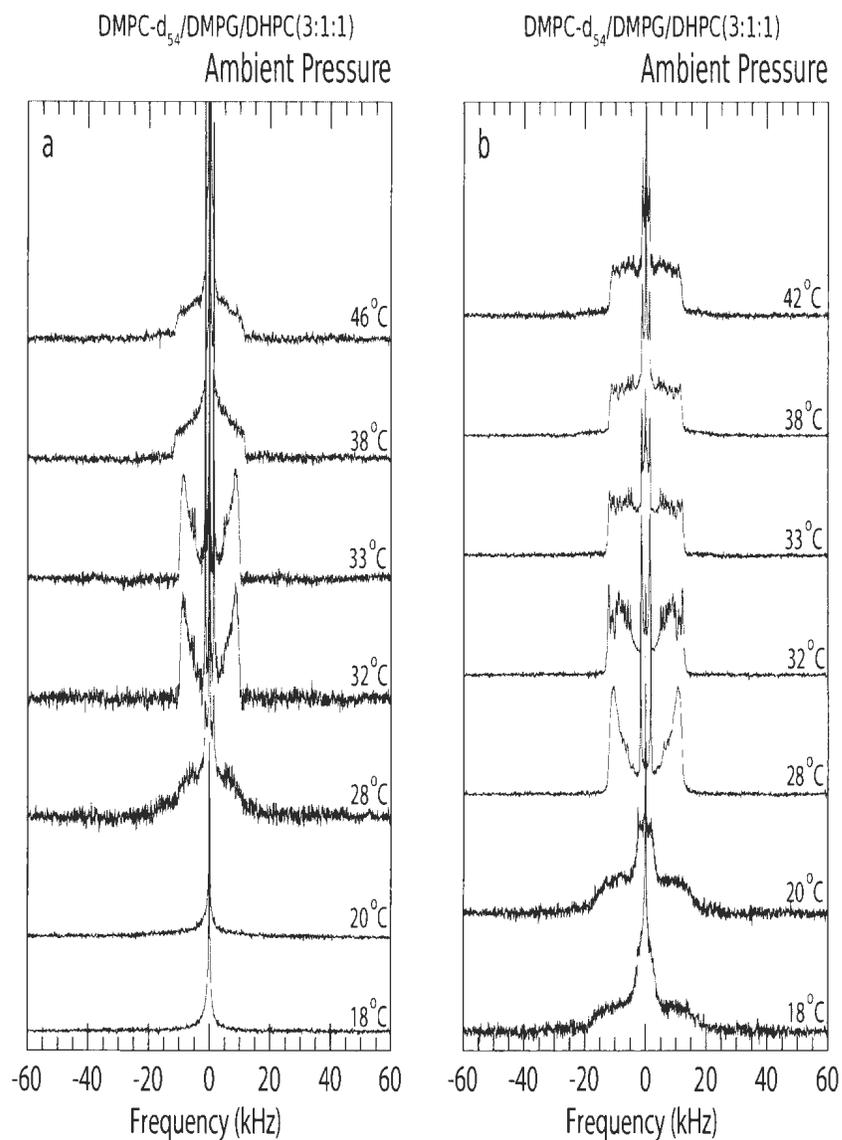
Fig. A. 25: Deuterium NMR spectra obtained with 3.5 T superconductive magnet at ambient for (a) DMPC/DMPG-d_{54}/DHPC (3:1:1) and (b) DMPC-d_{54}/DMPG/DHPC (3:1:1), duplicated from A.19. It should be noted that the DMPC/DMPG-d_{54}/DHPC (3:1:1) sample was denoted as AR12 while the DMPC-d_{54}/DMPG/DHPC (3:1:1) sample was denoted as AR11.
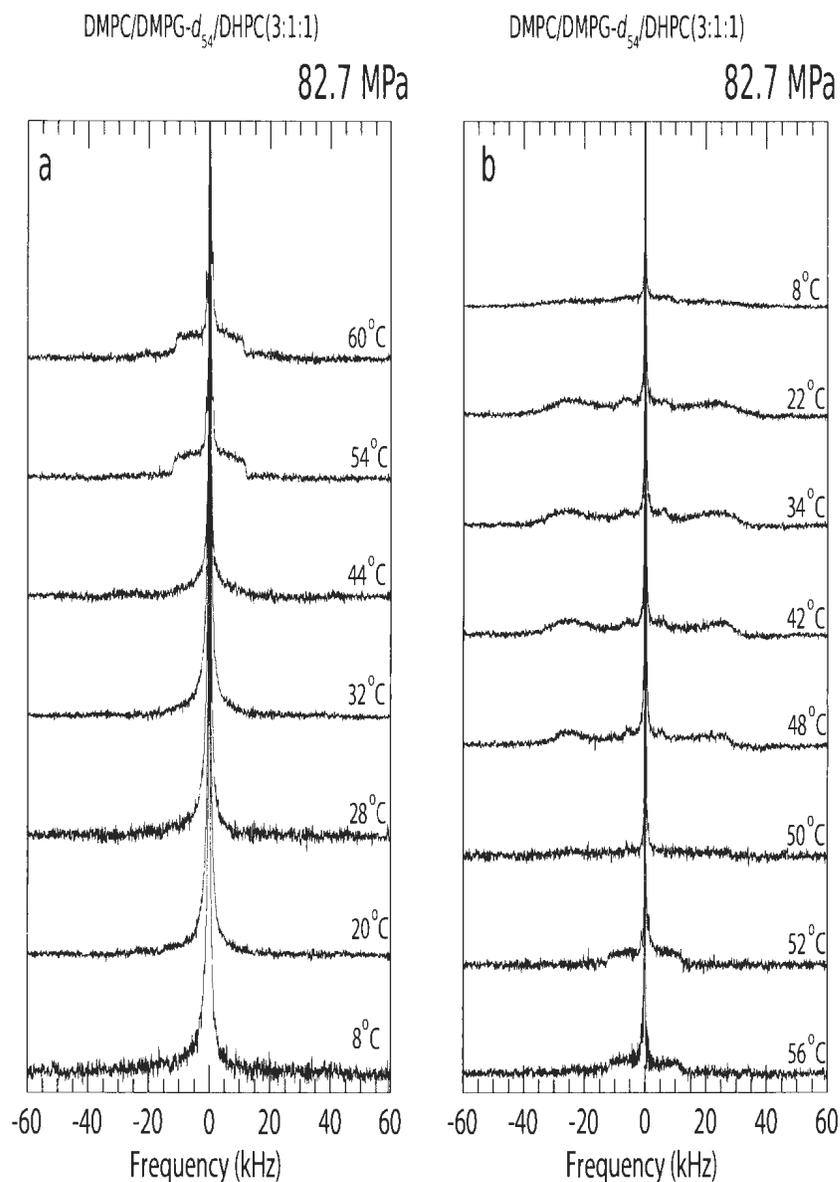
Fig. A. 26: Deuterium NMR spectra for DMPC/DMPG-d_{54}/DHPC (3:1:1) obtained with 3.5 T superconductive magnet at 85 MPa for the second cycle of (a) warming and (b) cooling. As can be seen, The spectra display characteristics of an interdigitated gel phase while cooling at 85 MPa (b). This sample was denoted as ARA12.
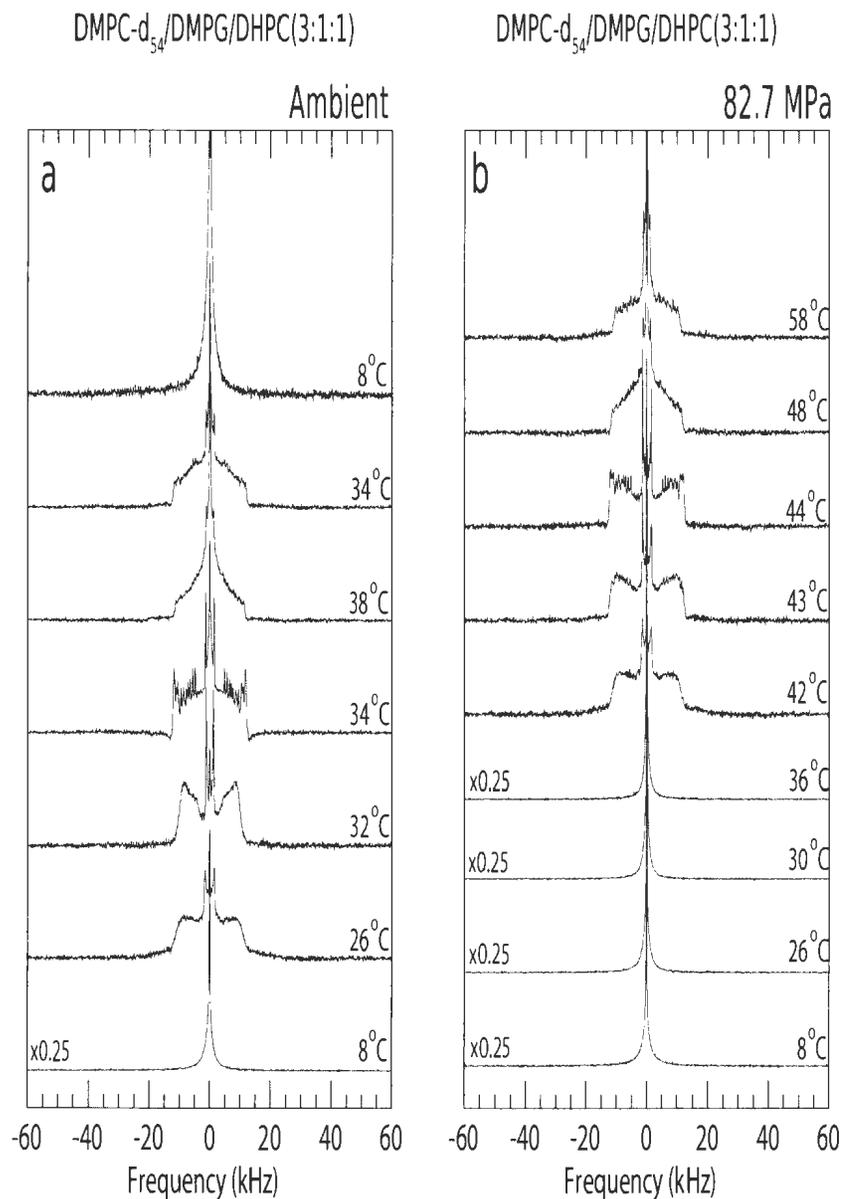
Fig. A. 27: Deuterium NMR spectra for non-sonicated DMPC-d_{54}/DMPG/DHPC (3:1:1) obtained with 3.5 T superconductive magnet at (a) ambient pressure while warming and cooling and (b) 85 MPa while warming. This sample was denoted as AR13 at ambient pressure and ARA13 at 85 MPa.

DMPC-d_{54}/DMPG/DHPC(3:1:1)

82.7 MPa
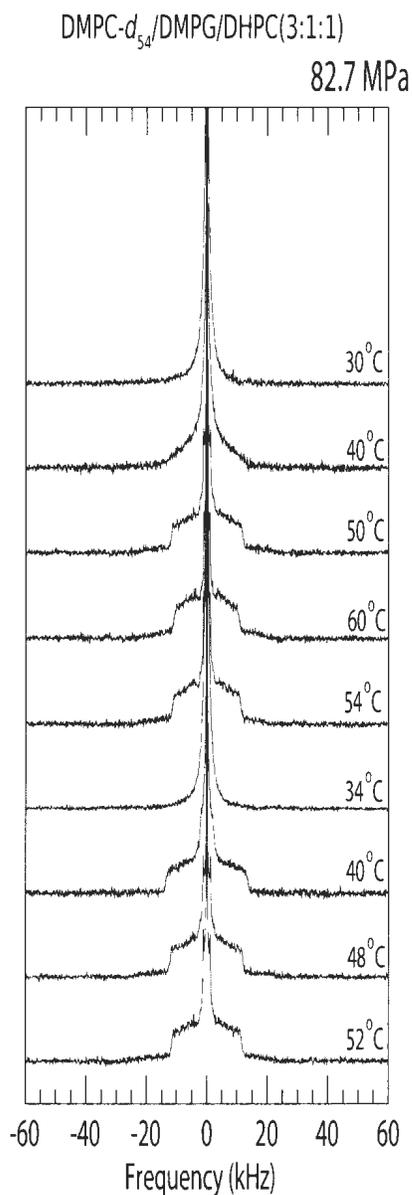
Fig. A. 28: Deuterium NMR spectra for non-sonicated DMPC-d_{54}/DMPG/DHPC (3:1:1) obtained with 3.5 T superconductive magnet at 85 MPa. This sample cooled from 52 °C to 34 °C at 85 MPa. The temperature was then raised to 60 °C while the pressure was kept constant. On decreasing the temperature, three spectra were obtained as shown. This sample was denoted as ARA13.